



Livestock Management Strategies in the 13th Century Mapungubwe Hinterland

By

Tyron D. Hopf

Submitted in fulfilment of the requirements for the degree of

Magister Artium (Archaeology)

in the Department of Anthropology, Archaeology, and Development Studies

in the

Faculty of Humanities

at the

University of Pretoria

Supervisor:

Dr. Alexander Antonites

Department of Anthropology, Archaeology, and Development Studies

Co-Supervisor:

Dr. Grant Hall

Mammal Research Institute

October 2023

Declaration

I, Tyron Denis Hopf, declare that this dissertation is my own original work. Where secondary material is used, this has been properly acknowledged and referenced in accordance with university requirements. This work has not been submitted before, in whole or in part, for any other degree or examination.

Signed: 

Date: 30 October 2023

Acknowledgement of Funding

This research was funded by a grant-holder linked studentship from the National Research Foundation (NRF) under the project “Mapungubwe Environment and Economy Project” (HSD170606237401).

Any opinions, findings, conclusions, or recommendations expressed in this dissertation are those of the author and the NRF is not liable for any of the above.

Abstract

Livestock were a key social and economic component of agropastoral Middle Iron-Age societies who occupied Middle Limpopo River valley between during the early second millennium CE.

This period witnessed rapid developments in regional social complexity underscored by an increased participation in the global trade network operating off the African east coast.

Agropastoral communities draw resilience from the effective management of domesticate stock which is shaped by a range of decisions regarding the mobility and diet of the animal herds.

These management practices take place against the backdrop of shifting environments, landscape resources, social networks, and economies.

This dissertation presents the results of stable isotope analysis of carbon and oxygen measured from the teeth of 35 domesticate and wild herbivores recovered from five archaeological sites in the hinterland of the Mapungubwe state. The results suggest that cattle and caprines were herded according to different regimes that may relate to their differing socio-economic roles in Middle Iron Age Society. Environmental variations and livestock management strategies among hinterland communities are examined in the rise of complexity that accompanied the transformation of southern Africa's first state-level civilisation.

Acknowledgements

My deepest thanks go first and foremost to my supervisors (past and present) — Dr. Xander Antonites, Dr. Grant Hall and Prof. Ceri Ashley — thank each one of you for the hand you have had in guiding, understanding, and encouraging, me through my research and writing. It is on your shoulders which I stand today.

A special thanks to Dr. Stephan Woodborne for the hours of invaluable assistance and teaching he provided with the running of (and battling with!) the mass spectrometer, isotope analysis, and data corrections.

I am infinitely grateful to those around me — my family, my friends, my Love — They have all supported me to the very last and kept me going when it mattered most, I love you all dearly. To hold values such as curiosity and the desire to *know* in reverence above the humdrum of life is a quality inspired by my grandfather and the wonder with which he regards the world — it is to him that I owe much of myself.

Contents

Chapter 1	Introduction.....	1
1.1	Significance of research	5
1.2	Dissertation structure.....	6
Chapter 2	Literature review.....	7
2.1	Early State Formation and the Greater Mapungubwe Landscape.....	7
2.2	Hinterlands and Heartlands	11
2.3	Herding and Livestock in the Middle Iron Age	14
2.4	Isotope Research on Middle Iron Age Agropastoralists	17
2.5	Background to sites used in this study.	21
2.5.1	Vryheid (MNR 04).....	21
2.5.2	Frampton I (MNR 74).....	23
2.5.3	Frampton II (MNR78).....	25
2.5.4	Mutamba	27
2.5.5	Stayt	29
Chapter 3	Background to Stable Isotopes.....	32
3.1	Principles of Stable Isotope Analysis.....	32
3.1.1	Carbon.....	34

3.1.2	Oxygen.....	36
3.2	Tooth Eruption and Enamel Mineralization.....	39
3.3	Applications of Stable isotopes on Tooth Enamel	42
Chapter 4	Materials and Methods.....	46
4.1	Sample Preparation and Pretreatment	46
4.2	Sample preparation.....	48
4.3	Sample Pre-treatment	49
4.4	Isotopic analysis	50
Chapter 5	Results of Serial $\delta^{13}\text{C}$ and $\delta^{18}\text{O}$ Tooth Enamel Analysis.....	52
5.1	Domesticated $\delta^{13}\text{C}$ and $\delta^{18}\text{O}$ Summary Results.....	52
5.2	Wild Grazer and Browser $\delta^{13}\text{C}$ and $\delta^{18}\text{O}$ results.....	61
5.3	Domesticated Serial tooththrow results.....	66
5.3.1	Mutamba	66
5.3.2	MNR 78	69
5.3.3	MNR 74	71
5.3.4	MNR04	74
5.3.5	Stayt (KON)	77
Chapter 6	Discussion and Conclusion.....	82
6.1	Discussion	82

6.1.1	Cattle	82
6.1.2	Caprines	89
6.1.3	Differences in livestock herd management: Cattle vs Caprines	92
6.2	Conclusion.....	95
	References.....	98
	Appendices.....	108

List of Figures

Figure 1.1. Map of the middle Limpopo River valley (grey rectangle) in regional perspective. Adapted from Ekblom et al. (2011).	2
Figure 2.1. Map of the south-eastern greater Mapungubwe landscape showing sites used in this research in relation to the Shashe-Limpopo Confluence Area. Adapted from Antonites et al. (2016).	12
Figure 2.2. Summer rainfall proxy records derived from <i>A. digitata</i> in the Kruger National Park (blue), and Mapungubwe National Park (red). Scale inverted to reflect lower values = higher moisture. The period under discussion is that which falls between AD 1180 and AD 1380. Source (Woodborne et al., 2016)	19
Figure 2.3. Radiocarbon dates from MNR04. Results are calibrated to the southern hemisphere calibration curve (Hogg et al. 2020) using OxCal v4.4.4 (Bronk Ramsey 2021). Uncalibrated dates from Lippert (2020).	23
Figure 2.4. Radiocarbon dates from MNR74. Results are calibrated to the southern hemisphere calibration curve (Hogg et al. 2020) and modelled using OxCal v4.4.4 (Bronk Ramsey 2021)..	25
Figure 2.5. Radiocarbon dates from MNR78. Results are calibrated to the southern hemisphere calibration curve (Hogg et al. 2020) using OxCal v4.4.4 (Bronk Ramsey 2021).	26
Figure 2.6. Calibrated radiocarbon dates from Mutamba. Results are calibrated to the southern hemisphere calibration curve (Hogg et al. 2020) using OxCal v4.4.4 (Bronk Ramsey 2021). Uncalibrated dates from Antonites (2012).	29

Figure 2.7. Calibrated radiocarbon dates from Stayt (KON). Results are calibrated to the southern hemisphere calibration curve (Hogg et al. 2020) using OxCal v4.4.4 (Bronk Ramsey 2021).

Uncalibrated dates from Prinsloo & Coetzee (2001)..... 31

Figure 4.1. Example of a serially sampled *B. taurus* (MUT/2012/F09) tooth from the present study..... 49

Figure 5.1. Variation in cattle $\delta^{13}\text{C}$ tooth enamel values grouped by tooth..... 53

Figure 5.2. Variation in caprine $\delta^{13}\text{C}$ tooth enamel values grouped by tooth..... 54

Figure 5.3. Variation in cattle $\delta^{18}\text{O}$ tooth enamel values grouped by tooth. 59

Figure 5.4. Variation in caprine $\delta^{18}\text{O}$ tooth enamel values grouped by tooth. 60

Figure 5.5. Variation in wild species $\delta^{13}\text{C}$ tooth enamel values. 62

Figure 5.6. Variation in wild species $\delta^{18}\text{O}$ tooth enamel values..... 63

Figure 5.7. Serial $\delta^{13}\text{C}$ and $\delta^{18}\text{O}$ values for wild species from all sites. 65

Figure 5.8. Serial $\delta^{13}\text{C}$ and $\delta^{18}\text{O}$ values for- *Bos taurus* MUT/2012/F10 M1, M2, and M3..... 66

Figure 5.9. Serial $\delta^{13}\text{C}$ and $\delta^{18}\text{O}$ values for two individual *Bos taurus* M3 MUT/2099/F09 and MUT/2167/F01 67

Figure 5.10. Serial $\delta^{13}\text{C}$ and $\delta^{18}\text{O}$ values for MUT/2177/F02 *Ovis/capra* M1 and M2 68

Figure 5.11. Serial $\delta^{13}\text{C}$ and $\delta^{18}\text{O}$ values for MUT/1170/F05 *Ovis/capra* M1, M2, and M3..... 68

Figure 5.12. Serial $\delta^{13}\text{C}$ and $\delta^{18}\text{O}$ values for MUT/2019/F20 *Ovis aries* M1, M2, and M3 69

Figure 5.13. Serial $\delta^{13}\text{C}$ and $\delta^{18}\text{O}$ values for MNR78/231/05 *Bos taurus* M2 and M3 70

Figure 5.14. Serial $\delta^{13}\text{C}$ and $\delta^{18}\text{O}$ values for MNR78/123/03 *Ovis/capra*..... 70

Figure 5.15. Serial $\delta^{13}\text{C}$ and $\delta^{18}\text{O}$ values for MNR74/B063 Bos taurus M2 and M3.....	71
Figure 5.16. Serial $\delta^{13}\text{C}$ and $\delta^{18}\text{O}$ values for MNR 74/B024 - Bos taurus M2.....	71
Figure 5.17. Serial $\delta^{13}\text{C}$ and $\delta^{18}\text{O}$ values for MNR 74/B065 Ovis/capra M1 and M2.....	72
Figure 5.18. Serial $\delta^{13}\text{C}$ and $\delta^{18}\text{O}$ values for MNR 74/B255 Ovis/capra M2 and M3.....	73
Figure 5.19. Serial $\delta^{13}\text{C}$ and $\delta^{18}\text{O}$ values for MNR04/341/08 - Bos taurus M1.....	74
Figure 5.20. Serial $\delta^{13}\text{C}$ and $\delta^{18}\text{O}$ values for MNR04/289/09 Ovis/capra M2 and M3	75
Figure 5.21. Serial $\delta^{13}\text{C}$ and $\delta^{18}\text{O}$ values for MNR04/2021/11 Ovis/capra M2 and M3	75
Figure 5.22. Serial $\delta^{13}\text{C}$ and $\delta^{18}\text{O}$ values for MNR04/239/09 Ovis aries M3.....	76
Figure 5.23. Serial $\delta^{13}\text{C}$ and $\delta^{18}\text{O}$ values for three individual Bos taurus M2s - KON/114, KON/T4, and KON/295.....	77
Figure 5.24. Serial $\delta^{13}\text{C}$ and $\delta^{18}\text{O}$ values for KON/100 Bos taurus M1	78
Figure 5.25. Serial $\delta^{13}\text{C}$ and $\delta^{18}\text{O}$ values for KON/106 Ovis/capra M1, M2, and M3.....	79
Figure 5.26. Serial $\delta^{13}\text{C}$ and $\delta^{18}\text{O}$ values for two individual Ovis/capra M3 KON/40 and KON/161.....	80
Figure 5.27. Serial $\delta^{13}\text{C}$ and $\delta^{18}\text{O}$ values for KON/192 Ovis/capra M2,.....	81
Figure 6.1 Serial $\delta^{13}\text{C}$ values for one cow from MNR78 and two hartebeest from Mutamba	88
Figure 6.2. Plot of all sampled cattle (top) and caprine (bottom) molar $\delta^{13}\text{C}$ values showing variance in diet over time.....	93

List of Tables

Table 2.1. Radiocarbon dates from MNR04. Results are calibrated to the southern hemisphere calibration curve (Hogg et al. 2020) using OxCal v4.4.4 (Bronk Ramsey 2021). Uncalibrated dates from Lippert (2020).	22
Table 2.2. Radiocarbon dates from MNR74. Results are calibrated to the southern hemisphere calibration curve (Hogg et al. 2020) and modelled using OxCal v4.4.4 (Bronk Ramsey 2021). Uncalibrated dates from Antonites & Ashley (2016).	24
Table 2.3. Radiocarbon dates from MNR78. Results are calibrated to the southern hemisphere calibration curve (Hogg et al. 2020) using OxCal v4.4.4 (Bronk Ramsey 2021). Uncalibrated dates from Antonites & Ashley (2016).	26
Table 2.4. Radiocarbon dates from Mutamba. Results are calibrated to the southern hemisphere calibration curve (Hogg et al. 2020) using OxCal v4.4.4 (Bronk Ramsey 2021). Uncalibrated dates from Antonites (2012).	28
Table 2.5. Radiocarbon dates from Stayt (KON). Results are calibrated to the southern hemisphere calibration curve (Hogg et al. 2020) using OxCal v4.4.4 (Bronk Ramsey 2021). Uncalibrated dates from Prinsloo & Coetzee (2001).	30
Table 4.1 Number of domesticates sampled from each site.	47
Table 4.2. List of wild species and their respective dietary preference sampled from each site. .	48
Table 5.1. Maximum, minimum, mean, and range of $\delta^{13}\text{C}$ and $\delta^{18}\text{O}$ serial enamel values for each Bos taurus tooth sampled.	55

Table 5.2. Maximum, minimum, mean, and range (range) of $\delta^{13}\text{C}$ serial enamel values for all caprines. 57

Table 5.3. Summary of wild species $\delta^{13}\text{C}$ and $\delta^{18}\text{O}$ enamel values grouped by dietary profile... 63

Table 6.1. Summary of cattle $\delta^{18}\text{O}$ values per tooth from each site, grouped as northern and southern clusters..... 86

Table 6.2 Mean values of the ranges of variation in the serial tooth $\delta^{13}\text{C}$ values for grouped cattle and caprines from each site..... 94

Chapter 1 Introduction

Agropastoral Iron Age communities have been present in the in Middle Limpopo River Valley for c.a. 1500 years during various periods of settlement density. Early Iron Age communities appear to have briefly entered the region prior to c.a. A.D. 500 (Voigt & Plug, 1984), however there is little evidence that these communities grew beyond sporadic settlements. Following an approximate three century hiatus, a new pulse of Iron Age communities entered the Shashe Limpopo Confluence Area – bringing with them well-established connections to global trade networks via the East African coast. This movement signals the regional commencement of the Middle Iron Age period that would last for c.a. 350 years (c.a. AD 900-1300) and would see the rise of an expanding complex state structure, which in northern South Africa culminates in the Mapungubwe civilization.

The Middle Limpopo River Valley is situated in the Mopane bioregion of the Savanna biome (Mucina et al., 2014). Between the town Alldays and the northern Kruger National Park, the landscape is currently predominated by the Musina Mopane Bushveld vegetation unit, with localised occurrences of the Limpopo Ridge Bushveld vegetation unit along with riparian thickets and reed beds typical of the azonal Subtropical Alluvial Vegetation unit occurring along the flat riverine terraces that form the banks of the Limpopo river (Mucina & Rutherford, 2006; Mucina et al., 2014). The present-day Middle Limpopo River Valley is considered to be generally unsuitable for commercial agriculture, being classified as a semi-arid environment with a mean annual precipitation of between 311mm and 334mm (Mucina & Rutherford, 2006: 482).

Located within the summer rainfall zone of southern Africa, precipitation is highly variable year-on-year and consecutive failed rainy seasons are not uncommon.

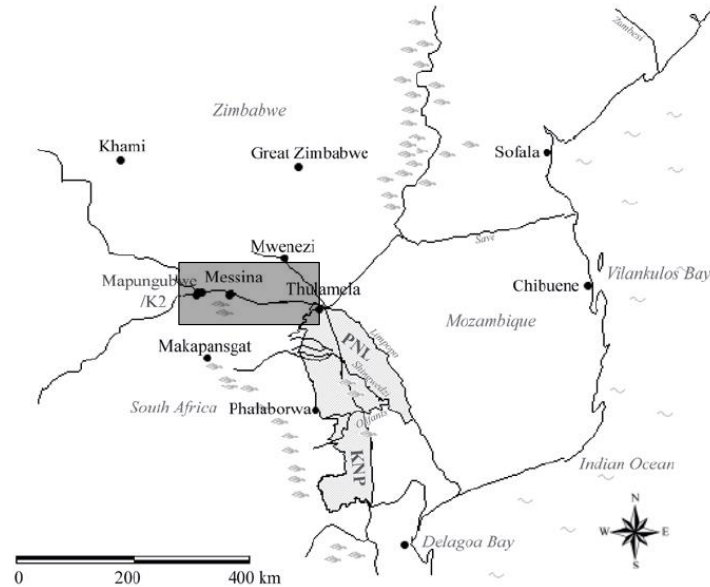


Figure 1.1. Map of the middle Limpopo River valley (grey rectangle) in regional perspective. Adapted from Ekblom et al. (2011).

Over the last 2000 years the southern Africa climate has been characterised by at least two major centennial scale climatic events which are typically characterised as the warmer, wetter Medieval Warm Period (ca. 900 – 1200 AD) and the cooler, drier Little Ice Age (ca. 1500 – 1800 AD) (Tyson et al., 2002; Ekblom, Gillson & Notelid, 2011; Woodborne et al., 2015, 2016).

Major trends in global climate are consistently discussed in tandem with trajectories of socio-cultural development (Huffman, 2008). Shifts in long term global climate will ultimately change the physical and social make-up of societies but it is through choices over an inter-generational time scale that these changes are enacted (Pauketat, 2001: 79). This leaves multiple opportunities for changes in the socio-political, material, and spatial make-up of society as adaptation

encourages more resilient ways of interacting with environmental variability (Ekblom et al. 2011).

The logic of a direct relationship between environmental extremes and significant cultural events appears a sound explanation of events in the archaeological record and as such, has faced relatively little critical examination (Kintigh & Ingram 2018:29). However, Kintigh and Ingram (2018) statistically assessed whether there was temporal correspondence between seven cultural traditions experiencing eleven periods of climatic transitions over respective periods of 400 – 600 years between AD 900 – AD 1500 in the Southwest USA. Their results were unable to find any statistical support for major cultural transitions and periods of extreme climate (Kintigh & Ingram, 2018: 29).

The study conducted by Kintigh and Ingram does not argue against the impact of extreme climate events on people but seeks rather to provide a means for assessing the extent to which cultural transitions are *determined* by shifts in a given climate regime. This leaves multiple opportunities for transformations in the socio-political, material, and spatial make-up of society across generations as adaptation encourages more dynamic ways of interacting with environmental variability (Ekblom et al. 2011).

Observed relationships between extreme climate events and cultural transitions on a macro scale serve as a broad means of understanding why a certain region may have been depopulated or inhabited at a given time but provide little to the understanding of how such a transition may have played out over multiple generations.

In an attempt to conceptualise the multiple dynamics that define the relationships between humans and their environment it is useful to imagine a socioecological system (SES) - a network of nested feedback loops that vary greatly between the long, slow processes and shorter, more rapid cycles (Redman, 2005). Key characteristics of ecosystems that align closely with the rhythms of societal change is that change is not usually a linear progression but manifests in, “episodic ... periods of slow accumulation of *natural* capital.” (Redman, 2005: 72). These episodes commonly culminate in a pulse of reorganisation in SES’s as either environmental and/or social inputs get altered.

The idea of natural capital mentioned above can be symmetrically conceived so that the concept of accumulation does not necessarily bear a ‘positive’ connotation. The multiple feedback loops that comprise the panarchy of systems conceived within an SES (Redman, 2005: 73) precludes the notion that human environment interactions can be represented by a single equilibrium.

Societal growth over a sustained period can be seen as an accumulation of natural capital in regional social systems through increased wealth in natural resources, trade, and people. The accumulation of natural capital in one sphere of a SES will ultimately have an altering effect on the inputs to other spheres, whereby they too will accumulate the altered inputs until such a point that a reorganisation of system dynamics is inevitable.

This scenario can be seen in the archaeological record of the Shashe-Limpopo Confluence Area where two centuries of growth among the ranked-based society at K2 (Meyer, 2000) would evolve into to a more stratified social pattern that would ultimately crystallise in the elite class-based society at Mapungubwe Hill by A.D. 1220 (Huffman, 1996).

Among the socioeconomic reorganisations that took place during this development, is an increasingly decentralised livestock herd management pattern (Smith, 2005; Smith et al., 2010). Using isotopic data of past diet and climate this shift in herd management has been interpreted as a response to increased population pressure on agricultural resources and overgrazing in the Shashe-Limpopo Confluence Area (Smith, 2005). The need to take livestock further from the capital simultaneously afforded communities the opportunity to permeate the landscape and establish themselves in order to draw from a wider pool of resources that would become the hinterlands of the Greater Mapungubwe Landscape.

1.1 Significance of research

Factors such as population increase leading to reduced local agricultural sustainability and variable climate patterns in the Shashe-Limpopo Confluence Area, present a possible rationale for the geographic expansion of settlement and pastoral management beyond the Shashe-Limpopo Confluence Area (Smith, Lee-Thorp & Hall, 2007; Smith et al., 2010). The occurrence of single-component Mapungubwe period sites as far south as the Soutpansberg mountains bear testament to such an expansion of people across the landscape. More evidence is required from the peripheries in order to facilitate a more symmetrical assessment of the regional conditions faced by the livestock who bore their people during this period of exploration.

Traditional zooarchaeological analyses offer suggestions into the roles of livestock in the lives of Middle Iron Age communities, however, many questions remain on how livestock herds were managed at a seasonal and region-specific scale. This thesis uses stable isotope data to reconstruct aspects of individual animal early life-histories in order to determine the conditions

under which herd management practices were negotiated at larger spatial and social scales during the rise of the Mapungubwe civilisation.

This research is centred on five relatively small to medium sized (0.1 -1.2 ha) Middle Iron Age settlements (encompassing levels 1-3 *sensu* Huffman and Hanisch, 1987) from the hinterland of the early second millennium Mapungubwe civilisation (see figure 2.1 in Chapter 2). These sites all bear a single Mapungubwe period occupation layer dating to the early second millennium (11th – 13th centuries AD) and can therefore be seen as largely contemporaneous glimpses of Mapungubwe hinterland life.

1.2 Dissertation structure

The dissertation begins with a background to the archaeology of the Middle Iron Age (Chapter 2) with reference to interpretations of paleoenvironmental conditions and a contextualisation of the five hinterland sites that were selected for sampling. Chapter 3 provides a background and overview of the principles of stable isotope analysis as well as a discussion and literature review of stable isotope research conducted on herbivore tooth enamel.

Chapter 4 presents the materials and methods used in the serial sampled IRMS analysis of 35 archaeological domesticate and wild animals. Chapter 5 presents the results of analysis beginning with a summary of the data and followed by combined plots of $\delta^{13}\text{C}$ and $\delta^{18}\text{O}$ values along the growth axis of the tooth for each individual. A discussion of broad observations and select individuals concludes the research in Chapter 6. Appendix A contains information about the archaeological samples and the full isotope data table is to be found in Appendix B.

Chapter 2 Literature review

2.1 Early State Formation and the Greater Mapungubwe Landscape

The research presented in this dissertation is concerned with the Middle Iron Age (Middle Iron Age), the period between ca. AD 900 – AD 1300 in the north-eastern region of South Africa, southwest Zimbabwe, and eastern Botswana (Huffman 2007:362). The Middle Iron Age can be characterised by an increase in both the number and scale of sites settled by iron-using agropastoral communities in the region and will ultimately see the florescence of social complexity in the Shashe-Limpopo Confluence Area (see Figure 2.1).

Prior to the 1970s archaeologists saw the first and second millennia in pre-colonial southern Africa as hosting two distinct Iron Age periods, namely the Early and Late Iron Age. The transition between these two periods was taken at roughly AD 1000, represented by changes in material culture (Summers, 1950) as well as shifts in settlement layout and an apparent shift in emphasis from grain cultivation to cattle herding (Huffman, 2007: 362). These changes were widely interpreted as indicative of new populations moving into the region and absorbing earlier societies (Evers, 1983).

Subsequent research into the transition between the Early and Late Iron Ages has revealed a sequence of events that, beginning in the 10th century, spanned a 300-year period which saw several shifts in the structure of Iron Age societies. In order to contextualise these myriad developments, archaeologists have employed the Middle Iron Age as a spatio-temporally discrete

term referring to the rise of social complexity in the Shashe-Limpopo Confluence Area (Huffman 2007: 362). However, as Bandama (2013: 15) notes, it is important to regard the usage of classifications for Early, Middle and Late Iron Age periods as convenient shorthand references to what should be viewed as a continuum of interweaving socio-political trajectories.

The Middle Iron Age sequence begins at ca. AD 900 with a southward expansion of Zhizo ceramic using peoples settling into the Shashe-Limpopo Confluence Area region from central Zimbabwe and eastern Botswana, under a similar climatic regime to our present day semi-arid conditions (Smith, 2005: 192; Huffman, 2007: 361; Du Piesanie, 2009: 16). The Limpopo Valley settlement known as Schroda has been identified as a major centre of Zhizo activity from the 9th to 10th century onwards and the occurrence of numerous imported glass beads alongside evidence of ivory working suggest that occupation of this region was intended to exploit large elephant herds for the ivory trade on the East coast markets (Wood, 2000: 87; Sinclair, Ekblom & Wood, 2012; Antonites, 2018: 223).

At ca. AD 1000 settlements with Zhizo type ceramics become less frequent in the Limpopo Valley, coupled with the contemporaneous appearance of settlements associated with a new ceramic style known as Leopard's Kopje. The sudden appearance of Leopard's Kopje ceramics has been typically interpreted as the arrival of a new demographic group. Over a period of 200 years, the Leopard's Kopje settlement known as K2, located in the Shashe-Limpopo Confluence Area, developed into a regional capital with a hitherto unprecedented diversity and scale of exotic imports from the Indian Ocean trade networks, extensive cattle kraals, and an exceptionally large population for the region (Huffman 2000:20). It is around this time that there is a rapid and considerable build-up of livestock numbers, which is seen in accumulation of very

deep dung deposits on archaeological settlements in the surrounding region of eastern Botswana, south-west Zimbabwe, and north-eastern South Africa (Denbow, 1999: 113). A rapid population increase is often observed when new species are introduced into a favourable environment as would be the case for expansion of cattle-based societies into this region. From about AD 1220 settlement at K2 appears to dwindle as a sharp increase in settlement activity is evinced about 1km to the north-east at the base of Mapungubwe Hill (Meyer 2000:6), the occupation of which signals the final period of the Middle Iron Age.

The Mapungubwe settlement is regarded as especially significant as the site layout indicates the emergence of a hereditary ruling elite (Calabrese, 2005; Huffman, 2007: 376). Prior to Mapungubwe, Iron Age sites followed an organisational pattern known as the Central Cattle Pattern (CCP) - where the cattle kraal is located at the centre of a settlement with discrete gendered divisions of space within the settlement (Huffman, 2001; Calabrese, 2005: 65; Badenhorst, 2009). In the relocation from K2 to Mapungubwe Hill, this settlement pattern was eschewed in favour of a more densely settled urban zone, with the main cattle kraal placed at the periphery of the settlement (Huffman, 2000: 20; Meyer, 2000: 11). Another notable change in settlement organisation is the elevation of the leader and his kin to a sacred position atop Mapungubwe Hill – a ritual seclusion from the commoner classes below emphasising the status of the newly founded elite (Huffman, 2000: 21; Calabrese, 2005: 363). Lending further legitimacy to the authority of sacred leadership is the symbolic act of taking up permanent residence on a powerful rainmaking hill and thereby asserting a metaphysical claim to the landscape through the power to wield rain (Huffman 2000:15). Taken together, these material shifts in settlement layout and social organisation at Mapungubwe represent some of the first

iterations of what is identified as the Zimbabwe settlement pattern. Significantly, the evolution of the Zimbabwe settlement pattern initially observed at Mapungubwe Hill did not take place at the smaller sites in the region, typically regarded as being of lower social status, which continued to observe a CCP type layout (Calabrese, 2005). The Zimbabwe pattern is therefore mostly regarded as a phenomenon associated with elite settlements, signifying an elevated social status.

The position of Mapungubwe being the southern African epicentre for the development of socially complex societies has been recast through increased investigation in regions beyond the Shashe-Limpopo Confluence Area (e.g., Chirikure et al. 2014). New surveys and excavations at Mapela demonstrate that the attributes indicative of a nascent stratified society were already in place at Mapela Hill contemporaneous to the occupation of K2 in the Shashe-Limpopo Confluence Area. The site at Mapela Hill is located two kilometres east of the confluence of the Shashe and Shashane Rivers, roughly 150 km north-west of Mapungubwe (Chirikure et al., 2014: 3).

These findings offer a revised perspective on the formation of early southern African states through emerging evidence indicating that a network of materially and culturally linked communities co-acted in the establishment of regional social complexity. This contrasts to the linear replacement model which currently isolates these developments to a pinpoint, or moment in time.

In conceiving the development of social complexity as a climate of fission and fusion between networks of multiple wealth or resource accumulating centres, the narrative of the crystallised state needs no longer collapse, or shatter, but can rather be seen as a transformation (Middleton,

2012: 264), or negotiation, to new ways of life. This recasting of the archaeological narrative is an important step in the redress of the lens through which early states in southern Africa are viewed, intentionally shirking the implication that the advent of socially complex societies in southern Africa resulted in the region's first failed state.

2.2 Hinterlands and Heartlands

The advent of social complexity during the Middle Iron Age was reliant on an evolving process of fission and fusion between communities. This is manifested on the landscape through the founding of multiple settlements during the 11th–13th centuries and represents a widening of the network of contact and exchange reaching beyond the immediate confines of the Shashe-Limpopo Confluence Area. Sites bearing testament to this with material-culture characteristic of the Mapungubwe civilisation have been documented at distances of up to 100km from the capital (Loubser, 1989; Prinsloo & Coetzee, 2001; Antonites, 2014; Antonites & Ashley, 2016; Antonites, Uys & Antonites, 2016) The elucidation of sites considered to be at the periphery of the Mapungubwe state have added interesting textures to current understandings of early state formation in southern Africa. Significantly, the machinations of early precolonial civilisations in southern Africa did not necessarily appear to follow the pursuit of political dominance through coercion or aggravation but chose rather to negotiate relationships of power through long distance networks of kinship, contact and exchange (*c.f.* Calabrese, 2001; Antonites, 2012, 2019a; Antonites & Ashley, 2016).

As a result, hinterland/peripheral sites have increasingly been integrated as key components to the larger Mapungubwe world. Examples of these sites include Mutamba on the southern slopes

of the Soutpansberg (Antonites, 2012) and sites in the wider Nzhelele River Valley (NRV), such as Vryheid (MNR04), Stayt (KON), and Frampton I and II (MNR74 and MNR78, respectively) (Figure 2.1). These sites bear a single cultural layer containing Mapungubwe type ceramics, Indian Ocean trade beads and worked metal objects (Prinsloo & Coetzee, 2001; Antonites, 2014; Antonites & Ashley, 2016). Radiocarbon dating (see section 2.5 below) and close material culture associations to Mapungubwe point to these sites forming nodes in a network of communities that have come to constitute part of the Greater Mapungubwe Landscape (GML).

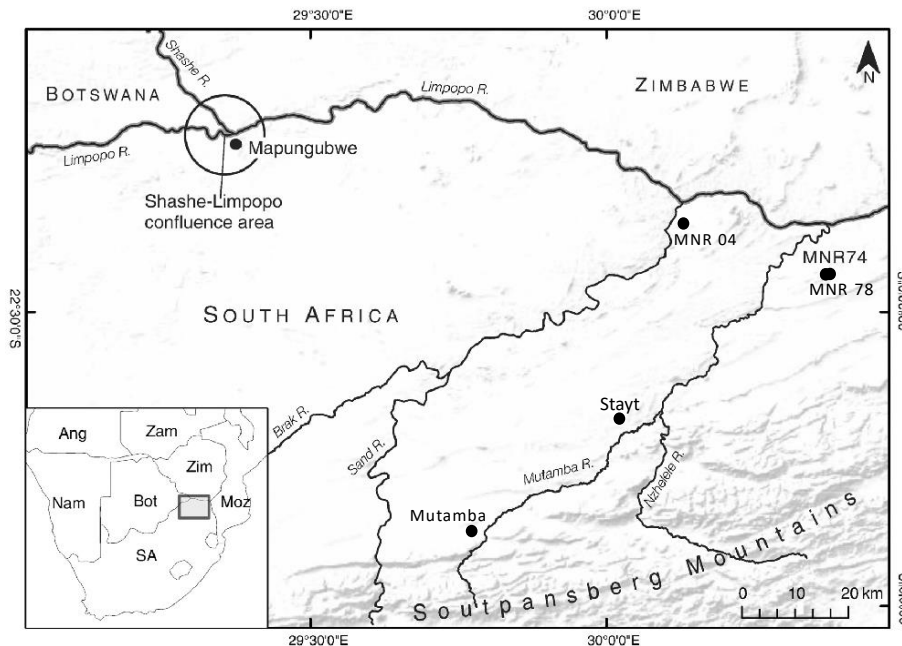


Figure 2.1. Map of the south-eastern greater Mapungubwe landscape showing sites used in this research in relation to the Shashe-Limpopo Confluence Area. Adapted from Antonites et al. (2016).

All sites examined in this research were excavated by members of the University of Pretoria Department of Anthropology and Archaeology and have revealed material culture profiles that provide new perspectives in understanding the well-established trajectory of socially complex societies in southern Africa. Excavated material from these peripheral sites is seemingly at odds

with patterns of prestige goods distribution among the large elite and small commoner sites of the Shashe-Limpopo Confluence Area region (Calabrese, 2000; *c.f.* Antonites, 2012). It has been suggested that there existed a system of Maussian ‘aggressive prestation’ among the various emergent classes which produced a settlement pattern reflecting a strict control over high-status prestige goods within the confines of the Shashe-Limpopo Confluence Area (Calabrese, 2005).

This pattern, however, does not seem to occur the further one moves from the Shashe-Limpopo Confluence Area, where relatively small communities had access to a variety of locally and globally traded objects, including gold, copper, iron, imported glass beads, as well as exotic ceramics (Antonites & Ashley, 2016; Moffett & Chirikure, 2016; Lippert, 2020). The relative abundance of high-status goods being observed at sites in the hinterland has been interpreted as the existence of a dual system of prestige goods control among communities that are differentially positioned within the greater state (Antonites & Ashley, 2016; Antonites, 2019a; Lippert, 2020). Such a system would seemingly present the state with the ability to cast its reach further into a landscape rich with economic opportunity, while still managing to keep a measure of control through the deployment (negotiation) of weak-ties (*sensu* Granovetter 1983) amongst its various actors and agents (Antonites & Ashley, 2016). Recent research has also suggested that economic and resource factors may have driven hinterland expansion. An example is the evidence of an intensified cotton spinning industry at Mutamba indicating that some communities may have exploited variable landscape resources, such as *Gossypium herbaceum* (African wild cotton), as leverage in exchange relationships within the politico-economic hierarchy of the Middle Iron Age (Antonites, 2019b: 106).

Societies grow as a culture through dialogue with others that are characterised as much by social flux as it is stability (Denbow, 1999). Through time these social negotiations are what form the matrix in which dynamics such as transformation and conservation are played out between the people, places, and things that make up their society. In the wake of the transition from K2 to Mapungubwe, and the opening-up of a greater landscape of influence, nascent hinterland communities may have found themselves in a position where they could enact new ways of leveraging their situation in the constant negotiation of socio-political relations.

2.3 Herding and Livestock in the Middle Iron Age

The arrival of large scale agropastoral groups in the middle Limpopo River valley at around the ninth century AD is signalled in the archaeological record of the region by the appearance of multiple, densely occupied sites with ubiquitous grainbin platforms (Huffman, 1996) and significantly larger kraals with up to 2m of dung deposit (Denbow, 1999). During this period, up until at least the 13th century, the density of settlements and scale productive activity seemed to have been in overall increase.

In terms of the increase in pastoral productivity, the fairly rapid expansion of herd sizes is a phenomenon that, as mentioned above, has been observed in the past as an ecological response to new herds entering a favourable environment (Denbow, 1999: 113). It is how these growing herds were managed, and the social exchanges that encoded these management practices, that would play a role in shaping the landscape.

When it comes to domesticate fauna two major themes emerge as central to interpretations of Middle Iron Age human-animal interactions. These are livestock as subsistence economy (Voigt,

1980, 1986; Plug, 2000) and livestock as symbolic wealth in social transactions (Huffman, 1982; Hall, 1986). Interestingly, both themes hold as central subjects the question of how prestige may be expressed through the faunal record. Where a higher proportion of wild to domesticate faunal remains may reflect the subsistence economy of a lower status settlement (Plug, 2000), a site that has a large proportion of domesticate remains is regarded as having command of a network of social relations (Huffman, 1982).

Some patterns in the faunal record of the Middle Iron Age that broadly emerge are a dominance in the number of ovicaprine stock in the late first millennium AD with a marked increase in the number of cattle emerging from sites dating to the around turn of the millennium (Voigt, 1986: 14; Badenhorst, 2015). This overall trend is however tempered with high levels of variability among the ratios of domesticate to wild animals in the faunal assemblages which have been interpreted as varying responses to subsistence, especially meat procurement (Plug, 2000).

These interpretations are viewed largely as responses to various ecological crises that may have undermined a particular mode of subsistence production. Changes in the faunal record explained in terms of local resource depletion, whether it be an over-reliance on hunted game for meat (Plug, 2000; Badenhorst, 2015) or exceeding veld carrying capacity (Voigt, 1983: 63) – present a passive picture of the society in which these animals are integral.

The role of cattle in southern Africa has been ethnographically demonstrated as being one that goes beyond subsistence economy (e.g., Stayt, 1931; Kuper, 1982). Cattle transactions are understood as signifying an acknowledgement of the mutual obligations woven into the social fabric of inter and intra community social relationships (Hall, 1986: 83). Most prominently,

cattle exchanges form the basis for marriage transactions and therefore serve to establish networks of kinship between communities (Huffman, 2001). The symbolic currency enshrined in cattle provide for the accumulation of political action-potential which may be deployed, or restricted, in the shaping of local labour forces or the establishment of contact networks across the landscape (Stayt, 1931:143).

Martin Hall makes the argument for livestock as a more suitable store of wealth in southern Africa given the “dialectic with nature” (Hall, 1987: 11) that underscores both day to day social reproduction as well as broader societal transformations. This idea is based on the notion that the environmental, logistical, and social mustering required to accumulate a significant store of cultivated grain would be fraught with myriad risks that are more difficult to mitigate. In keeping and deploying livestock through various social mechanisms, such as bridewealth payments and political loans, communities are afforded several hedges (Denbow, 1999: 113) against the pitfalls inherent in their ongoing socio-environmental negotiations.

The combined social and environmental concerns central to maintaining a pastoral economy make that, “for pastoralists, ecology is about livestock and politics is about pasture.” (Salzman, 2004: 2). Pastoralism is the practice of raising livestock on natural pastures unimproved by human intervention i.e., not actively cultivated or tended to. It must follow then that if the central ecological concern of a pastoralist society is directly related to concerns around livestock health, the management of livestock herds must then necessarily be the management of local pastures and the social relations that form the landscape.

Evidence for intensified seasonal herd management practices in conjunction with growing social complexity have been demonstrated to occur in the archaeological record of the region (Smith 2005; House 2021). Given the significant role that livestock played in forging the Middle Iron Age, insights into the livestock management practices of these societies reflect both the cultural and economic aims of the people behind the animals (Coertze, 1986).

If these themes are taken as variables informing the management of livestock over a landscape, it becomes clear then that a dynamic set of interactions between social and environmental factors inform the decisions resulting in the patterns observed in the archaeological record.

2.4 Isotope Research on Middle Iron Age Agropastoralists

Isotopic research on livestock management practices have been conducted on archaeological contexts within the geographic confines of the (Smith, 2005; Smith, Lee-Thorp & Hall, 2007; Smith et al., 2010) as well as in the broader southern Africa region (Denbow et al., 2008; House, 2021; House et al., 2021). The research in Shashe-Limpopo Confluence Area the chiefly examined local climate and shifts in herding patterns during the development of social complexity between AD 880 and 1290 (Smith et al., 2010). It was found that as the Shashe-Limpopo Confluence Area became more densely populated an increased need for environmental resources to support the agricultural requirements of a burgeoning population appears to have had a direct impact on the management and available rangeland of livestock herds (Smith et. al. 2010:94).

Through the analysis of $\delta^{15}\text{N}$ in cattle and ovicaprid remains as a proxy for rainfall levels during the Middle Iron Age, it was demonstrated that both the expansion and decline of settlement at

Mapungubwe took place under increased precipitation levels (Smith et. al. 2007:115). These results present alternatives in determining the role of the environment in the collapse of early southern African civilisations (Huffman, 2000: 24) and lend credence to the notion that organisation at the political or economic level operate in negotiation with environmental variability.

Further research into the paleoclimate of the Middle Iron Age has provided a clearer resolution with which to examine the role that climate played as a major determining force the abandonment of Mapungubwe (Smith, Lee-Thorp & Hall, 2007; Woodborne et al., 2015; Huffman & Woodborne, 2016). These include Smith *et. al.* (2007) study which examined the $\delta^{15}\text{N}$ values in the bone collagen of cattle and ovicaprines from the Shashe-Limpopo Confluence Area which found that the florescence of K2 and Mapungubwe between AD 1010 and AD 1290 took place under favourable, moist conditions. Their results further revealed that it was not until AD 1450 that drier conditions took hold, suggesting that factors beyond the environment need to play a role in considering the expansion of the GML and ultimate abandonment of Mapungubwe Hill (Smith *et. al.* 2007: 124). Other proxies for longer term climate records, such as a speleothem from Makapansgat in Limpopo, have indicated that the regional precipitation and temperature from the mid-Holocene onwards has displayed rapid changes at a centennial scale (Lee-Thorp et al., 2001)

More recently, high resolution (decadal/centennial) proxies for the summer rainfall region of southern Africa have been derived from stable isotope analysis of *Adansonia digitata* (Baobab) trees. Data from the Pafuri region of the Kruger National Park (in the Limpopo River Valley c.a. 200 km downriver from the Shashe-Limpopo Confluence Area), have demonstrated that there

existed a high level of variability in rainfall during the period that constitutes the Middle Iron Age, however an overall downward trend in rainfall events was noted (Woodborne et al., 2015). Significantly, the rainfall record derived from the Baobab trees confirmed that there was a period of cool, dry climate following the abandonment of Mapungubwe, however this is recorded as occurring slightly later than initially suggested, at around AD 1310 \pm 5 (Huffman & Woodborne, 2016: 468). A later study of 5 baobab trees some 200km west in the Mapungubwe National Park introduces an additional perspective on rainfall variation through space (Woodborne et al. 2016: 12). The Mapungubwe baobab record (fig 2.2) indicates that the localised climate around the Shashe-Limpopo Confluence Area followed a similar overall trend to that indicated by the KNP Pafuri record, but with comparably drier and more variable periods of moisture (Woodborne et al. 2016: 11–12).

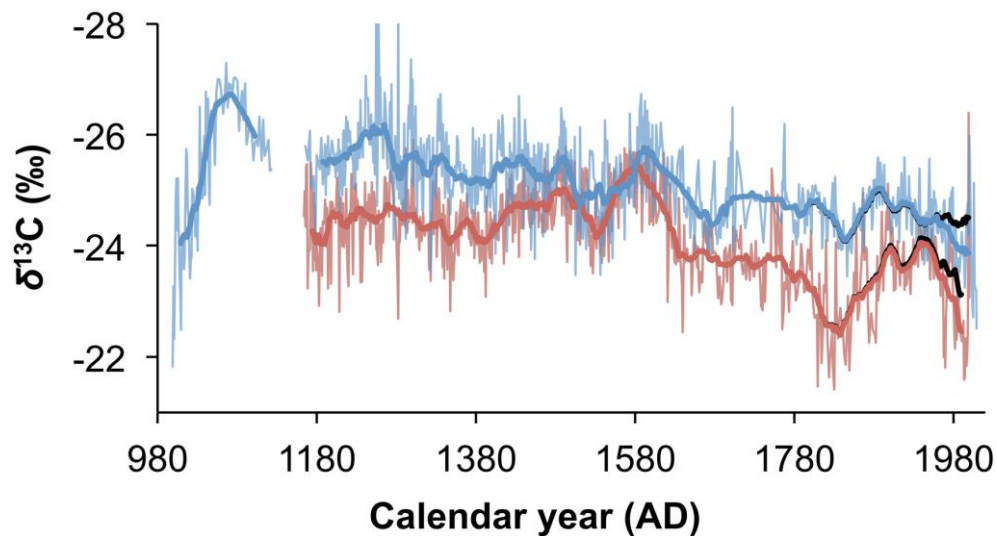


*Figure 2.2. Summer rainfall proxy records derived from *A. digitata* in the Kruger National Park (blue), and Mapungubwe National Park (red). Scale inverted to reflect lower values = higher moisture. The period under discussion is that which falls between AD 1180 and AD 1380. Source (Woodborne et al., 2016)*

Further afield, stable carbon and nitrogen isotopes have been used to investigate environmental impact of adaption during the Middle Iron Age from the site of Bosutswe, located on the eastern margin of the Kalahari in present day Botswana about 280 km north-west of Mapungubwe (Denbow et al., 2008). Here, a shift to a dispersed livestock management strategy documented at elite sites in the Shashe-Limpopo Confluence Area, also took place at around AD 1200 (Denbow et al., 2008). However, the shift at Bosutswe is argued in terms of the compounded environmental stress of long-term occupation (i.e., overgrazing, exhausted resources) and draws on insights from diet and rainfall derived from the characterisation of stable carbon and nitrogen isotopes from wild and domesticate faunal remains (Denbow et al., 2008:472). The findings indicate that livestock had year-round access to preferential fodder despite variable ecological conditions and are interpreted in tandem with the disappearance of large accumulations of dung layers at Bosutswe to indicate that cattle herds were being moved to outposts located near plentiful pastures.

Isotope research in the Shashe-Limpopo Confluence Area (Smith, 2005; Smith, Lee-Thorp & Hall, 2007; Smith et al., 2010; Woodborne et al., 2015, 2016; Huffman & Woodborne, 2016) and regionally important sites like Bosutswe (Denbow et al., 2008), provides an empirical dataset from which insights into the management of cattle and ovicaprine herds for the Middle Iron Age be drawn. However, there is a need to supplement this dataset with regional data from smaller and geographically peripheral sites and those located in the hinterland of politically central communities. The isotope data contained in this research serves as an initial step to augment the existing pool of data in order to present an expanded rendering of the systems of livestock management in the greater Mapungubwe landscape.

2.5 Background to sites used in this study.

The sites selected for analysis in this research are located in the south-eastern hinterland of the greater Mapungubwe landscape and fall in a corridor along the Nzhelele river. They range in size from class 3 to class 1 sites according to the size-status settlement hierarchy of Huffman and Hanisch which classifies sites of the region (Huffman & Hanisch, 1987). Excavations on these sites by members of the University of Pretoria's Archaeology and Anthropology department have yielded material culture which indicates that, despite being geographically distant from the capital at Mapungubwe hill, their material culture affinities suggest active participation in the Mapungubwe society.

2.5.1 Vryheid (MNR 04)

Vryheid is located 200m south-west of the Sand River on and around the spur of a ridge which overlooks the Limpopo River 3 km to the north. The river would have provided a perennial water source during the period of occupation and the occurrence of the ruderal sweet grasses such as blue seed grass (*Tricholaen monachne*) and Dinter's wiregrass (*Danthoniopsis dinteriz*) indicate that this locale would likely have been amenable to livestock.

One of the largest Mapungubwe period sites located in the Maremani nature reserve, work at MNR 04 has revealed at least three Middle Iron Age occupation areas. Area A is the slope and summit of the hill and comprises both kraal and domestic contexts. The two remaining areas are located at the base of a small dividing ridge about 150m to the east of Area A. Area B is represented by numerous grain-bin bases and domestic contexts the ridge while Area C is an area of ashy kraal deposit about 50 m to the north (Lippert, 2020).

The ubiquity of grain-bin bases at area B and significant layers of burnt dung at area A indicate that intensive agropastoral practices took place at MNR04. Material culture recovered from the excavations has provided evidence of fibre spinning and metal working, including finished non-utilitarian iron and cuprous objects. These objects reflect the potential status afforded to the inhabitants of MNR 04 and the presence of Indo-Pacific and Mapungubwe oblate series glass beads provide evidence of their contact with the greater Mapungubwe landscape.

Five charcoal samples recovered from kraal and midden deposits were submitted for dating (Lippert, 2020: 78). Raw dates were recalibrated using OxCal v4.4.4 (Bronk Ramsey 2021) along the updated southern hemisphere curve (Hogg et al., 2020) and are summarized in Table 2.1 and plotted in Figure 2.3.

Table 2.1. Radiocarbon dates from MNR04. Results are calibrated to the southern hemisphere calibration curve (Hogg et al. 2020) using OxCal v4.4.4 (Bronk Ramsey 2021). Uncalibrated dates from Lippert (2020).

Laboratory number	Uncalibrated age BP	95.4% Probability (cal. AD)
D-AMS 008688	917 ± 25	1050 – 1224
D-AMS 008690	822 ± 23	1220 – 1280
D-AMS 008691	1075 ± 22	986 – 1043
D-AMS 008692	952 ± 22	1044 – 1209
D-AMS 008693	902 ± 25	1150 – 1264

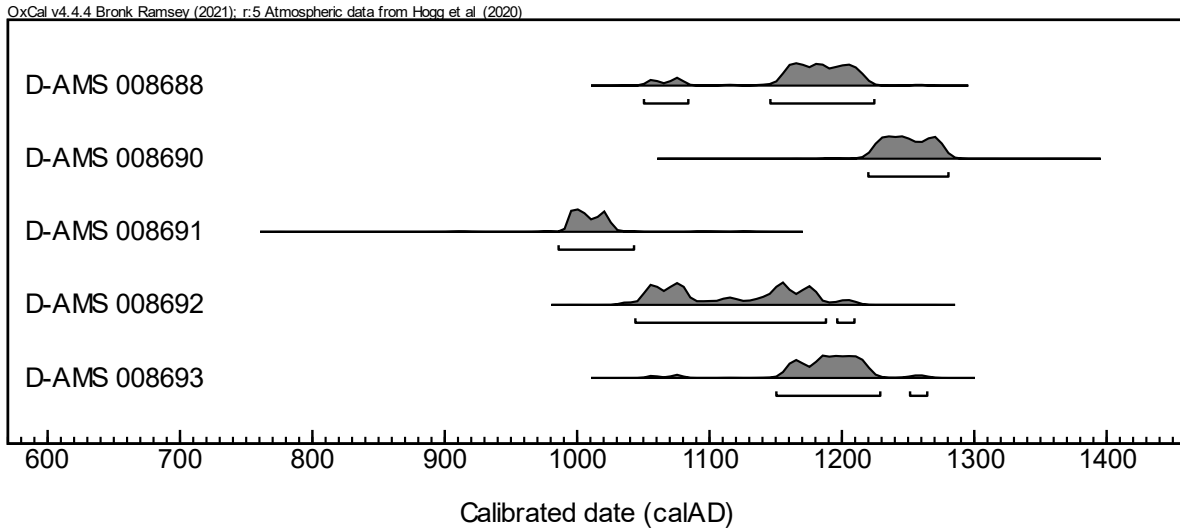


Figure 2.3. Radiocarbon dates from MNR04. Results are calibrated to the southern hemisphere calibration curve (Hogg et al. 2020) using OxCal v4.4.4 (Bronk Ramsey 2021). Uncalibrated dates from Lippert (2020).

2.5.2 Frampton I (MNR 74)

One of five small settlements on the farm Frampton, two of which were excavated in 2013 as MNR 74 and MNR 78 respectively, dotted along a low dolerite ridge in the Maremani Nature Reserve (Antonites & Ashley, 2016). Located 110km south-east of Mapungubwe Hill in the Mopane veld, the sites of the Frampton cluster would have probably consisted of no more than three to five huts each. Recent in field observations suggest evidence of ephemeral stock kraals but without significant buildup of dung and material as found in between the clusters on the western end of spur (Antonites *pers. comm* 2023)

The excavations comprised of five 2x2m units and three 1x1m test trenches. The deposits were comprised of one layer of cultural material \pm 5 – 10 cm thick suggesting a single, short lived

(Table 2.2), occupational component containing Mapungubwe type ceramics. Fine grey soil in the centre of the site indicates the presence of a small stock pen (Antonites & Ashley, 2016: 478).

Results of the faunal analysis indicate a predominately domesticate based subsistence economy while hunting, and trapping also played a part. Observations made on livestock tooth wear indicate that individuals were slaughtered after having reached sexual maturity as a potential strategy for maximising meat and dairy yields. The identification of *Rattus rattus* along with the presence of glass beads confirm that MNR 74 had some articulation to Indian ocean trade network. (Antonites, Uys & Antonites, 2016).

Table 2.2. Radiocarbon dates from MNR74. Results are calibrated to the southern hemisphere calibration curve (Hogg *et al.* 2020) and modelled using OxCal v4.4.4 (Bronk Ramsey 2021). Uncalibrated dates from Antonites & Ashley (2016).

Laboratory number	Uncalibrated age BP	95.4% Probability (cal. AD)
D-AMS-4206	837 ± 35	1185 - 1283
D-AMS-4205	729 ± 31	1275 - 1389
Combined date		1226 - 1298

Two charcoal samples excavated from the same midden context provided dates of 837 ± 35 BP (D-AMS-4206), and 729 ± 31 BP (D-AMS-4205) (Antonites & Ashley, 2016: 478). Calibrated using OxCal v4.4.4 (Bronk Ramsey 2021) along the updated southern hemisphere curve (Hogg *et al.* 2020), a combined modelled date of AD 1226 – 1298 is provided for the site (Figure 2.4).

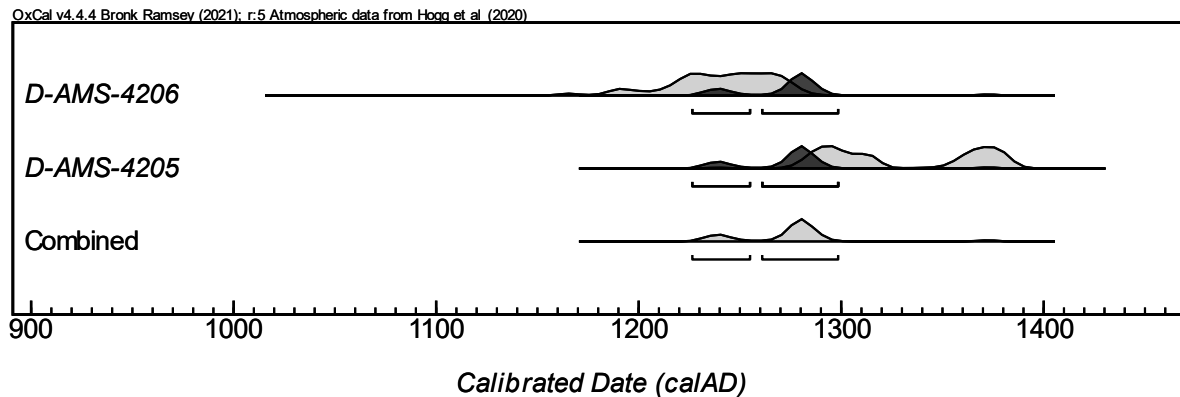


Figure 2.4. Radiocarbon dates from MNR74. Results are calibrated to the southern hemisphere calibration curve (Hogg et al. 2020) and modelled using OxCal v4.4.4 (Bronk Ramsey 2021).

2.5.3 Frampton II (MNR78)

The second site in the Frampton cluster (MNR78) is similarly located on the south-western slope of a small rocky hill. MNR78 is slightly larger than the neighbouring Frampton site and features low uncoursed stone walling which directs access to the site. Excavations confirmed the stone wall to be contemporaneous with a hut floor representing the 13th century occupation layer. A high proportion of non-utilitarian iron (n=6) and cuprous (n=24) metal fragments were recovered, along with glass beads as well as a high number of spindle whorls (n=18) (Antonites & Ashley, 2016: 480), suggesting that a healthy craft economy existed for the members of this community.

MNR78 was dated by means of a charcoal sample (D-AMS 008695) extracted from a midden as well as charred material (D-AMS 008694) that was associated with a hut floor (Lippert, 2020: 62). Raw dates (Antonites & Ashley 2016) were recalibrated using OxCal v4.4.4 (Bronk Ramsey 2021) along the updated southern hemisphere curve (Hogg *et. al.* 2020), the 95% probability dates provided for MNR78 fall within the 13th century from AD 1212 – 1298.

Table 2.3. Radiocarbon dates from MNR78. Results are calibrated to the southern hemisphere calibration curve (Hogg *et al.* 2020) using OxCal v4.4.4 (Bronk Ramsey 2021). Uncalibrated dates from Antonites & Ashley (2016).

Laboratory number	Uncalibrated age BP	95.4% Probability (cal. AD)
D-AMS 008694	785 ± 28	1222 – 1298
D-AMS 008695	835 ± 24	1212 – 1280

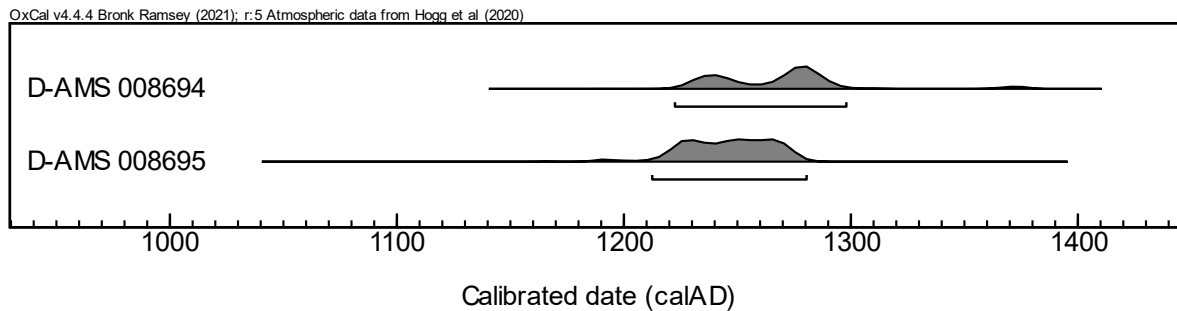


Figure 2.5. Radiocarbon dates from MNR78. Results are calibrated to the southern hemisphere calibration curve (Hogg *et al.* 2020) using OxCal v4.4.4 (Bronk Ramsey 2021).

2.5.4 Mutamba

The site of Mutamba is located in the northern foothills of the Soutpansberg mountains on the saddle of a long sandstone ridge which the Mutamba river bounds on the southern side (Loubser, 1991: 245). Mutamba is one of three in a cluster of Middle Iron Age sites. The nearby site known as Princess Hill has the spatial hallmarks of elite settlement with a residential zone located on a hilltop and the kraal around the base. Mutamba and Vhunyela share similar spatial layouts that resemble the central cattle pattern (Antonites, 2019b: 106). All three sites share a common material culture with ceramics typical of the Mapungubwe civilization demonstrating their links to the capital 80km north-east in the Shashe-Limpopo Confluence Area.

Intensive excavations during 2010 and 2011 (Antonites, 2012) shed light on the role that Mutamba, a relatively small (1.2 ha) site, played in the greater Mapungubwe political landscape. The recovery of iron, gold, and copper objects, accompanied by glass beads and marine shells during excavations (Antonites, 2019a), coupled with the evidence of intensified fiber spinning comes from the ubiquity of spindle whorls (n=187) found around domestic contexts at the site (Antonites, 2019b), indicate that residents at Mutamba were sufficiently agentive in its position to leverage consumption of elite objects.

A total of ten charcoal samples from three features of the site were submitted for dating. features 1 and 2 were domestic hut contexts while feature 3 represents an area in the centre of the site associated with burnt cattle dung (Antonites, 2019a). Raw dates were recalibrated using OxCal v4.4.4 (Bronk Ramsey 2021) along the updated southern hemisphere curve (Hogg *et. al.* 2020) and are summarized in Table 2.4 and plotted in Figure 2.6

Table 2.4. Radiocarbon dates from Mutamba. Results are calibrated to the southern hemisphere calibration curve (Hogg et al. 2020) using OxCal v4.4.4 (Bronk Ramsey 2021). Uncalibrated dates from Antonites (2012).

Laboratory number	Uncalibrated age BP	95.4% Probability (cal. AD)
AA-96452	692 ± 35	1286 – 1395
AA-96451	834 ± 35	1275 – 1389
AA-96455	862 ± 35	1160 – 1276
AA-96456	692 ± 35	1286 – 1395
AA-96457	803 ± 35	1212 – 1297
AA-96458	842 ± 35	1183 – 1282
AA-96454	832 ± 38	1184 – 1285
AA-96453	960 ± 35	1030 – 1210
AA-96459	955 ± 35	1033 – 1210
AA-96460	873 ± 35	1155 – 1275

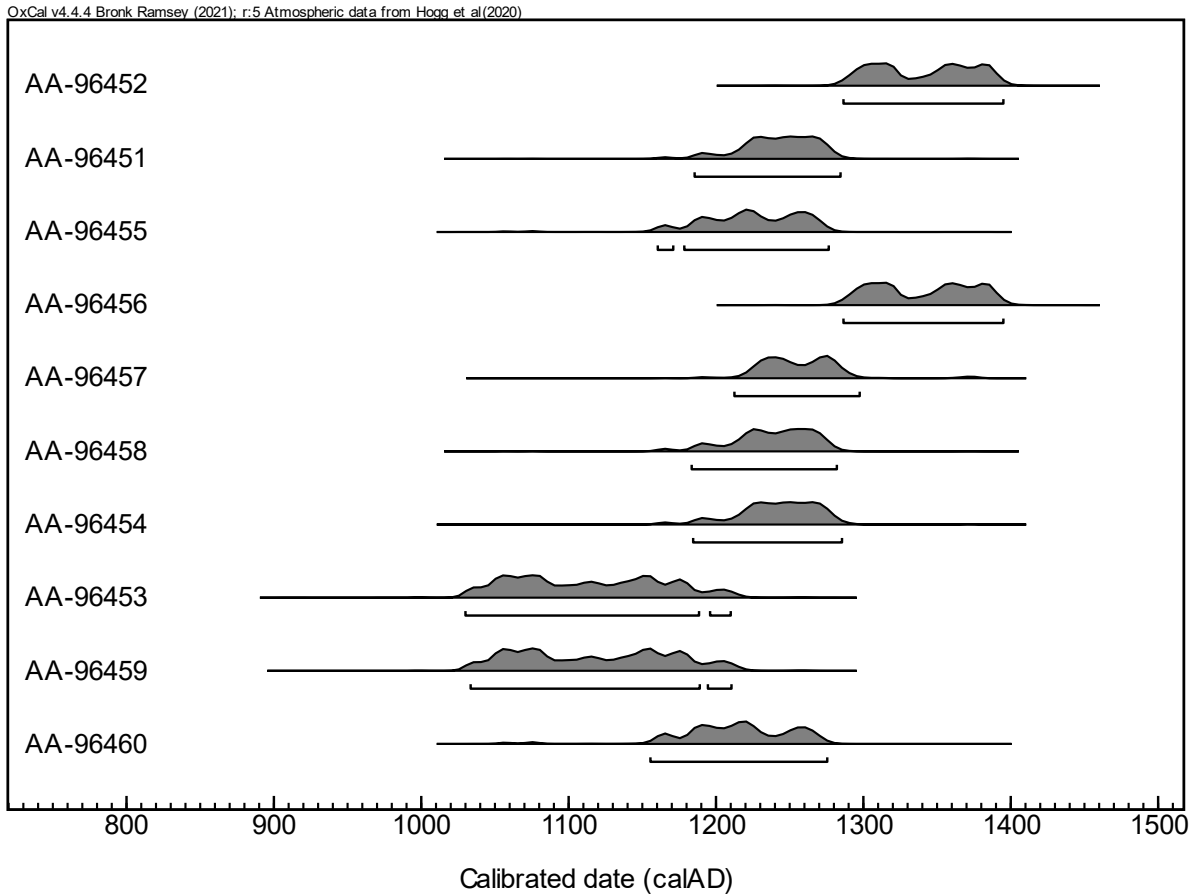


Figure 2.6. Calibrated radiocarbon dates from Mutamba. Results are calibrated to the southern hemisphere calibration curve (Hogg et al. 2020) using OxCal v4.4.4 (Bronk Ramsey 2021). Uncalibrated dates from Antonites (2012).

2.5.5 Stayt

Stayt is located on a sandstone spur 30km south-west of the town Tshipise. The site is about 160m long and 50m across and would have had a perennial water source from a spring located to the south. The site was settled at least twice over the last millennium and is accordingly divided into two sections. Section 1 is associated with Late Iron Age stone walling which represent an

unrelated occupation phase post-dating Section 2 where Mapungubwe type material culture was excavated in relatively shallow (0.5m) deposits (Prinsloo & Coetzee, 2001: 83).

Stayt was occupied during the warm and wet ‘medieval warm epoch’ (Huffman, 1996; Prinsloo & Coetzee, 2001). This would broadly suggest that favourable conditions for agropastoral settlement prevailed during the Middle Iron Age occupation at Stayt.

Comparisons between Voigt’s 1983 faunal study of Mapungubwe and K2 and the faunal report from Stayt (Plug 1989) indicate that considerably more animals were hunted and snared at Stayt than at Mapungubwe (Prinsloo & Coetzee 2001:87). This pattern may be explained by the access to large cattle herds at Toutswemogala enjoyed by the elite at Mapungubwe Hill (Hall 1987:8). This access was not available to the residents at Stayt and thus it is assumed that wild animals were hunted and snared in order to supplement their diet (Prinsloo and Coetzee 2001:87).

Table 2.5. Radiocarbon dates from Stayt (KON). Results are calibrated to the southern hemisphere calibration curve (Hogg et al. 2020) using OxCal v4.4.4 (Bronk Ramsey 2021). Uncalibrated dates from Prinsloo & Coetzee (2001).

Laboratory number	Uncalibrated age BP	95.4% Probability (cal. AD)
Pta-4363	820 ± 50	1158 – 1300
Pta-4328	910 ± 50	1045 – 1270

Newly calibrated radiocarbon dates from a piece of charcoal and bone respectively (based on the raw figures reported in Prinsloo & Coetzee 2001) indicate that Section 2 at Stayt was occupied between AD 1045 – 1270 (Pta-4328) and AD 1158 – 1300 (Pta-4363).

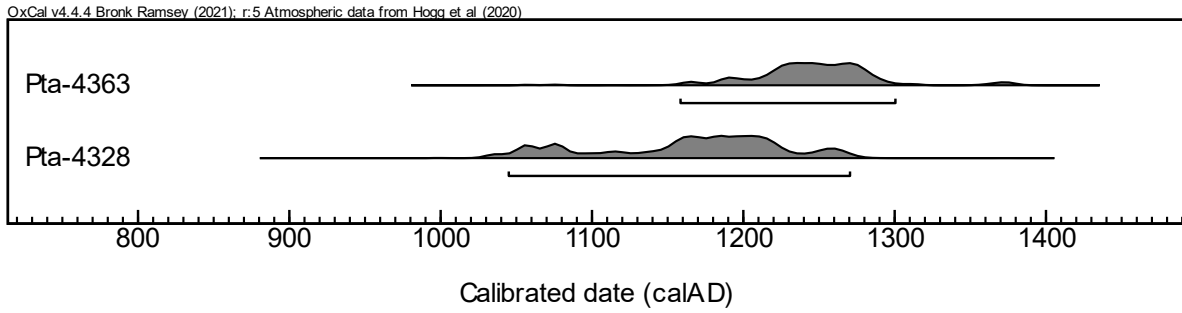


Figure 2.7. Calibrated radiocarbon dates from Stayt (KON). Results are calibrated to the southern hemisphere calibration curve (Hogg et al. 2020) using OxCal v4.4.4 (Bronk Ramsey 2021). Uncalibrated dates from Prinsloo & Coetzee (2001).

Chapter 3 **Background to Stable Isotopes**

This chapter serves to provide a background to stable isotope systems followed by an overview focusing on how carbon and oxygen isotopes pattern themselves throughout the environment in ways that can be meaningful to archaeologists.

3.1 Principles of Stable Isotope Analysis

An isotope of a given element has the same chemical properties (i.e., number of protons) but differs slightly in mass due to variations in the number of neutrons in the atom (Sharp, 2017: 2–1). The ratio of protons to neutrons determines the stability of a given isotope, if this is within a balanced range for a given element the isotope does not undergo radioactive decay and is consequently considered stable.

The ratio (R) of stable isotopes that have more neutrons (heavy) to those with fewer neutrons (light) is standardised according to an international element-specific expression known as delta notation (δ), with units measured in per mille (‰) derived from the formula (Coplen, 2011):

$$\delta = (R \text{ sample}) / (R \text{ standard}) - 1$$

The slight differences in mass between isotopes of an element foster a process known as isotopic fractionation, where reactions between elements in the environment predictably discriminate between lighter or heavier isotopes. Isotopic abundances are therefore patterned accordingly as elements flow through and are exchanged in the various physical and chemical processes that comprise our living world.

Fractionation systematically shapes isotopic abundances through various isotope effects as elements pass through different environmental and physiological processes, allowing for discrete food web systems to be quantified based on their isotopic signatures (O’Leary, 1981; Van der Merwe, 1982). The type of tissue sampled for isotopic analysis also has influence and limitation on the type of information able to be extracted from the analysis. Skeletal tissues undergo a life-long molecular remodelling process which results in an isotopic average of diet over several years, depending on the skeletal element sampled (Gerling et al., 2017: 4). Tooth enamel, however, provides an exception to this as it is biologically inert meaning that once mineralized the enamel does not remodel throughout the individual’s life (Pederzani & Britton, 2019: 82).

This provides researchers a boon in the form of being able to extract an isotopic snapshot, frozen in biogenic hydroxylapatite, of dietary and environmental inputs available at the time of tooth formation. (Fricke & O’Neil, 1996; Lee-Thorp, 2002; Balasse et al., 2003; Towers et al., 2014).

Understanding the systems relevant to the patterning of isotopic abundances across different ecological zones forms an empirical basis from which comparisons in the diet and environment of consumers across time and space are possible. The preservation of certain elements such as carbon and oxygen in tooth enamel are of particular use in making such dietary and environmental inferences, however an understanding of how the isotopes of these elements circulate in the biosphere is important to understand. These systems are briefly described below.

3.1.1 Carbon

Three naturally occurring isotopes of carbon are to be found in the environment, the most abundant being the two stable isotopes of carbon, namely ^{12}C and ^{13}C , while the third, ^{14}C , exists in very small quantities and undergoes radioactive decay (Van der Merwe, 1982).

The highest degree of fractionation in the carbon cycle takes place during photosynthesis in plants, which varies further depending on the photosynthetic pathway used by the plant when fixing CO_2 from the atmosphere (Cerling & Harris, 1999; House, 2021: 91). Three pathways of CO_2 metabolization have been identified in plants, known as C_3 , C_4 , and CAM photosynthesis, respectively.

A result of these varied pathways is that the $\delta^{13}\text{C}$ values in a given ecosystem will vary depending on whether the dominant plant species uses either the C_3 or C_4 photosynthetic pathway. Dicotyledonous plants such as trees and shrubs typically utilise the C_3 photosynthetic pathway which discriminates more against ^{13}C and results in a lower $\delta^{13}\text{C}$ values of between -20 to -37‰ (global mean -27.1 ± 1.6 ‰). Tropical *Kranz* grasses typically utilise the C_4 photosynthetic pathway which is more efficient in fixing CO_2 resulting in higher, or less negative, $\delta^{13}\text{C}$ values of between -9 to -17‰ (global mean -12.5 ± 1.1 ‰) (Ellis, Vogel & Fuls, 1980; Coutu et al., 2016: 420; Loftus, Roberts & Lee-Thorp, 2016: 3).

These distinct isotopic signatures are carried through as carbon moves up the trophic levels through consumption and have been demonstrated to reflect the proportions of graze and browse in ungulate diet (Vogel, 1978) within a region dominated by C_4 grasses. Through the analysis of $\delta^{13}\text{C}$ values from ungulate bone collagen (Vogel, 1978) demonstrated that because more than

90% of grasses in the summer rainfall region of South Africa use the C₄ pathway, the difference in δ¹³C values between C₃ and C₄ plants allows for the determination of grazing and browsing animals in this region (Vogel, 1978: 298). Therefore, the expectation is that herbivores that are predominantly browsers will mostly consume C₃ plants, and as a result will have higher δ¹³C values than grazers that preferentially subsist on C₄ plant species.

Expected ranges for the δ¹³C values of 100% grazing and browsing species have been derived through quantifying the fractionation that takes place in the movement of ¹³C from plant matter to tooth enamel (Cerling & Harris, 1999). Based on the analysis of animals with observed or known life-histories, and factoring in the plant-bioapatite spacing of ~-12.0 – ~-14.0‰, a range of ~-0.8 – 1.2‰ for pure grazing and ~-14.8 – ~-12.8‰ for pure browsing species has been suggested for modern herbivores in the region between the Soutpansberg and the Shashe-Limpopo confluence (Smith, 2005: 108). Accounting for the ~1.5‰ enrichment of ¹³C due to the burning of fossil fuels since the industrial revolution (the fossil fuel effect) expected ranges for archaeological herbivores are ~1.0‰ for pure grazers and ~-12.3‰ for pure browsers. (Smith, 2005: 131).

In a mixed C₃/C₄ biome such as the Mopane veld of the study area, seasonal dietary patterns are expected to be visible in the δ¹³C values of serial sampled tooth enamel as the availability of C₄ grasses reduces in the dry winter months. This provides an environmental snapshot of the early stages of an individual's life as the teeth mineralise. For bulk grazing animals, such as cattle, higher ranges in δ¹³C values indicate more browse incorporation into the diet (House, 2021: 148), as may be expected in winter when grasses are more scarce. Individuals that display either low variation or overall elevated δ¹³C values throughout the length of the tooth may therefore

suggest that other sources of grazing might have been provided through the lean months by the herders in attendance of the livestock (Balasse et al., 2012; Makarewicz, 2014). Local ethnographic observations of foddering practices such as allowing cattle to graze the stalks of harvested crops (Smith, 2005: 63) or, as has been documented among Cypriot pastoralists, the silage of plants such as *Amaranth sp.* for use during the lean months (Spyrou et al., 2023).

3.1.2 Oxygen

Oxygen has three stable isotopes ^{16}O , ^{17}O , and ^{18}O that occur throughout the universe in different abundances. The isotopes ^{16}O and ^{18}O are the most abundant of the three, together accounting for the majority of oxygen atoms (99.757 % and 0.205 % respectively) and are thus the most commonly measured pair of the element in isotope ratio mass spectrometry (Wright, 2017).

The oxygen isotopic ratio of meteoric water varies systematically in accordance with several environmental, geographic and seasonal effects, such as atmospheric temperature, distance from the ocean, latitude, elevation, and time of year (Rozanski, Araguás-Araguás & Gonfiantini, 2013; Wright, 2017) all of which influences the variation in $\delta^{18}\text{O}$ values of water throughout the year.

In the mid-latitude arid summer rainfall region of north-eastern South Africa, the two key drivers in shaping oxygen isotope abundances are the broader seasonal effect and the effects that variations in local precipitation, evaporation and temperature have on the water available to plants and animals (Smith, 2005: 117; House, 2021: 103). The seasonal effect has that more positive $\delta^{18}\text{O}$ values are recorded in the warmest months with the inverse being true in colder

months (Balasse et al., 2002; Rozanski, Araguás-Araguás & Gonfiantini, 2013), however the annual climatic conditions, and prevailing seasonal rainfall regime of a given region also has bearing on how ^{18}O is distributed in water. The sites that form the basis of this research are located in the arid summer rainfall zone of South Africa – a region which features cooler, dry winters and warmer, wetter summers. Work on modern faunal reference sets has demonstrated the seasonal variations of $\delta^{18}\text{O}$ values in herbivores from the Limpopo province display more positive $\delta^{18}\text{O}$ values in winter and lower values in the wetter summer months (Smith, 2005: 128). This pattern possibly point to a pronounced effect of evaporation combined with local weather systems as regional drivers for the seasonal enrichment/depletion of ^{18}O (Smith, 2005: 119).

Animals derive their oxygen from three input sources namely, respiration (atmospheric O_2), drinking water, and water contained in the food consumed (food water). It is in the last two of these inputs where the annual variability of $\delta^{18}\text{O}$ values is highest and therefore is of most use as a proxy for understanding a given environment.

A systematic variation in the $\delta^{18}\text{O}$ values of modern herbivores has been observed from individuals ranging from the cooler southern slopes of the Soutpansberg and the hotter, drier regions north of the Soutpansberg mountains (Smith, 2005). Key drivers postulated this patterning are the more arid conditions experienced in the north providing conducive conditions for the evaporative depletion of H_2^{16}O from standing water. Further, the manner in which a region receives its precipitation will also determine the degree to which the $\delta^{18}\text{O}$ values reflect the enrichment of H_2^{18}O . The region in which the sites analysed for this research would mostly have received the bulk of their rainfall in the form of short-term, high discharge thundershowers – weather systems that typically have water depleted in H_2^{18}O (Smith 2005:117). Considerations

around potential water sources are important when interpreting $\delta^{18}\text{O}$ values along patterns that seek to determine the seasonal variations in serial sampled teeth (Janzen, 2015: 148).

The $\delta^{18}\text{O}$ values of the precipitate minerals in tooth enamel is determined by the isotopic composition of water ingested through food or drinking and thus has the potential to act as a proxy for detecting sub-annual, or seasonal, variations in local temperature and water availability as the tooth mineralises (Loftus, Roberts & Lee-Thorp, 2016: 5). Comparisons between the ranges of variation in $\delta^{18}\text{O}$ values from mandibular and maxillary molars of sheep revealed that significant differences in oxygen isotope composition exist between animals depending on their physiology and drinking behaviour (Makarewicz, 2017a: 152).

Controlled studies have been performed in order to assess the isotopic effect of ingested water on the $\delta^{18}\text{O}$ ratios of tooth enamel (Fricke & O'Neil, 1996; Fricke, Clyde & O'Neil, 1998). Low amount of variation in the intra-tooth $\delta^{18}\text{O}$ of cattle that were provided with a controlled water source demonstrates that the $\delta^{18}\text{O}$ value of tooth enamel is representative of the oxygen isotope composition of ingested water (Fricke, Clyde & O'Neil, 1998).

Further variation is introduced to the oxygen isotope composition of tooth enamel through the mechanism by which a species ingests its water. The $\delta^{18}\text{O}$ values in tooth enamel from obligate drinking species such as cattle will be more closely associated with variations in ^{18}O of seasonal meteoric water. Non-obligate drinkers, such as goats, derive their corporeal water from ^{18}O enriched leaf water which has undergone an additional fractionation step during photosynthesis which results in their $\delta^{18}\text{O}$ values being generally higher (Sponheimer & Lee-Thorp, 1999).

It was previously believed that the first molars of cattle and sheep form *in-utero* and therefore their $\delta^{18}\text{O}$ values are not representative of local water sources as these teeth would mineralize using oxygen derived from the mother's body water which has already undergone fractionation (Fricke & O'Neil, 1996: 94). A result of this effect was purportedly that the M1 $\delta^{18}\text{O}$ values would be elevated compared to teeth formed post weaning weaned (Fricke & O'Neil, 1996). However, research on seven wild ungulate species in southwestern Africa (Luyt & Sealy, 2018) revealed that M1s were not enriched relative to the rest of the toothrow. That there are no systematic relationships in the patterning of inter-tooth $\delta^{18}\text{O}$ values may in part be because the mother's water still tracks the natural variations in ^{18}O , therefore large scale enrichment or depletion events (i.e., summer and winter) will still be passed on to the offspring (Luyt & Sealy, 2018: 151).

The multiple processes that influence the way in which oxygen isotopes are distributed through both environmental and biological stages introduce a level of complexity when attempting to interpret $\delta^{18}\text{O}$ values. Despite these challenges, sequential $\delta^{18}\text{O}$ values are still broadly indicative of seasonal changes in the study region and, when paired with $\delta^{13}\text{C}$ values, may provide insights into the relationship between diet and environment.

3.2 Tooth Eruption and Enamel Mineralization

Given that tooth enamel, if sampled appropriately, represents a time-sensitive record of isotopic abundances during the period of tooth mineralisation, it is necessary to understand the timing of the mineralization process and tooth eruption events in order for meaningful patterns to be discerned. Research into the dynamics of tooth growth has sought to clarify the way in which

elements are incorporated into tooth enamel and what implications this may have for interpreting the stable isotope values measured from teeth (Trayler & Kohn, 2017; Luyt & Sealy, 2018).

Isotopic analysis of tooth enamel has become a useful technique in assessments of animal diet and environment (Lee-Thorp & Van der Merwe, 1987; Fricke & O'Neil, 1996; Cerling, Harris & Passey, 2003; Copeland et al., 2009; Hare & Sealy, 2013; Luyt, Hare & Sealy, 2019). The process of tooth enamel formation occurs progressively from the root to tip and does not undergo further remodelling during its lifetime (Balasse et al., 2012; De Winter, Snoeck & Claeys, 2016). This provides an advantage in the use of tooth enamel when attempting to understand dietary and environmental aspects of an individual's life on a sub-annual scale. A further advantage, especially to archaeological teeth, is that the bioapatite in enamel is not susceptible to diagenetic alteration over time thus providing a reliable record of diet and environment at the time of mineralisation (Cerling & Harris, 1999).

This record can be recreated isotopically if the correct sampling procedures are used on the teeth. A key component to the analysis of stable isotope measurements from sequentially sampled tooth enamel is an understanding of how the mineral enamel is formed and matures.

Biological apatite, or bioapatite, is the mineral component of mammalian skeletal tissue presenting in a hexagonal calcium phosphate crystal form (Lee-Thorp, 2002). Small amounts of bioapatite are present in all bones; however, these are susceptible to distortion and substitution as the bone tissue remodels over time. Enamel bioapatite undergoes a once-off formation process that takes place in the early-life stages of an individual, producing larger and more stable crystals (Lee-Thorp, 2002: 437).

After formation, tooth enamel undergoes multiple discontinuous stages of maturation. Work conducted by Trayler and Kohn on enamel maturation in ungulate tooth enamel showed that tooth enamel does not mature at the same rate through the thickness of the tooth (Trayler & Kohn, 2017). Their research suggests that the central and inner areas of tooth enamel reach maturation before the outer layer. The implications of this research for time-resolved inferences from serially sampled enamel is that the isotopic profiles of teeth represent a dampened record of environment and diet (Trayler & Kohn, 2017: 32).

It is important to note that the process of enamel mineralization and tooth eruption do not have a direct developmental relationship as the former continues for some time after eruption and can be delayed by up to several months (Janzen, 2015: 136). While this does not preclude seasonal signals being observed in the isotopic record of serially sampled tooth enamel, care must be taken when interpreting the results.

Tooth mineralisation and eruption take place in a sequence which varies among different species. In cattle, the first molars (M1) begin mineralising *in utero* about 3 – 4 months before birth and mature at about 2-3 months. The second molar (M2) begins formation at 1 month and is completed after 12 – 13 months. The third molar (M3) begins mineralizing at 9 – 10 months and reaches maturity 24 months after birth (Towers et al., 2014: 210).

In caprines the chronology of tooth eruption commences with the first molars (M1) beginning mineralising *in utero*, about a month before birth, erupting at 3 months and are mature at about 6 – 9 months. M2 crown formation begins at 1 – 3 months and reaches completion at around 12 –

17 months. The M3 begins formation at 9 – 10 months after birth and is complete by 22 – 31 months (Janzen, 2015: 138).

3.3 Applications of Stable isotopes on Tooth Enamel

Sequentially sampled tooth enamel has found wide application in addressing archaeological questions around the annual rhythms of diet and mobility. There has been significant development of the field since its inception over 40 years ago with Nikolaas van der Merwe's pioneering study on human burials from the Phalaborwa region (Loftus, Roberts & Lee-Thorp, 2016). The growth of stable isotope based inferences into archaeological lifeways saw several analytical tropes emerge (for a review see Ventresca Miller & Makarewicz, 2017) as researchers began to clarify and refine the isotopic record and how it may be better interpreted.

Among the various avenues open to stable isotope research, specific questions regarding the nature of human-animal relations in pastoral societies has been a theme that has gained much traction (Balasse et al., 2002; Smith, 2005; Blaise & Balasse, 2011; Janzen, 2015; Balasse et al., 2017; Makarewicz, 2017b; Makarewicz & Pederzani, 2017; Pilaar Birch et al., 2019; House, 2021; Spyrou et al., 2023). The following section provides a brief review of some of the approaches to pastoral management practices.

A major aspect of animal husbandry is ensuring that the dietary requirements of the livestock are adequately met throughout the year. Consequently transhumance - on the seasonal movement of livestock between pastures to maintain their diet - is a common practice among pastoralists world-wide (e.g. Makarewicz, 2017; Makarewicz & Pederzani, 2017; Janzen, Balasse & Ambrose, 2020) . Another common strategy is the provisioning of fodder for animals during

winter through either the storage of feed gathered in summer (Spyrou et al., 2023) or allowing animals to forage among the harvested stalks of agricultural crops (Smith, 2005; Gillis et al., 2021: 16). Both of these management strategies are potentially isotopically visible if time-resolved sampling methods are used in conjunction with an understanding of the environmental and physiological parameters of the sampled individual.

In order to test the seasonal mobility pattern between coastal and inland pastures of Khoekhoe pastoralists in southern Africa (Balasse et al., 2002), a combination of carbon and strontium isotopes were analysed from domesticated and wild archaeological specimens. By using the range of variation in the sequential $\delta^{13}\text{C}$ values from the teeth of wild species the authors were able to determine a seasonal range for the local vegetation. The comparatively higher $\delta^{13}\text{C}$ ranges seen in domesticates suggested that domesticates were not foraging within the same areas as their wild counterparts.

Seasonal husbandry practices that seek to sustain year-round supply of animal products may also require levels of community cooperation, as has been inferred for the Late Neolithic Balkan Vinča culture communities (Gillis et al., 2021). By examining the range of intra-tooth carbon isotope change, the authors were able to differentiate between the diets of cattle and caprine. The tracking of $\delta^{13}\text{C}$ and $\delta^{18}\text{O}$ profiles when plotted along the length of the tooth suggests that the caprines analysed in this research were consuming food sources that varied considerably with the seasons (Gillis et al., 2021: 13). In addition, the caprines sample also had less inter-individual variability than cattle, leading the authors to suggest that the two livestock groups were herded using differing strategies (Gillis et al., 2021: 15). The lower variability among the caprines analysed suggests that the pooling of communal resources such as leaf-hay while the lack of such

patterning among cattle indicate that they were perhaps maintained at a household level (Gillis et al., 2021: 17). The result of this research provides major insight into the complexity of animal husbandry and the role it plays in society.

Winter foddering practices engaged in by pastoralists have also been inferred through the comparison of $\delta^{13}\text{C}$ values from wild and domesticated caprines in the northern Gobi steppe-desert (Makarewicz & Pederzani, 2017). The analysis found that domesticated caprines displayed high $\delta^{13}\text{C}$ values throughout the year as opposed to the wild specimens which had more variable $\delta^{13}\text{C}$ values recorded across the teeth. The domesticated caprines also displayed a larger intra-tooth range in $\delta^{18}\text{O}$ values than the wild caprines (Makarewicz & Pederzani, 2017: 1) which further support these data representing pastoral management practices.

The authors conclude that wild caprines displayed a relatively homogeneous seasonal drinking and feeding behaviour when compared to domesticated caprines that show clear signs of human intervention (Makarewicz & Pederzani, 2017: 26). Determining the exact form of intervention or strategy employed is however a more complex task. Due to differing strategies employed by herders in various responses to the needs of the livestock the drivers of the variation in $\delta^{18}\text{O}$ values for domesticated caprines is difficult to tease apart as these values reflect inputs from differing sources of water throughout the year (*ibid*).

Stable isotope analysis has also been used to elucidate animal husbandry strategies used by pastoralists, particularly as it relates to the management of birthing seasons through the year (Tornero et al., 2016). Work conducted by Blaise and Balasse on Neolithic sheep from south-

eastern France presents a methodology for determining birth seasonality using reference data from modern individuals (Blaise & Balasse, 2011).

The results of the analysis of sequentially sampled $\delta^{18}\text{O}$ values from the modern sheep with known life-histories confirmed that this technique allows for the distinction of individuals born in different seasons (Blaise & Balasse, 2011: 3091). It was found that the profile of $\delta^{18}\text{O}$ values along the length of the tooth differed in trajectory between sheep born in autumn to those born in winter (Blaise & Balasse, 2011: 3088). An important insight gained for incorporating a modern reference population is that enamel maturation in sheep may take up to 6 months as indicated by the pattern of variation between teeth $\delta^{18}\text{O}$ values.

From the above, it is clear that decisions made by pastoral herders may be evident in the isotopic patterns crystallised in animal teeth. The challenge to researchers is thus to distinguish environmental and other natural drivers of isotopic distribution from patterns that result from human intervention. This understanding is incrementally being built upon by the refinements of continued research in the field of stable isotope analysis.

Chapter 4 Materials and Methods

Stable isotope analysis in archaeology has by now a strong tradition in the assessment of the diet and mobility of pastoral livestock herds with the scope of studies ranging in scale and resolution (Balasse et al., 2002; Smith, Lee-Thorp & Hall, 2007; Smith et al., 2010; Janzen, 2015; Loftus, Roberts & Lee-Thorp, 2016; Ventresca Miller & Makarewicz, 2017; House, 2021).

In order to better understand the local environment a high-resolution method of stable isotope analysis involving the serial sampling of the mineral phase of tooth enamel, or biological apatite (hereafter bioapatite), was selected. This method is optimised for the broad determination of seasonal rhythms and characterisation of intra-annual dietary inputs. This chapter describes the sampling and analytic procedures involved in in this research.

4.1 Sample Preparation and Pretreatment

This research is based on the isotopic analyses of selected samples from existing collections housed in the University of Pretoria's Archaeology collections. All sites included in this research were excavated by members of the from the University of Pretoria Department of A&A between 1985 and 2013. Identification of both domestics and wild species for the sample sites were done archaeozoologists who worked in each collection: I. Plug (KON), AR Antonites (MNR74) and K. Scott, E. Grody and C. Abattino (Mutamba).

Where possible, sampling was standardised to select the same tooth from the same side of the mouth (e.g., right second upper molar) in order to differentiate individual animals within a given site. Where this was not possible, contextual evaluation of sample provenience, taphonomy, age

and wear patterns, as well as the integrity of the tooth enamel became the determining factors in selection. Teeth that were worn, cracked, or had stained patches on them were avoided to ensure as consistent enamel integrity and length of isotopic record as possible across the samples. The profiles for each sampled individual by site are provided in Appendix A.

The teeth of 12 cattle (*Bos taurus*) and 17 caprines (*Ovis aries*, *Capra hircus* & *Ovis/Capra*) were selected from the faunal assemblages of the five Middle Iron Age sites in this study (Table 4.1).

Table 4.1 Number of domesticates sampled from each site.

Site	Cattle	Caprines
Mutamba	4	5
MNR78	1	1
MNR74	2	3
MNR04	1	4
Stayt (KON)	4	4
Total	12	17

A selection of teeth (n=7) of 6 browsing and grazing wild animal species were additionally sampled (Table 4.2) for comparative isotope values of local grazer and browser diets against which it is possible to assess the values from domesticates(Makarewicz & Pederzani, 2017). The wild samples were sourced from the same archaeological collections as the domesticate samples. *Aepyceros melampus* (Impala) served as a mixed feeder signature for Mutamba and Stayt, the grazers sample were *Alcelaphus buselaphus* (Hartebeest) for Mutamba and equid from MNR04. *Pelea capreolus* (Grey rhebok) were used as a browser from Mutamba.

Table 4.2. List of wild species and their respective dietary preference sampled from each site.

Site	Species	Number of Individuals	Diet
Mutamba	<i>Aepyceros melampus</i>	1	Mixed feeder
Mutamba	<i>Alcelaphus buselaphus</i>	2	Grazer
Mutamba	<i>Pelea capreolus</i>	1	Browser
MNR74	Equid	1	Grazer
Stayt (KON)	<i>Aepyceros melampus</i>	1	Mixed feeder
Total		6	

4.2 Sample preparation

Sample preparation took place at the Mammal Research Institute laboratory at the University of Pretoria. The selected teeth were first removed from their sockets (where present) and cleaned with a combination of dry brushing followed by ultrasonic bathing in ultra-purified water for 10 minutes followed by overnight drying at 70°C.

The cleaned teeth were then serially sampled using a handheld rotary drill set to low-medium speed to avoid heat damage to the bioapatite mineral phase. A 2mm diamond tipped burr was used to drill a series of \approx 2-3mm wide transverse lines along the growth axis of the tooth.



Figure 4.1. Example of a serially sampled B. taurus (MUT/2012/F09) tooth from the present study.

The resultant powder from each line of drilling was captured in a 2ml microcentrifuge tube in preparation for the pretreatment process. This method of serial sampling allows for a time-sensitive determination of isotopic signatures which are recorded in the enamel bioapatite at the time of tooth enamel mineralisation (Fricke, Clyde & O'Neil, 1998; Wiedemann et al., 1999; Gerling et al., 2017).

4.3 Sample Pre-treatment

Sample preparation and pretreatment followed the protocols outlined by Lee-Thorp (Lee-Thorp, Manning & Sponheimer, 1997). Pretreatment was applied to purify the enamel powder of diagenetic carbonates. The first step in this process involves neutralising the organic phase of the bioapatite sample. 1.0ml of 1.75% v/v of sodium hypochlorite (24% NaOCl:76% ultrapurified water) was introduced to the microcentrifuge tubes and allowed to steep for 45 minutes, with frequent agitation to ensure maximum saturation of the sample with the reagent. The tubes were then centrifuged for 5 minutes at 7500 RPM before the NaOCl solution was vacuum suctioned

out and the sample rinsed with ultrapurified water. The rinsing step was repeated three times, with runs in the centrifuge between each rinse ensuring minimal loss of sample material.

The samples were then introduced to 1ml of 0.1 molarity (M) acetic acid (CH_3COOH) for 15 minutes in order to remove exogenous minerals which may be present in the bioapatite sample. Koch et al. (1997) has shown that a 0.1M acetic acid solution causes minimal alteration to the bioapatite while an increase to 1M, with a steeping time exceeding 15 minutes, may result in the recrystallisation of exogenous minerals in the bioapatite. (Lee-Thorp, Manning & Sponheimer, 1997). Following the acid wash, samples were centrifuged, and the-acetic acid solution was vacuum suctioned out before being triple rinsed with ultrapurified water. In some samples this step led to a notable reduction in sample material (n=9). These instances mainly occurred when the sampled enamel powder had a yellowish tinge. The treated samples were stored in a chest freezer prior to freeze-drying.

4.4 Isotopic analysis

Aliquots of the purified enamel bioapatite samples were weighed to 0.8mg, when possible, while the internal standard GS-35 was weighed at 0.1mg per sample. Each weighed sample was placed in a borosilicate glass sample vial and sealed. The vials were placed in a GC PAL autosampler with the heating block set to 72°C. Each vial was then purged with helium removing any atmospheric CO_2 , in preparation for the reaction with 100% phosphoric acid (H_3PO_4) which produces CO_2 gas.

Once the sample has reacted the measurement of the resultant CO_2 gas takes place. Helium is used as a carrier gas that ushers the CO_2 through a network of ingenious valves and hair-like

glass capillaries housed inside a Finnigan II Gas Bench before being delivered to a Thermo Scientific Delta V-plus isotope-ratio mass spectrometer for measurement of carbon and oxygen isotopic composition. A series of technical (and global) challenges¹ arose during the course of the analysis which resulted in complications with some of the instrumentation.

Reproducibility and analytical precision were determined from 70 runs of the internal laboratory standard for enamel carbonates GS-35. These provided mean corrected $\delta^{13}\text{C}$ values of $1.18\text{‰} \pm 0.17\text{‰}$ (1σ) and mean corrected $\delta^{18}\text{O}$ values of $-2.96 \pm 0.24\text{‰}$ (1σ). Mean analytical precision within each run – measured from 7 to 10 samples of the GS-35 standard – varied between 0.03‰ to 0.06‰ for $\delta^{13}\text{C}$ and from 0.04‰ to 0.1‰ for $\delta^{18}\text{O}$.

¹ The Covid-19 pandemic and ensuing supply chain issues resulted in challenges to laboratory access as well as sourcing replacement components for the mass spectrometer.

Chapter 5 Results of Serial $\delta^{13}\text{C}$ and $\delta^{18}\text{O}$ Tooth Enamel

Analysis

This chapter presents the summarized results of all isotope samples (n=492) analysed across the teeth (n=52) of 35 individual animals from five 13th century Middle Iron Age sites. The first section presents the mean values a range for $\delta^{13}\text{C}$ and $\delta^{18}\text{O}$ ratios (derived from the minimum and maximum values) respectively for each sampled tooth in summary tables below. The complete data tables are located in Appendices B and C. Serial results plotted for individual cattle and caprines will be reported on separately for each site, followed by the results of the wild species recovered from all sites. Serial comparison graphs are plotted along the distance from the enamel-root junction (ERJ - reversed scale), allowing for a time resolved record of variation in $\delta^{13}\text{C}$ and $\delta^{18}\text{O}$ values over the period of tooth mineralisation (see Chapter 2).

5.1 Domesticate $\delta^{13}\text{C}$ and $\delta^{18}\text{O}$ Summary Results.

The mean $\delta^{13}\text{C}$ value across 211 drilled samples for all cattle sampled in this study (n=12) is $0.2 \pm 1.68\%$. The mean $\delta^{13}\text{C}$ value across 230 samples for all caprines sampled in this study (n=17) is $-5.1 \pm 2.14\%$.

The mean $\delta^{18}\text{O}$ value across 211 drilled samples for all cattle sampled in this study (n=12) is $-3.1 \pm 1.53\%$. The mean $\delta^{18}\text{O}$ value across 230 samples for all caprines sampled in this study (n=17) is $-3.1 \pm 1.82\%$

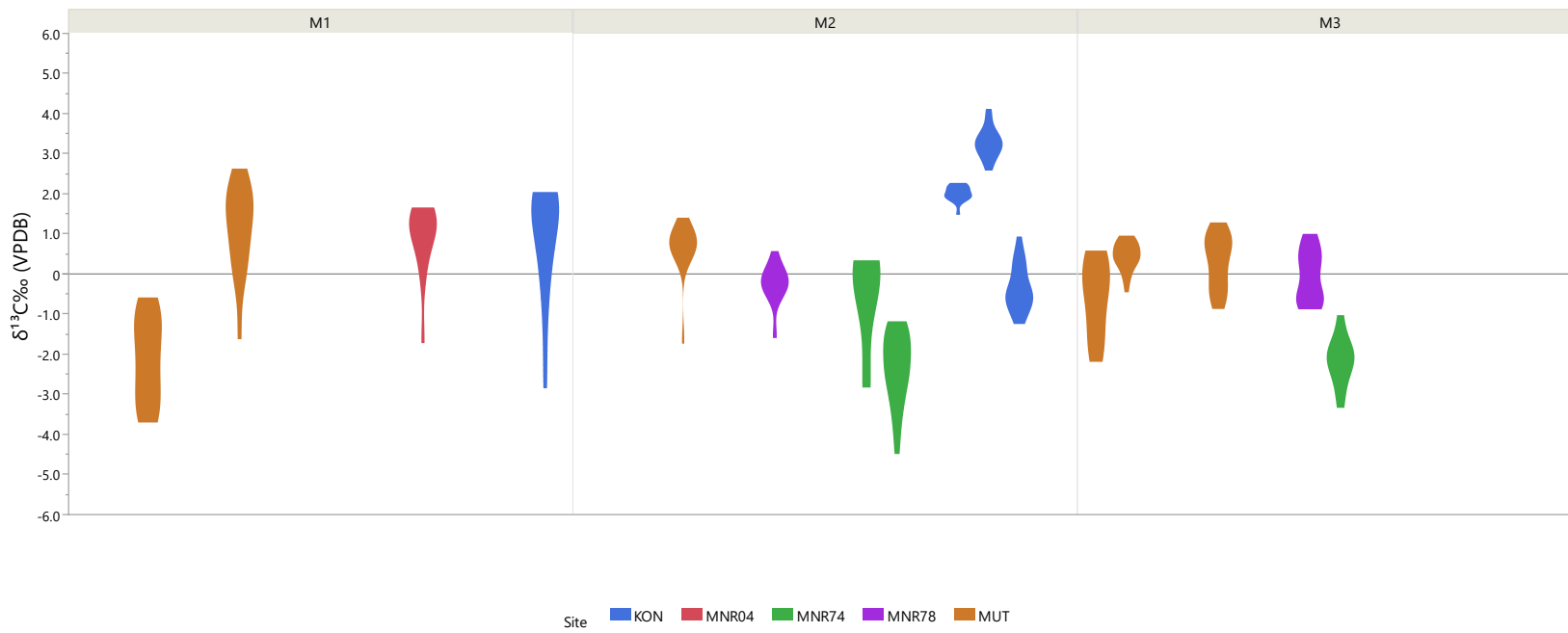


Figure 5.1. Variation in cattle $\delta^{13}C$ tooth enamel values grouped by tooth

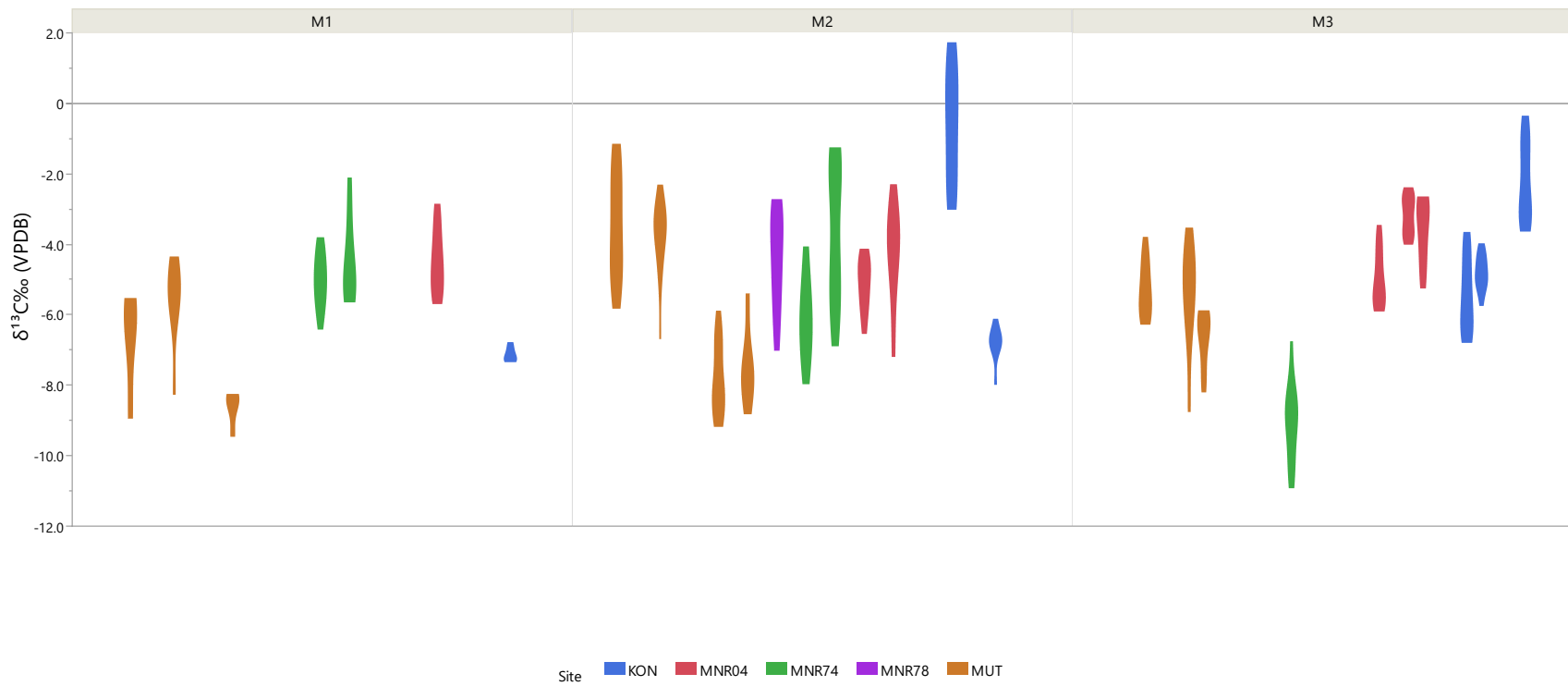


Figure 5.2. Variation in caprine $\delta^{13}\text{C}$ tooth enamel values grouped by tooth.

Table 5.1. Maximum, minimum, mean, and range of $\delta^{13}\text{C}$ and $\delta^{18}\text{O}$ serial enamel values for each *Bos taurus* tooth sampled.

Site/Sample ID (Tooth)	Max. $\delta^{13}\text{C}\text{‰}$	Min. $\delta^{13}\text{C}\text{‰}$	Mean $\delta^{13}\text{C}\text{‰}$	$\delta^{13}\text{C}$ Range	Max. $\delta^{18}\text{O}\text{‰}$	Min. $\delta^{18}\text{O}\text{‰}$	Mean $\delta^{18}\text{O}\text{‰}$	$\delta^{18}\text{O}$ Range
Mutamba								
MUT/1031/F07 (M1)	2.57	-1.55	1.1	4.12	0.23	-3.07	-1.1	3.30
MUT/2012/F10 (M1)	-0.63	-3.73	-2.14	3.1	-0.18	-3.10	-2.04	2.92
MUT/2012/F09 (M2)	1.37	-1.7	0.65	3.07	0.4	-4.2	-2.57	4.6
MUT/2012/F08 (M3)	1.25	-1.10	0.3	2.35	-1	-4.1	-3.1	3.1
MUT/2167/F01 (M3)	0.54	-2.13	-0.59	2.67	-0.88	-4.07	-2.31	3.19
MUT/2099/F09 (M3)	0.94	-0.44	0.44	1.38	-0.19	-2.89	-1.84	2.7
MNR 78								
MNR78/231/06 (M2)	0.54	-1.56	-0.3	2.1	-1.7	-3.20	-2.5	1.5
MNR78/231/05 (M3)	1.0	-0.8	-0.04	1.8	-1.61	-3.9	-2.88	2.3
MNR 74								
MNR74/B024 (M2)	-1.22	-4.43	-2.36	3.21	0.32	-5.87	-2.64	6.19
MNR74/B063/01 (M2)	0.29	-2.76	-0.60	3.05	-4.25	-5.36	-4.87	1.11
MNR74/B063/02 (M3)	-1.06	-3.30	-2.2	2.24	-2.9	-6.5	-4.8	3.6
MNR 04								
MNR04/341/08 (M1)	1.62	-1.7	0.9	3.32	-1.78	-4.22	-3.2	2.44

Site/Sample ID (Tooth)	Max. $\delta^{13}\text{C}\text{‰}$	Min. $\delta^{13}\text{C}\text{‰}$	Mean $\delta^{13}\text{C}\text{‰}$	$\delta^{13}\text{C}$ Range	Max. $\delta^{18}\text{O}\text{‰}$	Min. $\delta^{18}\text{O}\text{‰}$	Mean $\delta^{18}\text{O}\text{‰}$	$\delta^{18}\text{O}$ Range
Stayt (KON)								
KON/T4 (M $\bar{2}$)	2.26	1.49	2.00	0.77	-1.50	-5.91	-3.67	4.41
KON/295 (M $\bar{2}$)	4.10	2.60	3.27	1.50	-2.78	-6.47	-4.55	3.69
KON/114 (M $\bar{2}$)	0.91	-1.21	-0.35	2.12	-3.46	-5.98	-4.86	2.52
KON/100 (M $\bar{1}$)	1.98	-2.77	0.82	4.75	-2.59	-6.52	-4.26	3.93

The mean $\delta^{18}\text{O}$ value for all *Bos taurus* teeth sampled is -3.1‰ while the mean $\delta^{18}\text{O}$ value for all *Bos taurus* excluding the values (n=56) for sampled M1 teeth (n=4) is slightly more negative at -3.3‰. This difference may be due to the result of enriched $\delta^{18}\text{O}$ values being received via the ingestion of water through milk (suckling) during the mineralisation of the M1 of the calf. (Towers et al., 2014) or other climatic and factors related to life-history (Luyt & Sealy, 2018)

Table 5.2. Maximum, minimum, mean, and range (range) of $\delta^{13}\text{C}$ serial enamel values for all caprines.

Site/Sample ID <i>Species</i> (Tooth)	Max. $\delta^{13}\text{C}\%$	Min. $\delta^{13}\text{C}\%$	Mean $\delta^{13}\text{C}\%$	$\delta^{13}\text{C}$ Range	Max. $\delta^{18}\text{O}\%$	Min. $\delta^{18}\text{O}\%$	Mean $\delta^{18}\text{O}\%$	$\delta^{18}\text{O}$ Range
Mutamba								
MUT/2019/F20/03 <i>Ovis aries</i> M $\bar{1}$	-4.66	-7.33	-5.58	2.67	-1.06	-3.60	-2.39	2.54
MUT/2019/F20/04 <i>Ovis aries</i> M $\bar{2}$	-2.36	-4.96	-3.58	2.6	-2.04	-3.66	-3.08	1.62
MUT/2019/F20/05 <i>Ovis aries</i> M $\bar{3}$	-3.82	-7.03	-5.46	3.21	-3.10	-6.07	-4.82	2.97
MUT/1011/F13/02 <i>Ovis aries</i> M $\bar{2}$	-5.46	-8.75	-7.53	3.29	-0.80	-4.75	-3.17	3.95
MUT/2003/F04 <i>Capra hircus</i> M $\bar{3}$	-3.59	-8.67	-5.48	5.08	-4.17	-7.72	-5.66	3.55
MUT/2177/F02 <i>Ovis/Capra</i> M $\bar{1}$	-5.8	-8.87	-6.82	3.07	-1.20	-2.41	-1.93	1.21
MUT/2177/F03 <i>Ovis/Capra</i> M $\bar{2}$	-1.21	-6.49	-3.77	5.23	0.84	-3.45	-0.62	2.61
MUT/1170/F05/01 <i>Ovis/Capra</i> M $\bar{1}$)	-8.27	-9.83	-8.94	1.56	0.22	-1.56	-0.6	1.78
MUT/1170/F05/02 <i>Ovis/Capra</i> M $\bar{2}$	-5.49	-9.12	-7.81	3.63	0.46	-5.77	-2.43	6.23
MUT/1170/F05/03 <i>Ovis/Capra</i> M $\bar{3}$	-5.92	-8.16	-6.70	2.24	-1.5	-6.14	-3.78	4.64
MNR 78								
MNR78/123/03 <i>Ovis/Capra</i> M $\bar{2}$	-2.79	-6.93	-4.47	4.14	-1.72	-4.74	-2.93	3.02
MNR 74								
MNR74/B255/02 <i>Ovis/Capra</i> M $\bar{2}$	-4.12	-7.89	-6.11	3.7	-1.48	-4.25	-3.25	2.77
MNR74/B255/02 <i>Ovis/Capra</i> M $\bar{3}$	-6.81	-10.85	-9.04	4.04	-0.98	-4.62	-2.11	3.64

Site/Sample ID <i>Species</i> (Tooth)	Max. $\delta^{13}\text{C}\text{‰}$	Min. $\delta^{13}\text{C}\text{‰}$	Mean $\delta^{13}\text{C}\text{‰}$	$\delta^{13}\text{C}$ Range	Max. $\delta^{18}\text{O}\text{‰}$	Min. $\delta^{18}\text{O}\text{‰}$	Mean $\delta^{18}\text{O}\text{‰}$	$\delta^{18}\text{O}$ Range
MNR74/B068 <i>Ovis/Capra M1</i>	-3.83	-6.38	-5.03	2.55	-3.21	-5.81	-4.56	2.6
MNR74/B065/01 <i>Ovis/Capra M1</i>	-2.17	-5.57	-4.41	3.4	-0.84	-2.48	-1.71	1.64
MNR74/B065/02 <i>Ovis/Capra M2</i>	-1.33	-6.79	-3.71	5.46	-0.52	-4.01	-2.33	3.49
MNR 04								
MNR04/289/10 <i>Ovis/Capra M2</i>	-2.37	-7.10	-4.31	4.73	-1.83	-4.44	-3.44	2.61
MNR04/289/09 <i>Ovis/Capra M3</i>	-2.40	-4.61	-3.32	2.21	-2.35	-6.24	-4.69	3.89
MNR04/2021/11/02 <i>Ovis/Capra M2</i>	-4.16	-6.50	-5.15	2.34	-3.69	-5.45	-4.62	1.70
MNR04/2021/11/01 <i>Ovis/Capra M3</i>	-3.48	-5.79	-4.95	2.31	-3.50	-5.39	-4.27	1.89
MNR04/205/10 <i>Ovis aries M1</i>	-2.89	-5.64	-4.46	2.75	-3.79	-6.11	-5.13	2.32
MNR04/239/09 <i>Ovis aries M3</i>	-2.69	-5.19	-3.65	2.50	-1.74	-4.04	-3.07	2.30
Stayt (KON)								
KON/40 <i>Ovis/Capra M3</i>	-0.39	-3.58	-2.19	3.19	-3.58	-8.78	-5.46	5.20
KON/192 <i>Ovis/Capra M2</i>	1.66	-2.92	-0.64	4.58	-1.55	-4.88	-3.25	3.33
KON/161 <i>Ovis/Capra M3</i>	-3.70	-6.74	-5.41	3.04	-0.92	-2.95	-1.91	2.03
KON/106/01 <i>Ovis/Capra M1</i>	-6.79	-7.33	-7.12	0.54	-1.27	-3.70	-2.38	2.43
KON/106/02 <i>Ovis/Capra M2</i>	-6.14	-7.96	-6.73	1.82	-0.61	-5.23	-2.56	4.62
KON/106/03 <i>Ovis/Capra M3</i>	-2.37	-5.72	-4.81	3.35	1.62	-2.37	-0.07	3.99

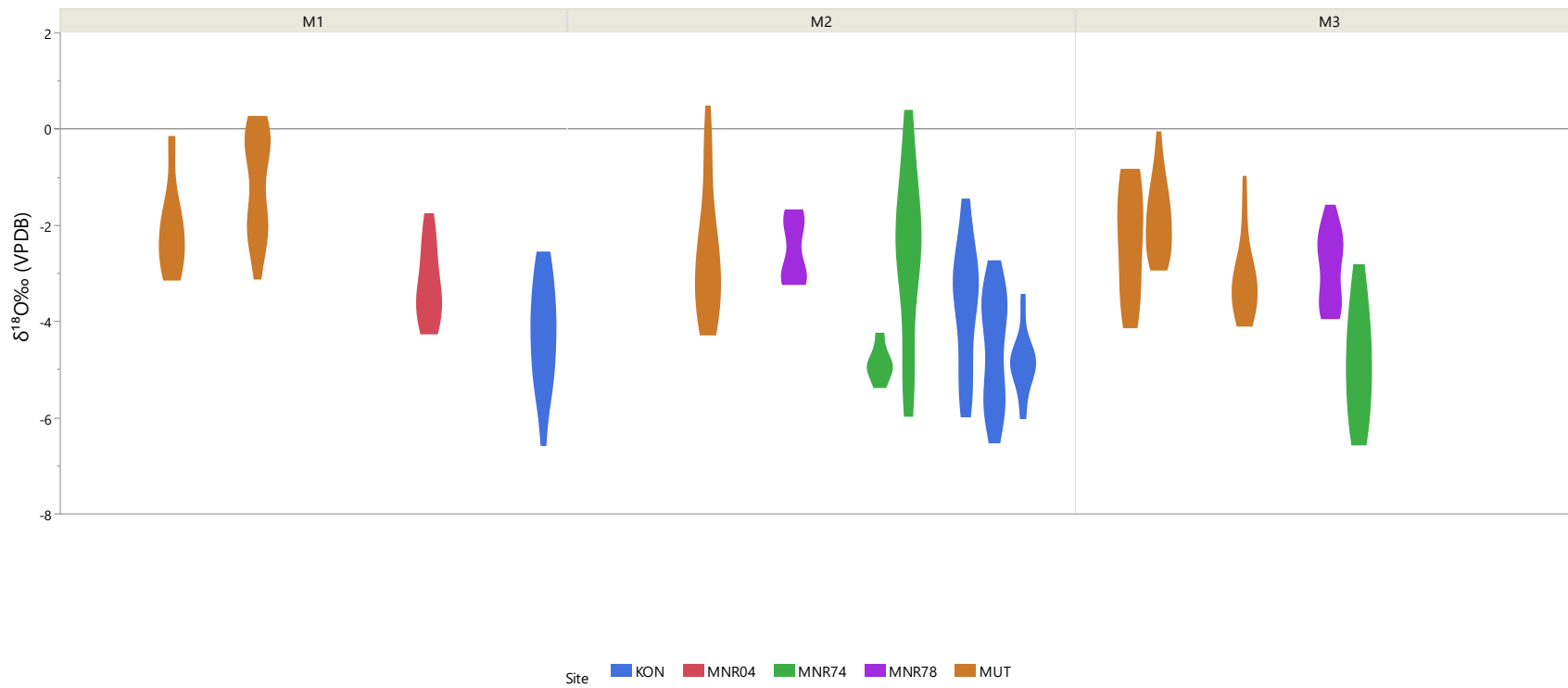


Figure 5.3. Variation in cattle $\delta^{18}O$ tooth enamel values grouped by tooth.

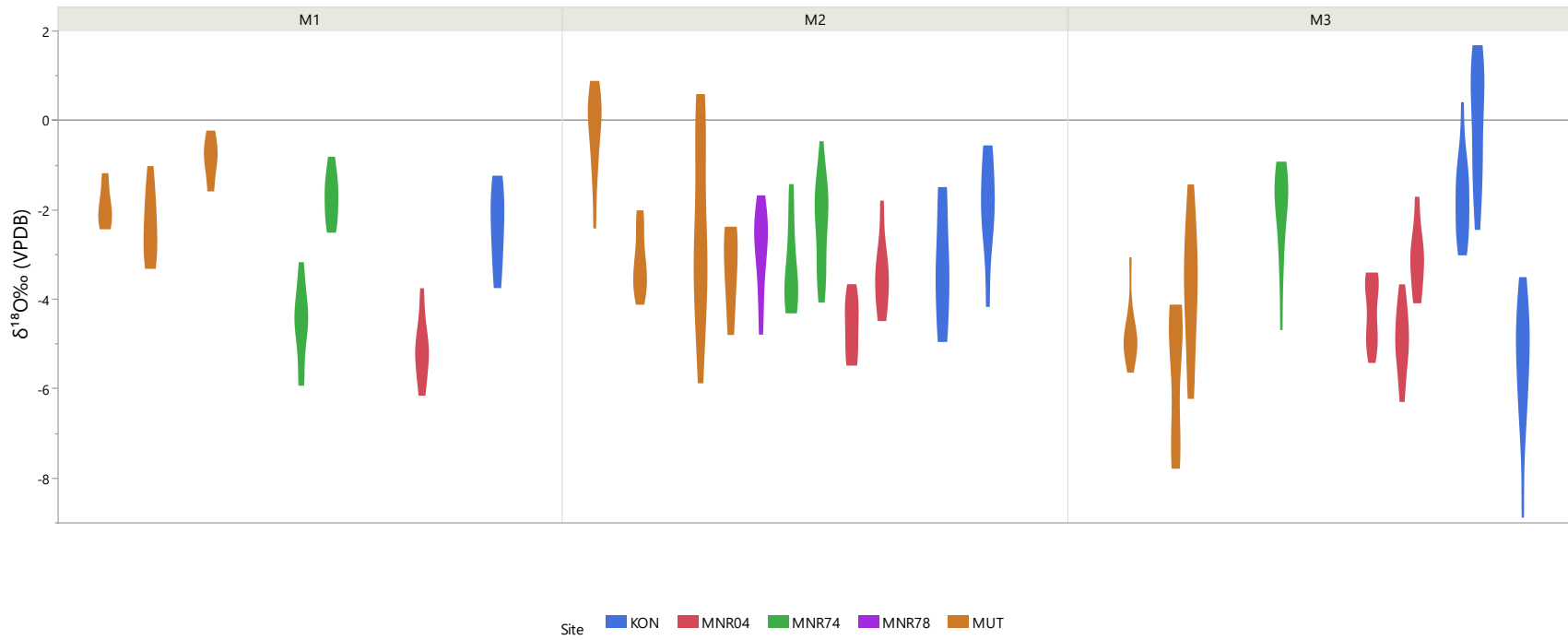


Figure 5.4. Variation in caprine $\delta^{18}\text{O}$ tooth enamel values grouped by tooth.

5.2 Wild Grazer and Browser $\delta^{13}\text{C}$ and $\delta^{18}\text{O}$ results

The mean $\delta^{13}\text{C}$ value for all wild browser samples (n=6) is $-7.71 \pm 0.4\%$. The mean $\delta^{18}\text{O}$ value for all wild browser samples (n=6) is $-1.53 \pm 1.13\%$.

The mean $\delta^{13}\text{C}$ value for all wild grazer samples (n=37) is $-1.03 \pm 1.73\%$. The mean $\delta^{18}\text{O}$ value for all wild grazer samples (n=37) is $-3.15 \pm 1.12\%$.

The mean $\delta^{13}\text{C}$ value for all wild mixed-feeder samples (n=13) is $-7.89 \pm 0.66\%$. The mean $\delta^{18}\text{O}$ value for all wild mixed-feeder samples (n=13) is $-0.92 \pm 1.63\%$.

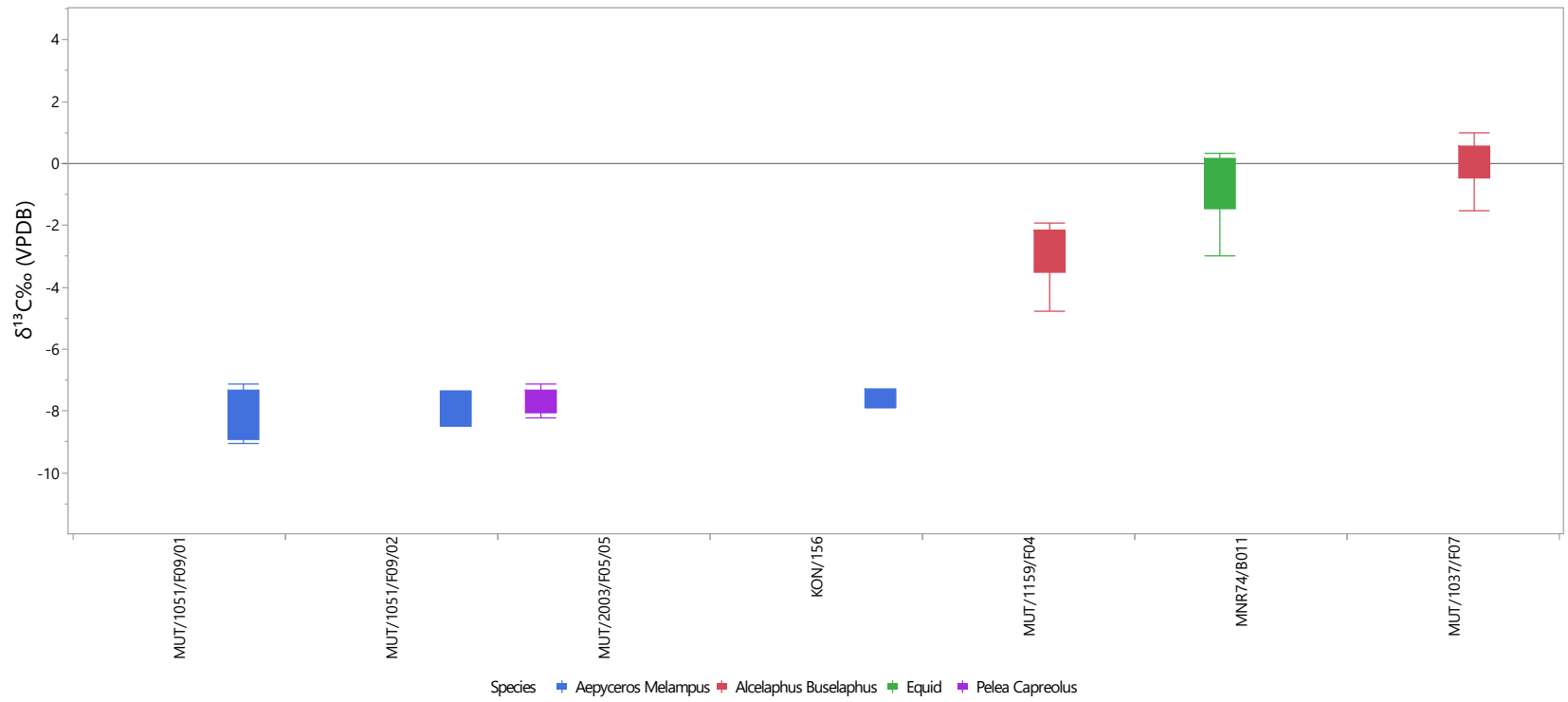


Figure 5.5. Variation in wild species $\delta^{13}C$ tooth enamel values.

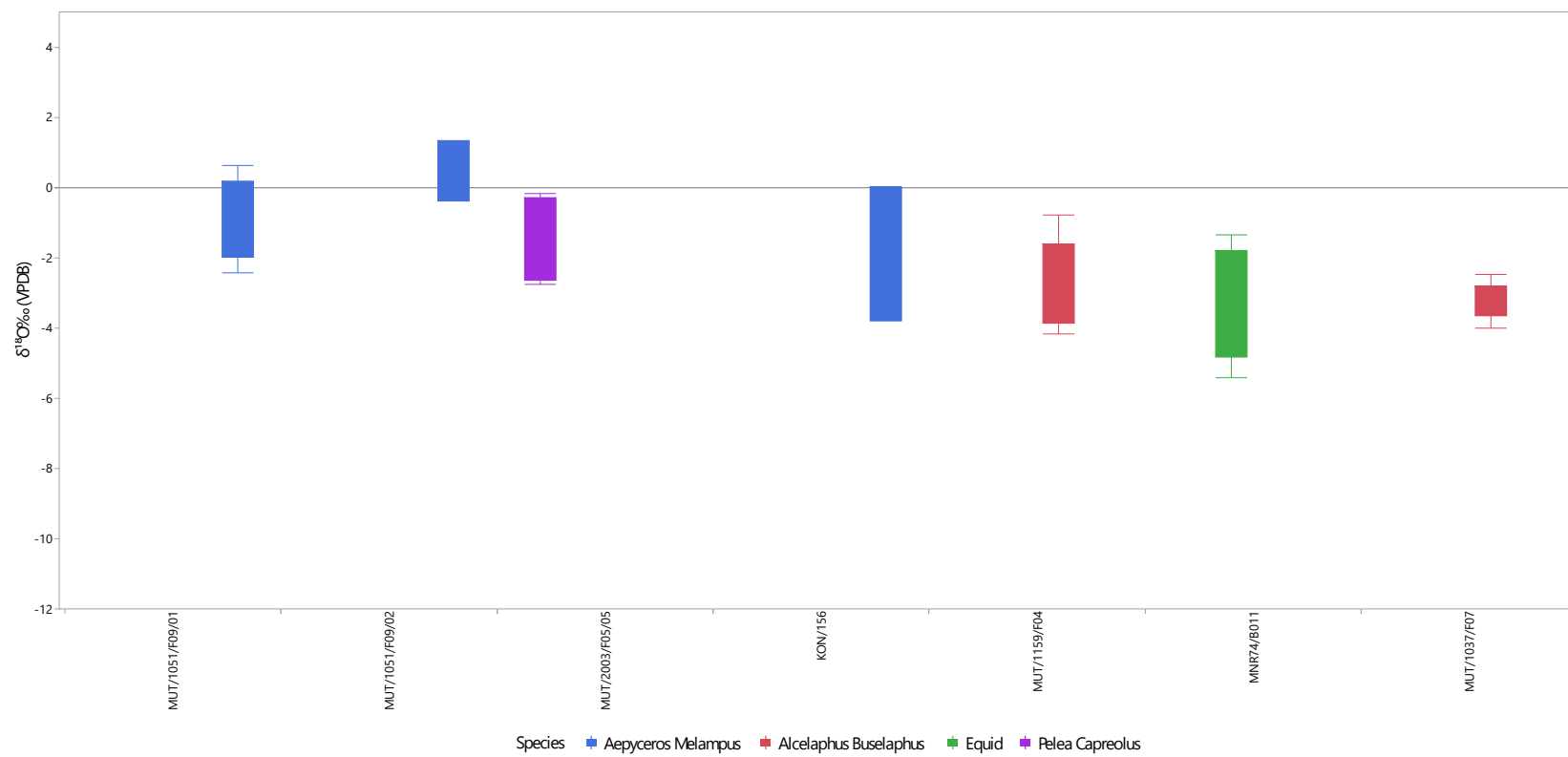


Figure 5.6. Variation in wild species $\delta^{18}O$ tooth enamel values.

Table 5.3. Summary of wild species $\delta^{13}C$ and $\delta^{18}O$ enamel values grouped by dietary profile.

Site/Sample ID Species ID (Tooth)	Max. $\delta^{13}\text{C}$	Min. $\delta^{13}\text{C}$	Mean $\delta^{13}\text{C}$	Range	Max. $\delta^{18}\text{O}$	Min. $\delta^{18}\text{O}$	Mean $\delta^{18}\text{O}$	Range
Browser								
MUT/2003/F05/05 <i>Pelea capreolus</i> (M1)	7.14	8.21	7.72	1.07	-0.08	-4.43	-1.92	4.35
Grazer								
MUT/1159/F04 <i>Alcelaphus buselaphus</i> (M2)	1.96	4.74	3.04	2.78	-0.44	-4.06	-2.47	3.62
MUT/1037/F07 <i>Alcelaphus buselaphus</i> (M2)	1.00	1.51	0.09	2.51	-2.49	-4.02	-3.21	1.53
MNR74/B011 <i>Equid</i> (M1)	0.31	6.16	1.05	6.47	-1.35	-5.41	-3.37	4.06
Mixed Feeder								
MUT/1051/F09/02 <i>Aepyceros melampus</i> (M1)	7.35	8.49	7.74	1.32	1.14	-0.38	0.35	0.18
MUT/1051/F09/01 <i>Aepyceros melampus</i> (M2)	7.14	9.05	8.16	1.91	0.62	-2.44	-0.84	1.29
KON/156 <i>Aepyceros melampus</i> (M1)	7.30	7.90	7.61	0.6	0.01	-3.80	-2.34	3.81

The difference of 3.13‰ in the mean $\delta^{13}\text{C}$ values of the two *Alcelaphus buselaphus* M2 specimens (Table 5.3) indicate a potential tentative range that grazer diets can display.

The wide range in $\delta^{18}\text{O}$ values for the equid (*c.f.* Zebra) MNR74/B011 likely represents mobility over a large tract of land as Zebra are known to cover hundreds of kilometres during their seasonal migrations.

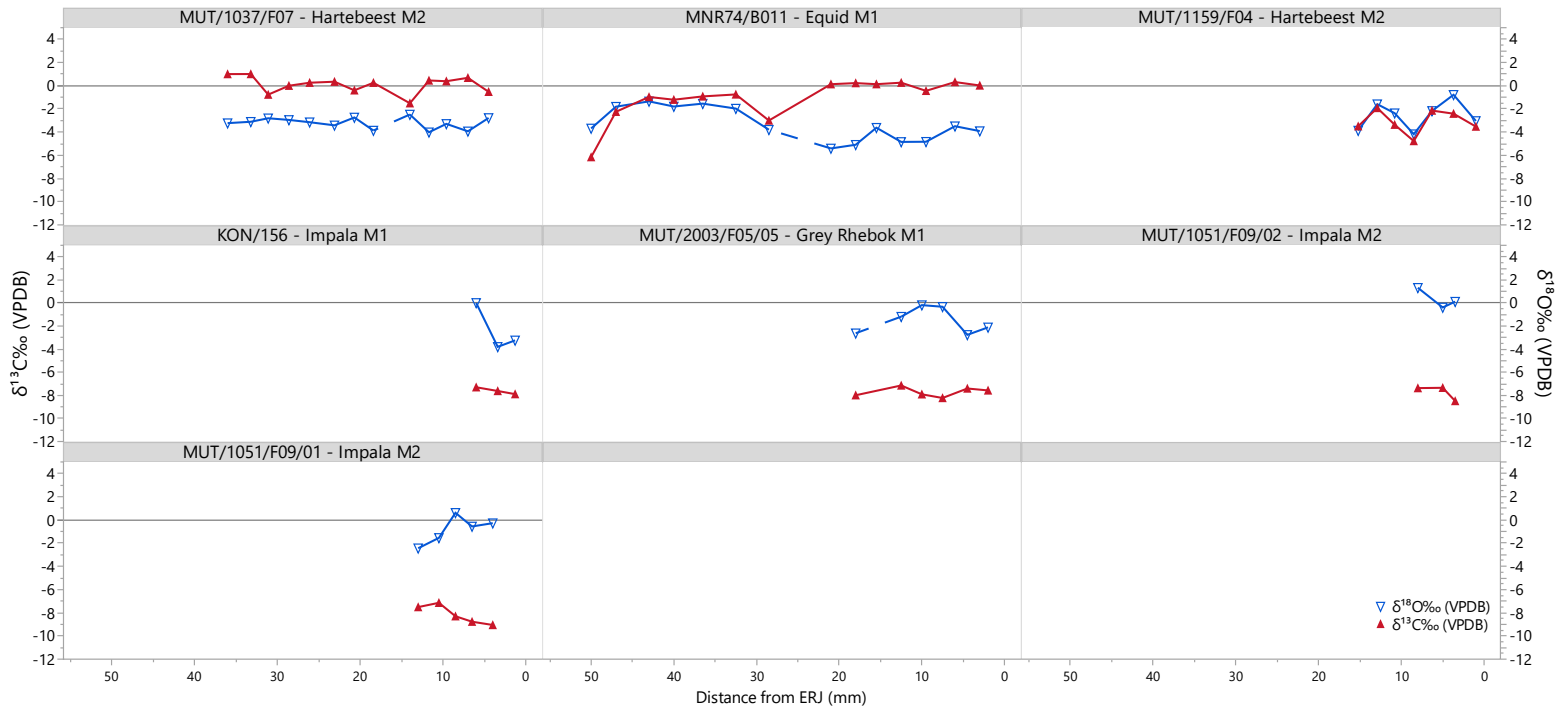


Figure 5.7. Serial $\delta^{13}\text{C}$ and $\delta^{18}\text{O}$ values for wild species from all sites.

5.3 Domesticate Serial tooththrow results.

This section presents the combined $\delta^{13}\text{C}$ and $\delta^{18}\text{O}$ values measured along the growth axis of the tooth for individual animals from each site. The respective $\delta^{13}\text{C}$ and $\delta^{18}\text{O}$ values (y axes) are plotted against the distance from the enamel root junction (ERJ) for each tooth, represented by 0 on the x axis. This provides a time-resolved record of isotopic inputs for the period of individual tooth mineralisation.

5.3.1 Mutamba

Cattle

The mean $\delta^{13}\text{C}$ value for all cattle samples (n=85) from Mutamba is $0.05 \pm 1.34\text{‰}$ with a range of 6.22‰ . The mean $\delta^{18}\text{O}$ value for all cattle samples (n=85) from Mutamba is $-2.15 \pm 1.19\text{‰}$ with a range of 4.63‰

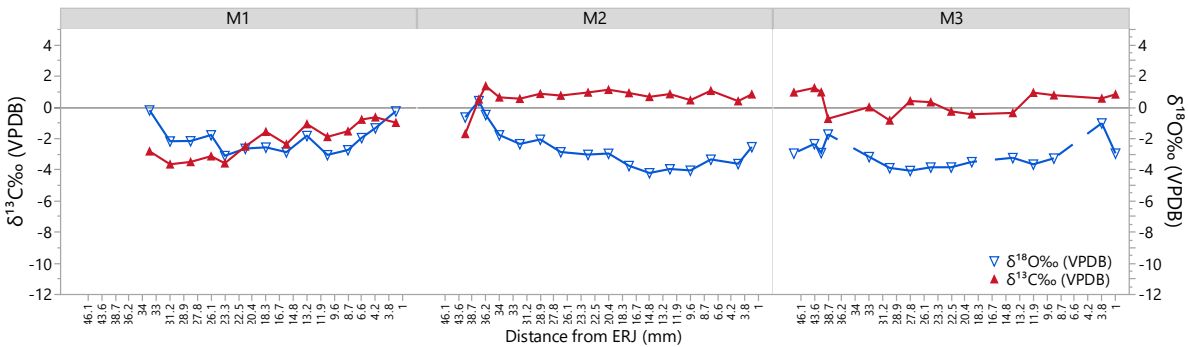


Figure 5.8. Serial $\delta^{13}\text{C}$ and $\delta^{18}\text{O}$ values for- *Bos taurus* MUT/2012/F10 M1, M2, and M3

The mean $\delta^{13}\text{C}$ value for all samples (n=45) across the serially sampled tooththrow of *Bos taurus* MUT/2012/F10 (Figure 5.8) is $-0.33 \pm 1.48\text{‰}$ with a range of 5.02‰ . The mean $\delta^{18}\text{O}$ for the

serially sampled tooththrow is $-2.58 \pm 1.14\text{‰}$ with a range of 4.63‰ .

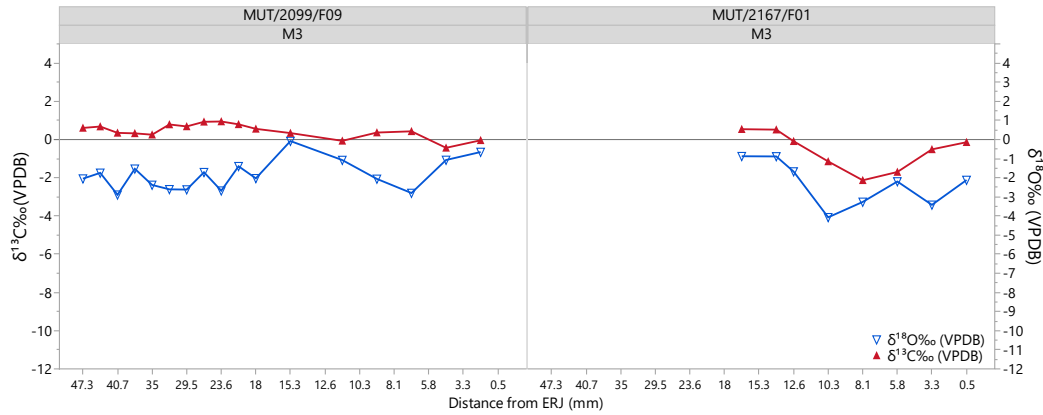


Figure 5.9. Serial $\delta^{13}\text{C}$ and $\delta^{18}\text{O}$ values for two individual *Bos taurus* M3 MUT/2099/F09 and MUT/2167/F01

The two individual M3s from MUT/2099/F09 and MUT/2167/F01 (Figure 5.9) display variability among the dietary patterns of cattle at Mutamba. The mean $\delta^{13}\text{C}$ value for all samples ($n=17$) from the M3 of *Bos taurus* MUT/2099/F09 is $0.44 \pm 0.37\text{‰}$ with a range of 1.38‰ . The mean $\delta^{18}\text{O}$ for all samples ($n=17$) from the M3 of *Bos taurus* MUT/2099/F09 is $-1.85 \pm 0.8\text{‰}$ with a range of 2.81‰ .

The mean $\delta^{13}\text{C}$ value for all samples ($n=8$) from the M3 of *Bos taurus* MUT/2167/F01 is $-0.59 \pm 1\text{‰}$ with a range of 2.67‰ . The mean $\delta^{18}\text{O}$ value for all samples ($n=8$) from the M3 of *Bos taurus* MUT/2167/F01 is $-2.32 \pm 1.18\text{‰}$ with a range of 3.19‰ .

Caprines

The mean $\delta^{13}\text{C}$ value for all caprine samples ($n=78$) from Mutamba is $-5.82 \pm 1.98\text{‰}$ with a range of 8.22‰ . The mean $\delta^{18}\text{O}$ value for all caprine samples ($n=78$) from Mutamba is $-2.96 \pm 1.95\text{‰}$ with a range of 8.55‰ .

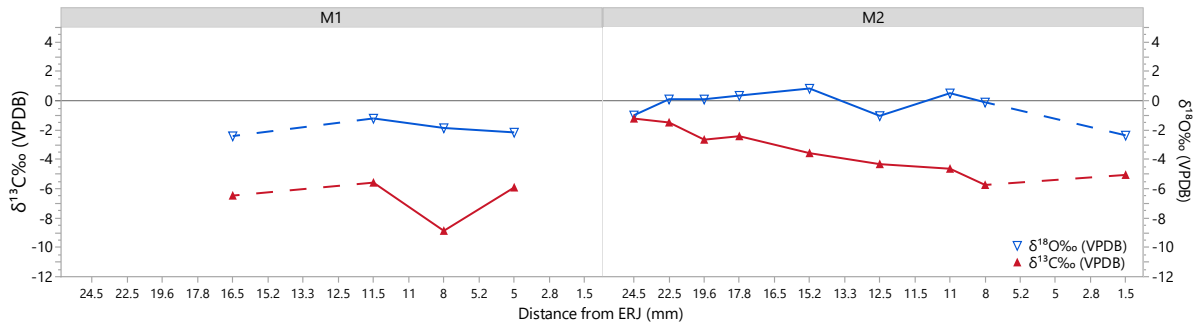


Figure 5.10. Serial $\delta^{13}\text{C}$ and $\delta^{18}\text{O}$ values for MUT/2177/F02 Ovis/capra M1 and M2

The mean $\delta^{13}\text{C}$ value for all samples ($n=13$) across the tooththrow of MUT/2177/F02 Ovis/capra (Figure 5.10) is $-4.46 \pm 2.17\text{‰}$ with a range of 7.66‰ . The mean $\delta^{18}\text{O}$ for the tooththrow is $-0.78 \pm 1.16\text{‰}$ with a range of 3.24‰ .

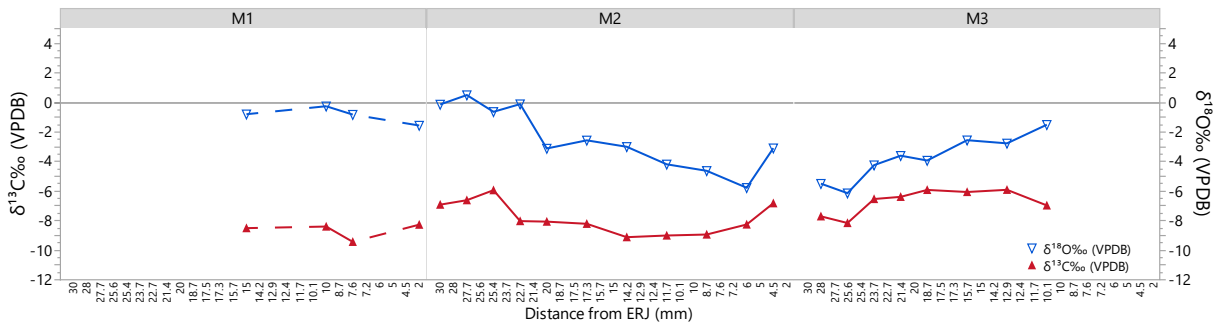


Figure 5.11. Serial $\delta^{13}\text{C}$ and $\delta^{18}\text{O}$ values for MUT/1170/F05 Ovis/capra M1, M2, and M3

The mean $\delta^{13}\text{C}$ value across all samples ($n=23$) for the tooththrow of MUT/1170/F05 *Ovis/capra* (

Figure 5.11) is $-7.57 \pm 1.14\text{‰}$ with a range of 3.52‰ . The mean $\delta^{18}\text{O}$ for the tooththrow is $-2.62 \pm 1.95\text{‰}$ with a range of 6.64‰ .

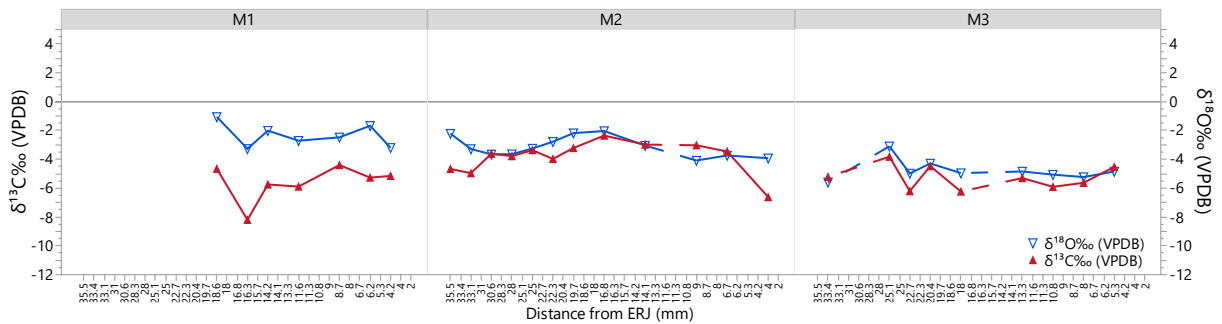


Figure 5.12. Serial $\delta^{13}\text{C}$ and $\delta^{18}\text{O}$ values for MUT/2019/F20 *Ovis aries* M1, M2, and M3

The mean $\delta^{13}\text{C}$ value across all samples ($n=28$) for the tooththrow of MUT/2019/F20 *Ovis aries* (Figure 5.12) is $-4.74 \pm 1.32\text{‰}$ with a range of 5.84‰ . The mean $\delta^{18}\text{O}$ for the tooththrow is $-3.47 \pm 1.2\text{‰}$ with a range of 4.54‰ .

5.3.2 MNR 78

Cattle

A single individual *Bos taurus* M2 and M3 tooththrow provide the only values for cattle at MNR 78.

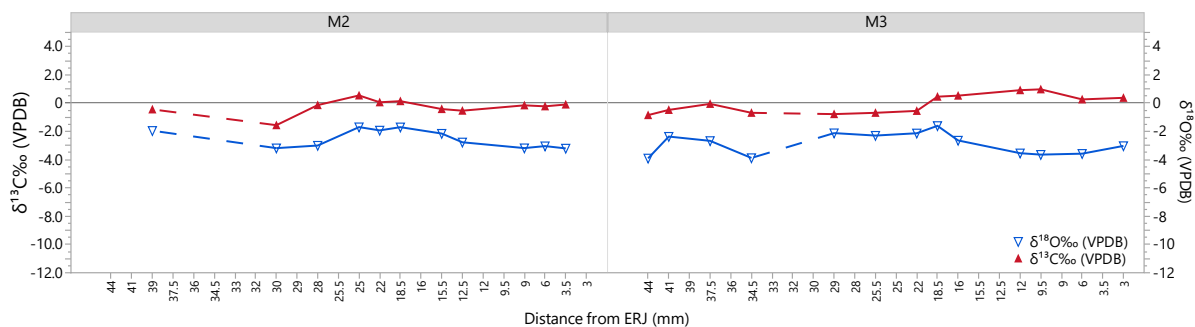


Figure 5.13. Serial $\delta^{13}\text{C}$ and $\delta^{18}\text{O}$ values for MNR78/231/05 *Bos taurus* M2 and M3

The mean $\delta^{13}\text{C}$ value across all samples (n=24) for the tooththrow of for MNR78/231/05 *Bos taurus* (Figure 5.13) is $-0.14 \pm 0.6\text{‰}$ with a range of 2.54‰. The mean $\delta^{18}\text{O}$ for the tooththrow is $-2.72 \pm 0.72\text{‰}$ with a range of 2.3‰.

Caprines

A single *Ovis/capra* M2 provides the only values for caprines at MNR78.

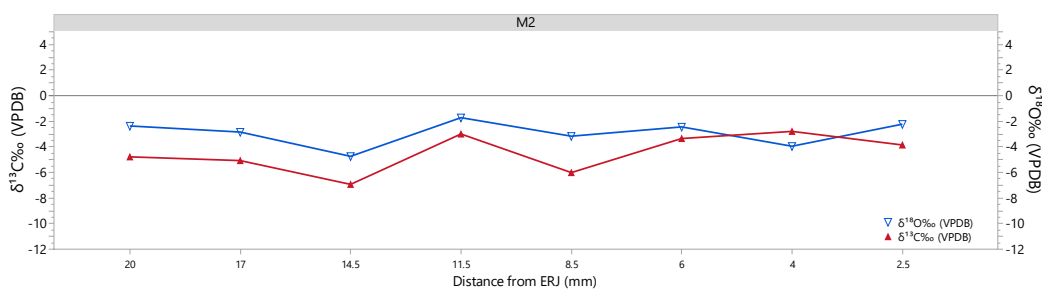


Figure 5.14. Serial $\delta^{13}\text{C}$ and $\delta^{18}\text{O}$ values for MNR78/123/03 *Ovis/capra*

The mean $\delta^{13}\text{C}$ value across all samples (n=8) for the M2 of MNR78/123/03 *Ovis/capra* (Figure 5.14) is $-4.47 \pm 1.49\text{‰}$ with a range of 4.14‰. The mean $\delta^{18}\text{O}$ for the tooththrow is $-2.93 \pm 1\text{‰}$ with a range of 3.02‰.

5.3.3 MNR 74

Cattle

The mean $\delta^{13}\text{C}$ value for all cattle samples (n=30) from MNR74 is $-2.01 \pm \%$ with a range of 4.72%. The mean $\delta^{18}\text{O}$ value for all cattle samples (n=30) from MNR74 is $-3.67 \pm 1.84\%$ with a range of 6.82%.

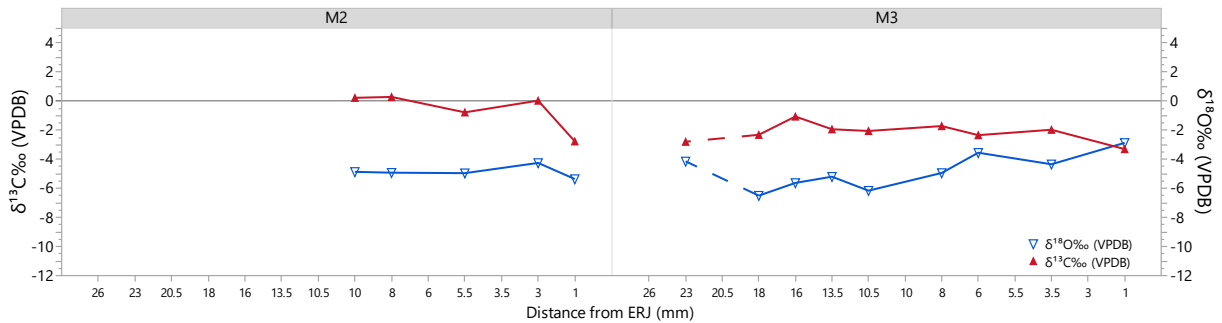


Figure 5.15. Serial $\delta^{13}\text{C}$ and $\delta^{18}\text{O}$ values for MNR74/B063 *Bos taurus* M2 and M3

The mean $\delta^{13}\text{C}$ value across all samples (n=14) for the tooththrow of MNR74/B063 *Bos taurus* (Figure 5.16) is $-1.6 \pm 1.17\%$ with a range of 3.59%. The mean $\delta^{18}\text{O}$ for the tooththrow is $-4.83 \pm 0.97\%$ with a range of 3.63%.

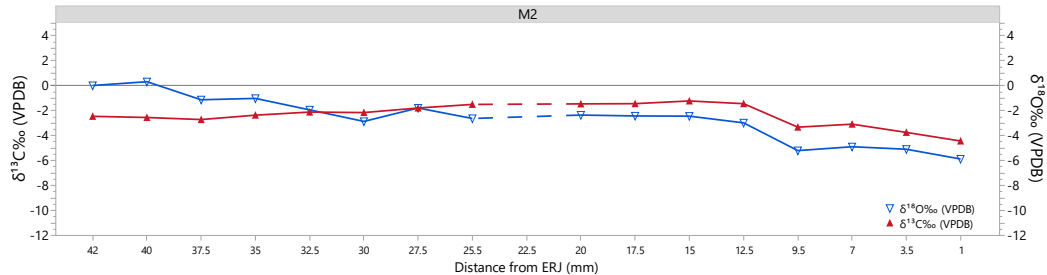


Figure 5.16. Serial $\delta^{13}\text{C}$ and $\delta^{18}\text{O}$ values for MNR 74/B024 - *Bos taurus* M2

The mean $\delta^{13}\text{C}$ value across all samples ($n=16$) for the M2 of MNR74/B024 *Bos taurus* (Figure 5.16) is $-2.36 \pm 0.92\text{‰}$ with a range of 3.21‰ . The mean $\delta^{18}\text{O}$ for the M2 is $-2.64 \pm 1.83\text{‰}$ with a range of 6.19‰ .

Caprines

The mean $\delta^{13}\text{C}$ value for all caprine samples ($n=44$) from MNR74 is $-5.62 \pm 2.47\text{‰}$ with a range of 9.52‰ . The mean $\delta^{18}\text{O}$ value for all caprine samples ($n=44$) from MNR74 is $-2.78 \pm 1.38\text{‰}$ with a range of 5.36‰ .

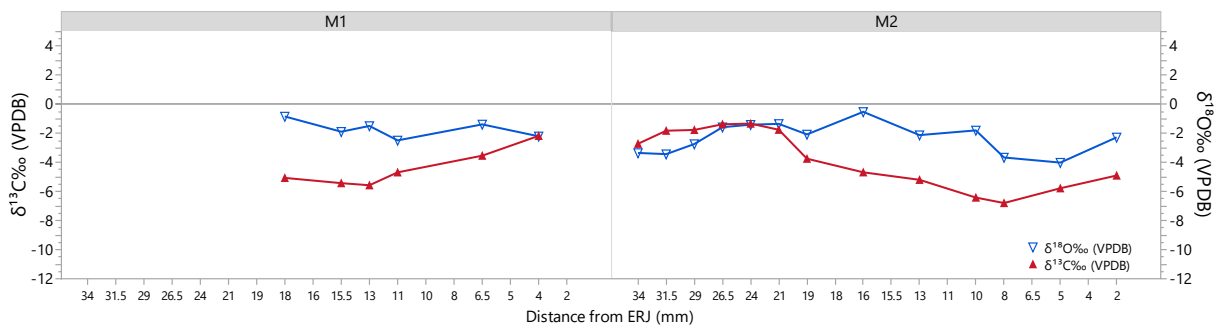


Figure 5.17. Serial $\delta^{13}\text{C}$ and $\delta^{18}\text{O}$ values for MNR 74/B065 Ovis/capra M1 and M2.

The mean $\delta^{13}\text{C}$ value across all samples ($n=19$) for the tooththrow of MNR 74/B065 Ovis/capra (

Figure 5.17) is $-3.93 \pm 1.82\text{‰}$ with a range of 5.46‰ . The mean $\delta^{18}\text{O}$ for the tooththrow is $-2.13 \pm 0.95\text{‰}$ with a range of 3.49‰ . Further, there seems to be no indication that a weaning induced enrichment shift in the isotope values between M1 and M2 occurred for this individual (Luyt & Sealy, 2018).

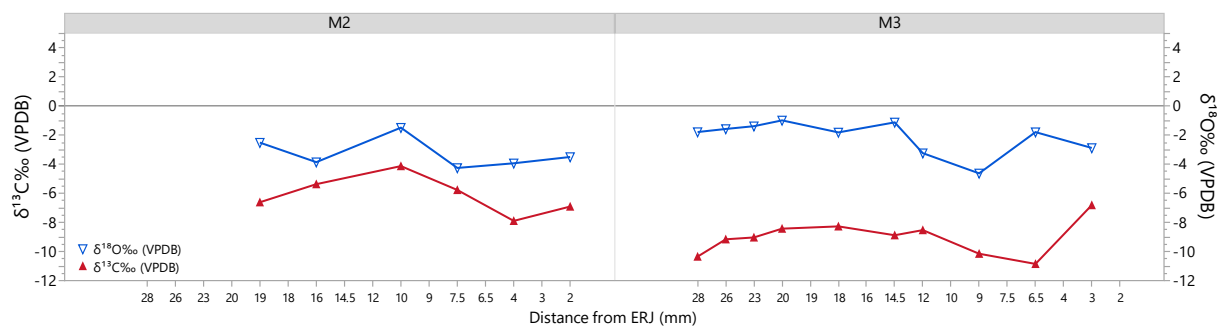


Figure 5.18. Serial $\delta^{13}\text{C}$ and $\delta^{18}\text{O}$ values for MNR 74/B255 Ovis/capra M2 and M3

The mean $\delta^{13}\text{C}$ value across all samples (n=16) for the toothrow of MNR 74/B255 Ovis/capra Figure 5.18) is $-7.94 \pm 1.89\text{‰}$ with a range of 6.73‰ . The mean $\delta^{18}\text{O}$ for the toothrow is $-2.54 \pm 1.21\text{‰}$ with a range of 3.64‰ .

5.3.4 MNR04

Cattle

A single *Bos taurus* M1 provides the only values for cattle at MNR04.

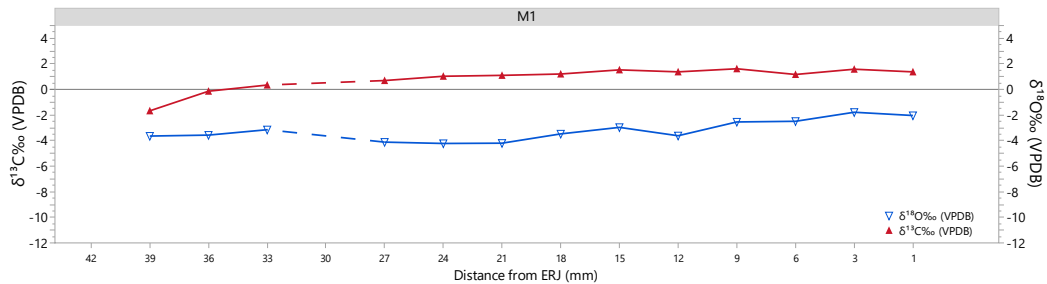


Figure 5.19. Serial $\delta^{13}\text{C}$ and $\delta^{18}\text{O}$ values for MNR04/341/08 - *Bos taurus* M1

The mean $\delta^{13}\text{C}$ value for all samples ($n=13$) across the M1 of MNR04/341/08 (Figure 5.19) is $0.87 \pm 0.92\text{‰}$ with a range of 3.29‰ . The mean $\delta^{18}\text{O}$ for the tooththrow is $-3.22 \pm 0.81\text{‰}$ with a range of 2.44‰ .

Caprines

The mean $\delta^{13}\text{C}$ value for all caprine samples ($n=50$) from MNR04 is $-4.3 \pm 1.16\text{‰}$ with a range of 4.72‰ . The mean $\delta^{18}\text{O}$ value for all caprine samples ($n=50$) from MNR04 is $-4.33 \pm 1.01\text{‰}$ with a range of 4.50‰ .

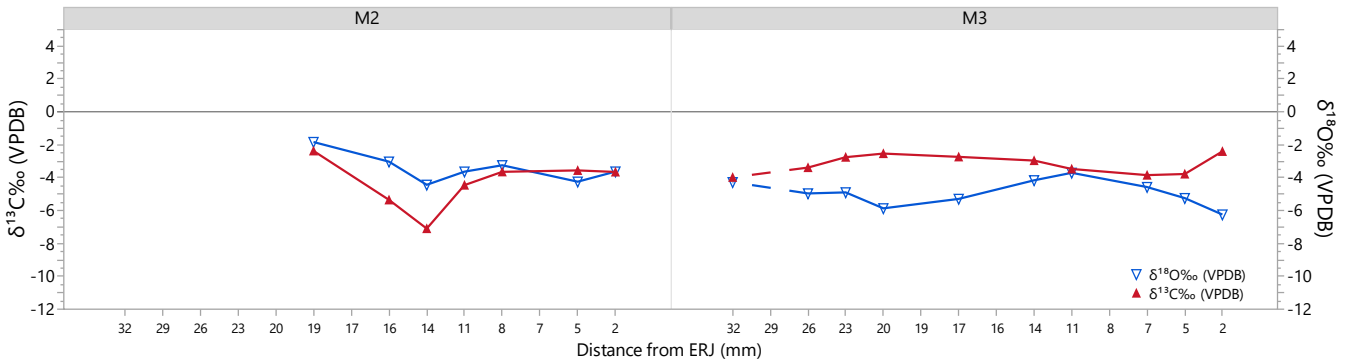


Figure 5.20. Serial $\delta^{13}\text{C}$ and $\delta^{18}\text{O}$ values for MNR04/289/09 *Ovis/capra* M2 and M3

The mean $\delta^{13}\text{C}$ value across all samples (n=17) for the tooththrow of *Ovis/capra* MNR04/289/09 (Figure 5.20) is $-3.65 \pm 1.18\text{‰}$ with a range of 4.72‰. The mean $\delta^{18}\text{O}$ for the tooththrow is $-4.31 \pm 1.09\text{‰}$ with a range of 4.41‰

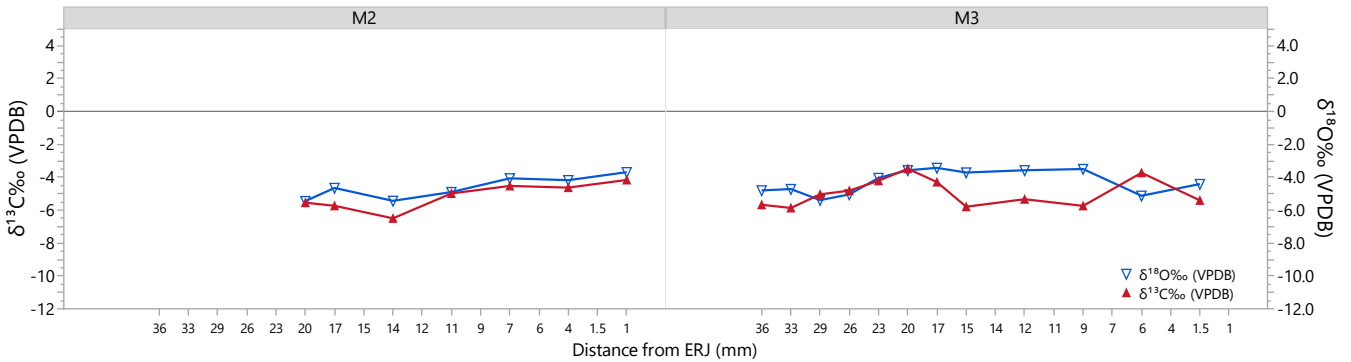


Figure 5.21. Serial $\delta^{13}\text{C}$ and $\delta^{18}\text{O}$ values for MNR04/2021/11 *Ovis/capra* M2 and M3

The mean $\delta^{13}\text{C}$ value across all samples (n=19) for the tooththrow of *Ovis/capra* MNR04/2021/11 (Figure 5.21) is $-5.02 \pm 0.81 \text{‰}$ with a range of 3.02‰. The mean $\delta^{18}\text{O}$ for the tooththrow is $-4.4 \pm 0.71\text{‰}$ with a range of 2.02‰

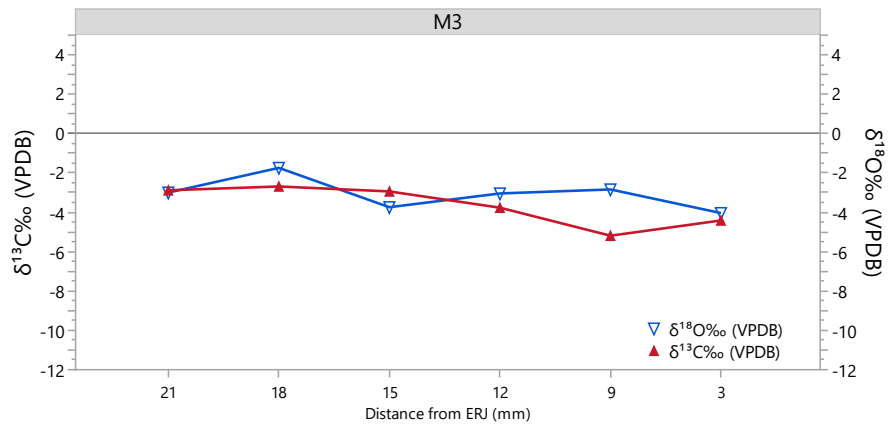


Figure 5.22. Serial $\delta^{13}\text{C}$ and $\delta^{18}\text{O}$ values for MNR04/239/09 *Ovis aries* M3

The mean $\delta^{13}\text{C}$ value across all samples (n=6) for the M3 of MNR04/239/09 *Ovis aries* (Figure 5.22) is $-3.69 \pm 1\text{‰}$ with a range of 2.5‰. The mean $\delta^{18}\text{O}$ for the M3 is $-3.07 \pm 0.8\text{‰}$ with a range of 2.3‰.

5.3.5 Stayt (KON)

Cattle

The mean $\delta^{13}\text{C}$ value for all cattle samples (n=59) from Stayt is $1.41\text{‰} \pm 1.59\text{‰}$ with a range of 6.87‰ . The mean $\delta^{18}\text{O}$ value for all cattle samples (n=59) from Stayt is $-4.36 \pm 1.15\text{‰}$ with a range of 5.02‰ .

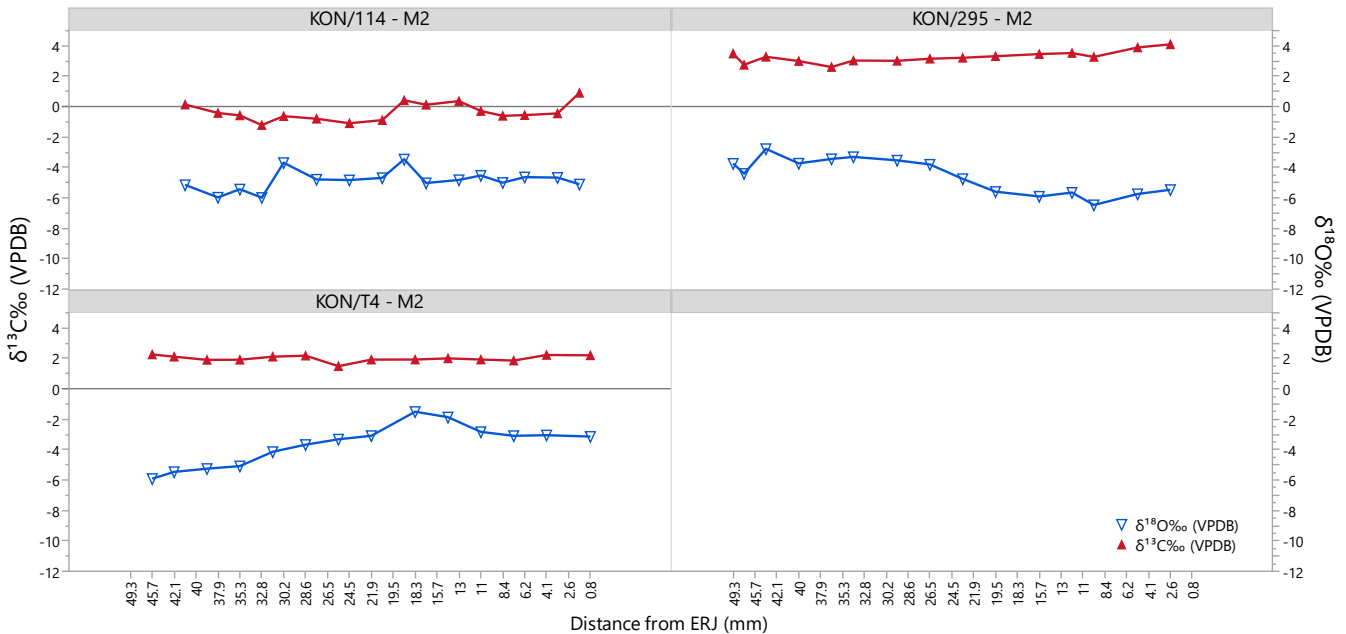


Figure 5.23. Serial $\delta^{13}\text{C}$ and $\delta^{18}\text{O}$ values for three individual *Bos taurus* M2s - KON/114, KON/T4, and KON/295

Three individual cattle M2s were sampled from Stayt (Figure 5.23). The mean $\delta^{13}\text{C}$ value for all samples from KON/114 (n=16) is $-0.35 \pm 0.59\text{‰}$ with a range of 2.12‰ . The mean $\delta^{18}\text{O}$ value for all samples from KON/114 is $-4.86 \pm 0.66\text{‰}$ with a range of 2.52‰ .

The mean $\delta^{13}\text{C}$ value for all samples from KON/T4 (n=14) is $2 \pm 0.2\text{‰}$ with a range of 0.77‰.

The mean $\delta^{18}\text{O}$ value for all samples from KON/T4 is $-3.67 \pm 1.33\text{‰}$ with a range of 4.41‰.

The mean $\delta^{13}\text{C}$ value for all samples from KON/295 (n=15) is $3.27 \pm 0.39\text{‰}$ with a range of 1.49‰. The mean $\delta^{18}\text{O}$ value for all samples from KON/295 is $-4.55 \pm 1.16\text{‰}$ with a range of 3.69‰.

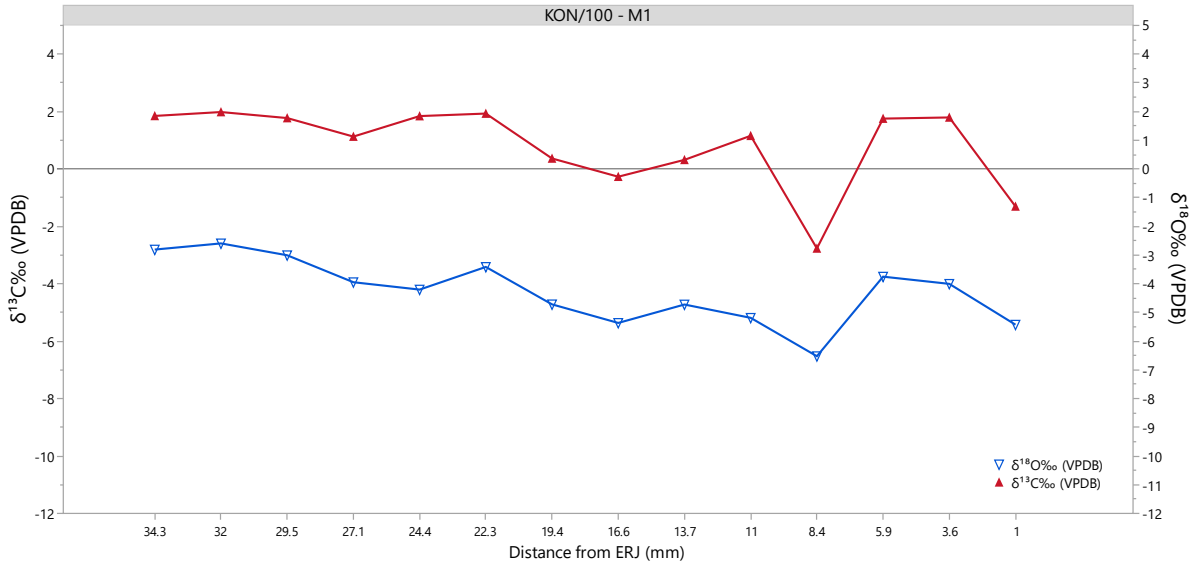


Figure 5.24. Serial $\delta^{13}\text{C}$ and $\delta^{18}\text{O}$ values for KON/100 *Bos taurus* M1

The mean $\delta^{13}\text{C}$ value across all samples (n=14) for the M1 of KON/100 *Bos taurus* (Figure 5.24) is $0.82 \pm 1.43\text{‰}$ with a range of 4.75‰. The mean $\delta^{18}\text{O}$ for the M1 is $-4.26 \pm 1.13\text{‰}$ with a range of 3.93‰.

Caprines

The mean $\delta^{13}\text{C}$ value for all caprine samples (n=50) from Stayt is $-4.3 \pm 2.44\text{‰}$ with a range of 9.61‰ . The mean $\delta^{18}\text{O}$ value for all caprine samples (n=50) from Stayt is $-2.55 \pm 2.18\text{‰}$ with a range of 10.41‰

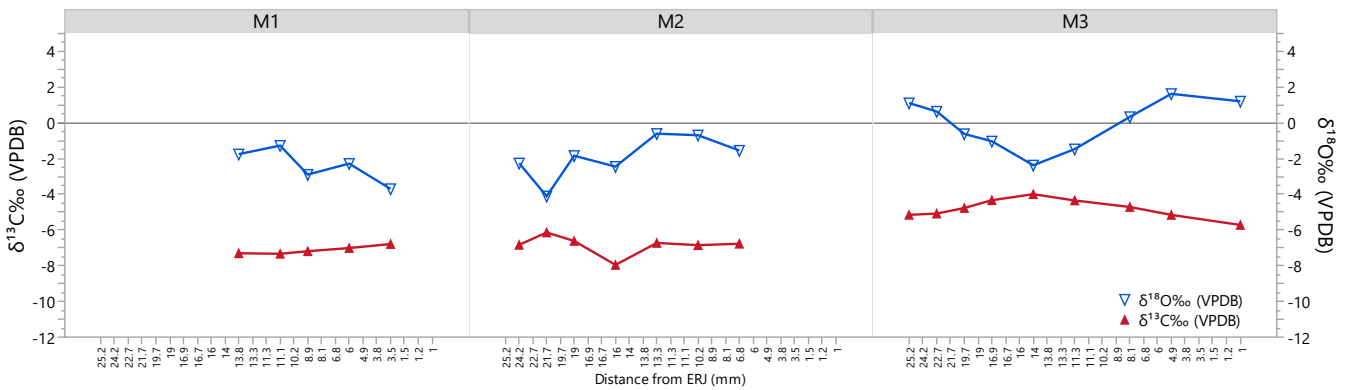


Figure 5.25. Serial $\delta^{13}\text{C}$ and $\delta^{18}\text{O}$ values for KON/106 Ovis/capra M1, M2, and M3

The mean $\delta^{13}\text{C}$ value across all samples (n=21) for the toothrow of *Ovis/capra* KON/106 (Figure 5.25) is $-6.04 \pm 1.19\text{‰}$ with a range of 3.96‰ . The mean $\delta^{18}\text{O}$ for the toothrow is $-1.24 \pm 1.57\text{‰}$ with a range of 5.73‰

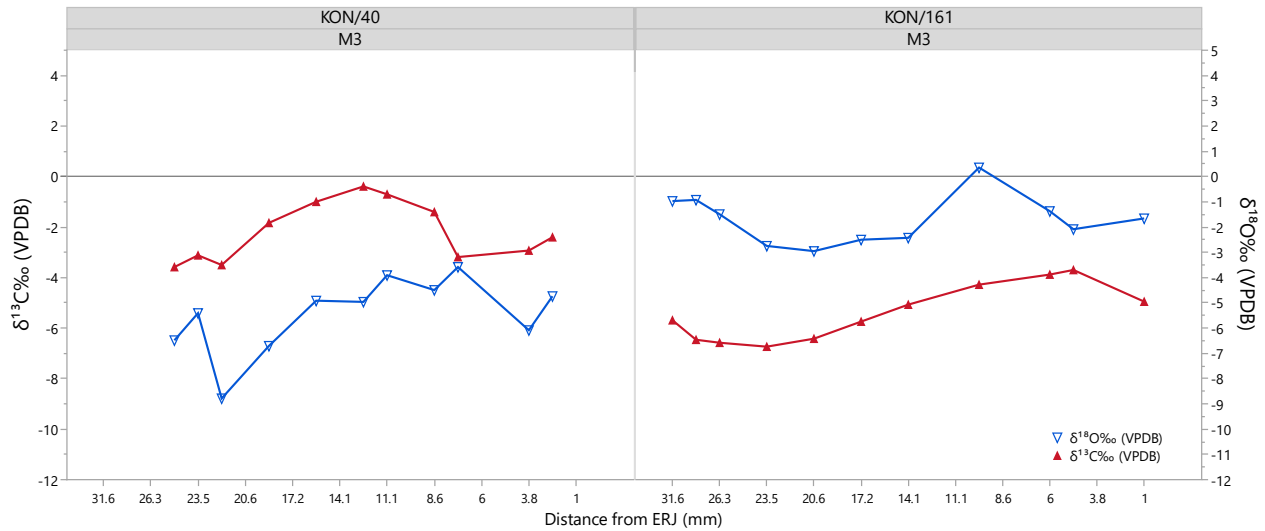


Figure 5.26. Serial $\delta^{13}\text{C}$ and $\delta^{18}\text{O}$ values for two individual *Ovis/capra* M3 KON/40 and KON/161

Two individual *Ovis/capra* M3 were sampled at Stayt (Figure 5.26). The mean $\delta^{13}\text{C}$ value for all samples from KON/40 (n=11) is $-2.19 \pm 1.17\text{‰}$ with a range of 3.19‰. The mean $\delta^{18}\text{O}$ value for all samples from KON/40 is $-5.46 \pm 1.48\text{‰}$ with a range of 5.20‰. The mean $\delta^{13}\text{C}$ value for all samples from KON/161 (n=11) is $-5.41 \pm 1.11\text{‰}$ with a range of 3.04‰. The mean $\delta^{18}\text{O}$ value for all samples from KON/161 is $-1.71 \pm 0.97\text{‰}$ with a range of 3.31‰

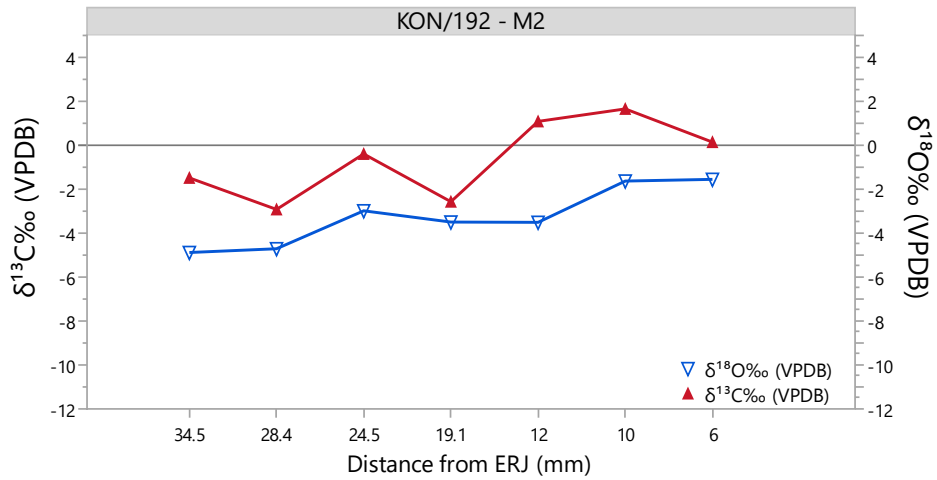


Figure 5.27. Serial $\delta^{13}\text{C}$ and $\delta^{18}\text{O}$ values for KON/192 Ovis/capra M2,

The mean $\delta^{13}\text{C}$ value across all samples ($n=7$) for the M2 of KON/192 Ovis/capra (Figure 5.27) is $-0.64 \pm 1.76\text{‰}$ with a range of 4.58‰. The mean $\delta^{18}\text{O}$ for the M2 is $-3.25 \pm 1.32\text{‰}$ with a range of 3.33‰

Chapter 6 Discussion and Conclusion

6.1 Discussion

The first section will provide a broad-level discussion in terms of the results for select cattle, caprine, and wild individuals presented in Chapter 5. Complete data tables (including reference standards) can be found in Appendix B. Concluding remarks highlight the implications of this data regarding livestock diets and pastoral management practices in the Middle Iron Age.

6.1.1 Cattle

Carbon

Overall, the cattle sampled as part of this research were able to maintain a graze dominant diet for most of the year suggested by a mean $\delta^{13}\text{C}$ value of $0.17 \pm 1.68\text{‰}$ and a median $\delta^{13}\text{C}$ value of 0.35‰ for all cattle sampled ($n = 11$). A total of three wild bulk grazer individuals were sampled from MNR 74 and Mutamba. Despite the small sub-sample size, the $\delta^{13}\text{C}$ and $\delta^{18}\text{O}$ values derived from these individuals provide at least some indication as to the natural rhythms of the local and regional pastures. This is because the diets of wild animals can be assumed to be reflective of the natural ecological context unimproved or unaltered by human intervention.

Previous work on modern faunal enamel conducted in the northern Limpopo province (Smith, 2005) which accounted for the fossil fuel effect (Dombrosky, 2020: 477) in the $\delta^{13}\text{C}$ values found an enrichment factor of $\sim 1.5\text{‰}$ between modern and archaeological samples. These results suggest that a likely archaeological range for pure grazing (C_4) and pure browsing (C_3) animals falls between $\sim 1\text{‰}$ and $\sim -12.3\text{‰}$ respectively (Smith, 2005: 131). Using these bounds as broad

parameters in forming an archaeological region-specific scale, inferences can be made as to the quality of diet for different individuals and livestock groups.

The single equid from MNR 74 recorded a mean $\delta^{13}\text{C}$ value of $-1.04 \pm 1.77\text{‰}$ of all samples ($n=14$) across the height of the tooth. The two *A. buselaphus* individuals sampled from Mutamba provide a mean $\delta^{13}\text{C}$ value of $-1.03 \pm 1.75\text{‰}$. The ranges for the two *A. buselaphus* and the equid are within the published expected ranges (above) of 100% grazing and browsing species (see chapter 3 for a more detailed discussion).

Given that modern domesticated and wild species in the region are unable to access year-round graze and are reliant on supplemental browse or the provisioning of graze (Smith, 2005: 169), the archaeological cattle diets sampled in this research suggests that they too were seasonally managed to some extent (see Figure 6.2.). There is, however, a degree of internal variation in this pattern at an inter-site scale allowing for discussion on aspects of the management practices that accompanied the livestock across the hinterland landscape.

The cattle samples from Stayt and Mutamba, both representing larger settlements, show a demonstrably higher proportion of C_4 plant consumption than those from the contemporaneous cattle-post sites in the sample (MNR 74 and MNR 78) (Figure 5.1). This is supported by the mean $\delta^{13}\text{C}$ value for cattle at the larger both settlements being $0.6 \pm 1.59\text{‰}$ as opposed to the lower mean $\delta^{13}\text{C}$ values of $-0.86 \pm 1.27\text{‰}$ from the cattle-post sites. This suggests that at least some of the cattle at the smaller sites may have been supplementing their diet with a degree of browsing.

The browsing pattern observed in the diets of cattle may reflect the highly variable and, at times, fairly limited grazing capacity available between the Thsirundu mountains and the Limpopo river (van Rooyen, 2002) – an environment in which the use of a cattle-post based transhumant management practice likely have been employed to ensure optimal cattle diets year-round.

Other factors such as general animal health should also be considered when dealing with $\delta^{13}\text{C}$ values of herbivore tooth enamel. This is because *in-vivo* taphonomic processes such as wear, and disease will alter the isotopic record contained within the tooth post-mineralisation. The M2 crown heights for the individuals from MNR 74 and MNR 78 were lower than that of M2s from Mutamba and Stayt. In addition, cavities/hypoplasia were observed on the upper part of the tooth for MNR74/B063/01. The crown height and tooth pathology suggest poorer animal condition at MNR 74 and MNR 78, suggesting that sickly or older individuals may have been selected for consumption at the cattle posts. Since the inhabitants of cattle posts would be tending cattle on behalf of higher status clients, it is possible that this power asymmetry was reflected in the selection of animals being killed for meat and would therefore be individuals in poorer condition.

In contrast to the cattle post animals, two individual *Bos taurus* from the larger settlement at Stayt, KON/T4 and KON/295, were both able to sustain pure grazing diets with mean tooth $\delta^{13}\text{C}$ values of $2.0 \pm 0.2\text{‰}$ and $3.27 \pm 0.39\text{‰}$ respectively. These diets were maintained throughout variations in the prevailing seasonal profile indicated by rising $\delta^{18}\text{O}$ values characterising KON/T4 and declining $\delta^{18}\text{O}$ values characterising KON/295 (see Figure 5.23).

Oxygen

As detailed in chapter 3, assessing the potential water sources for livestock is also an important consideration when interpreting seasonal variations in the $\delta^{18}\text{O}$ values of tooth enamel. Beyond the broad season effect on $\delta^{18}\text{O}$ values, local variations in moisture and aridity are also important drivers to be considered when interpreting patterns observed in the oxygen isotope ratios of the animals from this region. The overprinting (Makarewicz & Pederzani, 2017: 21) of these environmental effects in tooth enamel complicates the interpretation of seasonal information and limits the level to which one is able to draw meaningful inferences from observed patterns.

The comparatively high range in $\delta^{18}\text{O}$ values for MNR74/B024 (Table 6.1) may be explained by higher levels of climatic variability either through local variability in climate or movement through different regions. Given the cattle post context which is in essence a system of mobile herd management, the latter is likely the case.

Discrete differences in the ecotones of the research area allow for a larger landscape pattern to be potentially visible. By comparing the amplitudes of $\delta^{18}\text{O}$ values in cattle from sites closer to the moister and more temperate Soutpansberg mountains (Mutamba, Stayt) to those further north in a more arid region (MNR sites) a pattern emerges. Cattle from the two southern sites, Mutamba and Stayt display broader ranges of variation in $\delta^{18}\text{O}$ values (mean = 3.45) as opposed to cattle from the northern sites in the Maremani Nature Reserve where the amplitudes in $\delta^{18}\text{O}$ values are overall more compressed (mean = 2.86) as can be seen in Table 6.1. below.

Table 6.1. Summary of cattle $\delta^{18}O$ values per tooth from each site, grouped as northern and southern clusters.

Tooth ID	Site	Mean	Std Dev	Range
Northern Sites				
MNR04/341/08	MNR04	-3.22	0.81	2.44
MNR74/B024	MNR74	-2.64	1.83	6.19
MNR74/B063/01	MNR74	-4.87	0.39	1.11
MNR74/B063/02	MNR74	-4.81	1.20	3.63
MNR78/231/05	MNR78	-2.88	0.76	2.30
MNR78/231/06	MNR78	-2.53	0.64	1.51
Southern Sites				
KON/100	KON	-4.26	1.13	3.93
KON/114	KON	-4.86	0.66	2.52
KON/295	KON	-4.55	1.16	3.69
KON/T4	KON	-3.67	1.33	4.41
MUT/1031/F07	MUT	-1.14	1.07	3.31
MUT/2012/F08	MUT	-3.09	0.85	3.05
MUT/2012/F09	MUT	-2.57	1.37	4.63
MUT/2012/F10	MUT	-2.04	0.93	2.92
MUT/2099/F09	MUT	-1.84	0.80	2.81
MUT/2167/F01	MUT	-2.32	1.18	3.19

This patterning is likely the result of a combination of mechanisms (see chapter 3) such as higher rates of evaporation coupled with rainfall type (short, heavy storms) being a more potent driver of variability in the more arid northern regions, whereas the foothills of the Soutpansberg offered a more stable annual climate with a higher Mean Annual Precipitation (Smith, 2005: 72).

Variation is also introduced through the type of water source consumed such as, for example, streams, pans, and springs. Given that the sites sampled in this region are located near rivers, it is likely that these were the primary source of water.

The isotopic characterisation of cattle $\delta^{13}C$ and $\delta^{18}O$ enamel also provide some insight into the management strategies of herds in the Mapungubwe hinterland. Tentative patterns emerge that may be indicative of either i.) seasonal regional mobility, or ii.) winter fodder provisioning and

perhaps localised transhumant practices. In order to properly address the point of regional mobility, a study incorporating strontium isotopes would be the most suitable methodology in an attempt to reach a meaningful conclusion on the movement across the landscape of livestock.

Foddering

Foddering is the practice of gathering and storing food during times of abundance for livestock to feed on in the leaner months of the year. The resolution afforded through the serial sampling method allows for more time sensitive signals of dietary contribution to be analysed. It is possible to infer foddering practices by archaeological communities through the occurrence of carbon isotope ratios that reflect vegetation types that the animal would otherwise not have had usual seasonal access to (Janzen, 2015: 147). Further, the amplitude of $\delta^{13}\text{C}$ values may also be an indicator of quality of diet as cattle with higher amplitudes suggest that more C_3 browse was incorporated into the diet (House, 2021: 148).

By comparing the $\delta^{13}\text{C}$ values of co-localised wild bulk grazing species (in this case *A. buselaphus*) to those of cattle an assessment of grazer diets with and without human intervention is made possible (Makarewicz & Pederzani, 2017). A comparison (Figure 6.1) of the variance in the serial $\delta^{13}\text{C}$ values of the mandibular M2s of two *A. buselaphus* individuals to that of a lower M2 of a *B. taurus* individual from MNR 78 indicate a much greater degree of variability through time in the diet of the wild species ($2\sigma = 0.52$ and 1 , respectively) than that of the cattle ($2\sigma = 0.28$).

The relatively low variance ($2\sigma = 0.36$) in diet across the combined $\delta^{13}\text{C}$ values of MNR78/231 M2 and M3 contrasts to the more variable seasonal pattern indicated by the $\delta^{18}\text{O}$ values across

the toothrow (see Figure 5.13). The mean $\delta^{13}\text{C}$ value for the M2 and M3 of MNR78/231 is $-0.26 \pm 0.53\text{‰}$ and $-0.04 \pm 0.66\text{‰}$, respectively, which indicates that this individual was able to access C_4 food fairly consistently, potentially offset slightly by the incorporation of some browse during the mineralisation of the M2.

The amplitude of $\delta^{13}\text{C}$ values for the two *A. buselaphus* individuals is 2.52 and 2.85, respectively. When compared to the more attenuated amplitudes of *B. taurus* MNR78/231 M2 (2.1‰) and M3 (1.51‰) it appears the domesticate had more consistent access to C_4 food than the wild *A. buselaphus*. The mean $\delta^{18}\text{O}$ for both cattle teeth and both *A. buselaphus* teeth are within similar ranges ($-2.72 \pm 0.72\text{‰}$ and $-2.9 \pm 0.84\text{‰}$, respectively) suggesting that these individuals shared similar environmental conditions during their early lives. Taken together these data may suggest that cattle wintering in the same environmental conditions as wild grazers were receiving a steadier supply of C_4 fodder throughout the winter.

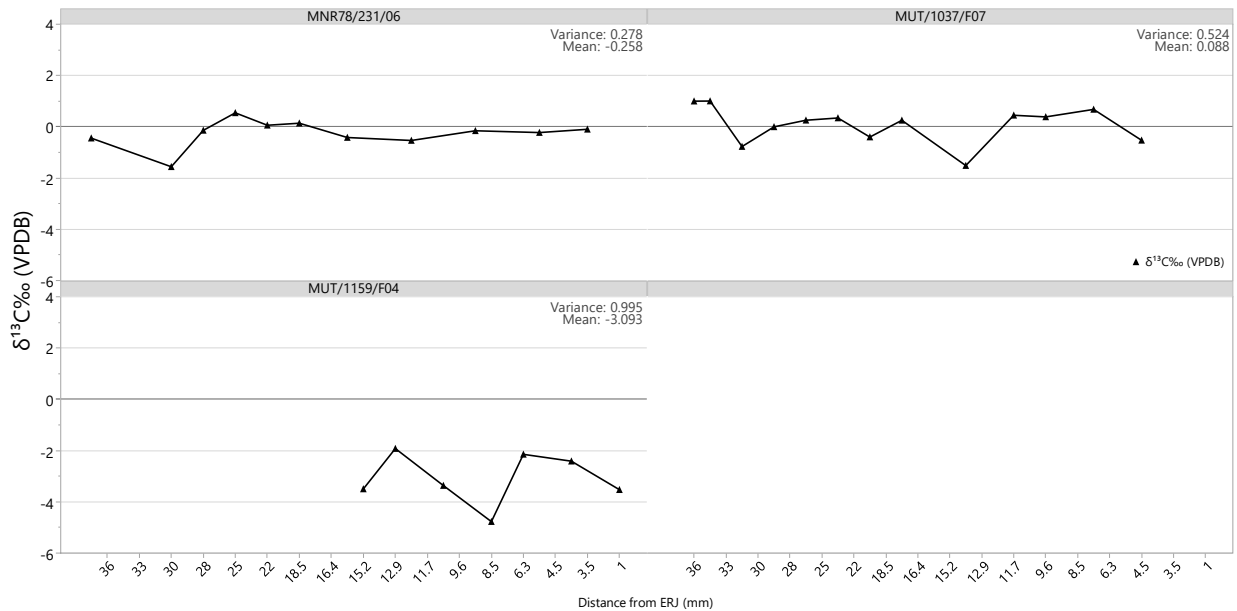


Figure 6.1 Serial $\delta^{13}\text{C}$ values for one cow from MNR78 and two hartebeest from Mutamba

The above insights remain inconclusive as only a limited number of suitably comparable skeletal analogues (in this case second mandibular molars) are available in the present study, however a more exhaustive application of the highlighted example above to the complete dataset will certainly further clarify any interpretation.

6.1.2 Caprines

The category *Caprines* is a taxonomic phenomenon that arises directly out of the difficulty faced by zooarchaeologists in assigning a species level identification to the remains of *O. aries* and *C. hircus*. The close similarities between sheep and goat skeletal and dental morphology combined with the fragmentary nature of zooarchaeological remains presents myriad challenges to attaining a species-level identification using traditional techniques (Jeanjean et al., 2022). A consequence of this is that the often-encountered category of sheep/goat, or caprine, contains both grazers (e.g., *O. aries*) and browsers (e.g., *C. hircus*) which must be taken into consideration when dealing with a livestock group categorised as caprine.

Attempts at identifying sheep and goat based on $\delta^{13}\text{C}$ enamel serial values have found success in C_4 dominated grasslands as the feeding habits of the two species differ. In a C_4 grassland environment sheep would prefer graze over browse while the converse is true for goats (Balasse & Ambrose, 2005). Some overlap may exist as animals may be compelled to deviate from their preferred diet, however the lack of overlap in mean values of $\delta^{13}\text{C}$ have been demonstrated as being useful in distinguishing between the two species (Balasse & Ambrose, 2005). This manifests isotopically as goats displaying overall lower $\delta^{13}\text{C}$ tooth averages and a greater intra-tooth range compared to sheep.

The mean $\delta^{13}\text{C}$ value of $-7.49 \pm 1.09\text{‰}$ (table 4.1) for one *O. aries* from Mutamba (MUT/1011/F13) show that this individual had a diet that was dominated by C_3 browse. These results raise some potential interesting questions as the species ID (based on a maxillary tooththrow) for this particular individual (*O. aries*) indicates that this was a preferentially grazing animal, however the $\delta^{13}\text{C}$ values are consistent with a browser diet. While many physiological and environmental reasons may account for this anomaly, the most likely explanation is the difficulty in distinguishing the archaeological remains of sheep from goat.

Differences in the amplitude of the intra-tooth $\delta^{18}\text{O}$ are potentially influenced by different inputs of water sources utilised by the sheep and goats i.e. water through open sources of water or leaf water respectively (Makarewicz & Pederzani, 2017: 26). The close tracking of the serially plotted $\delta^{18}\text{O}$ and $\delta^{13}\text{C}$ values (Table 5.2) observed in the M2 and M3 of a sheep from Mutamba (MUT/2019/F20) suggests that this animal derived most of its water from its diet as opposed to open-stand sources of water (Makarewicz & Pederzani, 2017; Gillis et al., 2021).

The steep elevation in mean $\delta^{13}\text{C}$ values from -6.82‰ in M1 and -3.77‰ in the M2 of *Ovis/capra* MUT/2177 (Figure 5.10) is potentially related to a shift in diet during the respective tooth mineralisation phases that take place before (M1) and after (M2) weaning. M2, producing in some cases more elevated values, however this phenomenon has subsequently been shown to be highly variable across different species and climates (Towers et al. 2014:232 cf. Luyt and Sealy 2018) therefore more controlled species-specific work is required to better quantify this effect, especially for the summer rainfall region of southern Africa. Taking this into account, the increased $\delta^{13}\text{C}$ values observed alongside increasing $\delta^{18}\text{O}$ values in the first portion (25-15mm

from ERJ) of the M2 (Figure 5.10) suggest that this individual had some access to C4 graze during the initial period of mineralisation.

Ingestion of water via milk has similarly been believed to distort the seasonal pattern of the $\delta^{18}\text{O}$ values across the M1 relative to subsequent molars. This phenomenon, however, has yet to be demonstrated as a systematic inter-tooth pattern due to differences in suckling behaviour, while research into this topic (Luyt & Sealy, 2018) has indicated that weaning signals are likely overridden by prevailing seasonal patterns.

A clear seasonal relationship can be seen in the diet of MNR74/B065 *Ovis/capra* where lower $\delta^{18}\text{O}$ values — characterising summer in the arid Limpopo province, based on modern reference samples (Smith, 2005: 128) — inversely coincide with higher $\delta^{13}\text{C}$ values in a sinusoidal pattern (Figure 5.17). Further, there seems to be no indication that a weaning induced enrichment shift in the isotope values between M1 and M2 occurred for this individual (Luyt & Sealy, 2018). The dietary profile of this *Ovis/capra* is reminiscent of the feeding behaviour of *O. aries* that will preferentially graze when grass is accessible (typically mid-late summer in northern Limpopo).

A very different seasonal feeding behaviour can be seen in the *Ovis/capra* MNR74/B255 (Figure 5.18) which exhibits overall much lower $\delta^{13}\text{C}$ values (mean = $-7.94 \pm 1.88\%$) consistent with that of a browsing species. Similarly to MNR74/B065, this individual displays a sinusoidal pattern along the tooththrow however the relationship between the $\delta^{13}\text{C}$ and $\delta^{18}\text{O}$ plotted profiles are different. The largely direct relationship between the amplitude of both values for MNR74/B255 may possibly be driven by the source of body water and diet being the same (i.e. leaf browse) in this individual (Makarewicz & Pederzani, 2017: 22) which further supports a

tentative interpretation of this individual being a semi-obligate drinking (Makarewicz, 2017b) browser such as *C. hircus*.

The $\delta^{13}\text{C}$ values across the tooththrow of *Ovis/capra* KON/106 (Figure 5.25) are consistent with a browser type diet. This may be further confirmed by the variability displayed in the $\delta^{18}\text{O}$ values as they are influenced, amongst other factors, by variances in leaf water $\delta^{18}\text{O}$ values. The signal derived from the $\delta^{18}\text{O}$ series indicates that environmental variability was significant with and increasing arid trend over the period of tooththrow mineralisation.

The exploration of such distinctions is, however, beyond the immediate scope of this research therefore the values for sheep, goats, and sheep/goat (i.e., caprines) will be discussed in broad terms of general patterns related to climate and overall herd management.

6.1.3 Differences in livestock herd management: Cattle vs Caprines

The patterns observed in the $\delta^{13}\text{C}$ values of cattle and caprine teeth sampled across the five sites forms the basis for broad inferences about livestock management practices. Work in Shashe-Limpopo Confluence Area has shown that a coordinated approach to pastoral management was adopted as a possible response to environmental challenges faced by a growing population (Smith et al., 2010). Such coordination is logical against the backdrop of the growing socio-political complexity evidenced through the establishment of the settlement at Mapungubwe Hill. Furthermore, the spread of Mapungubwe type ceramics across the region (Antonites & Ashley, 2016) points toward a nascent civilisation operating under an expansionist paradigm in a landscape that provided multiple opportunities.

Overall, cattle from five single-component sites in the Mapungubwe hinterland appear to have had more consistent $\delta^{13}\text{C}$ values over time (Figure 6.2) displaying lower variance ($2\sigma = 2.83$) as opposed to more the more variable caprine values ($2\sigma = 4.61$) which can be interpreted as cattle having a more consistent diet over time.

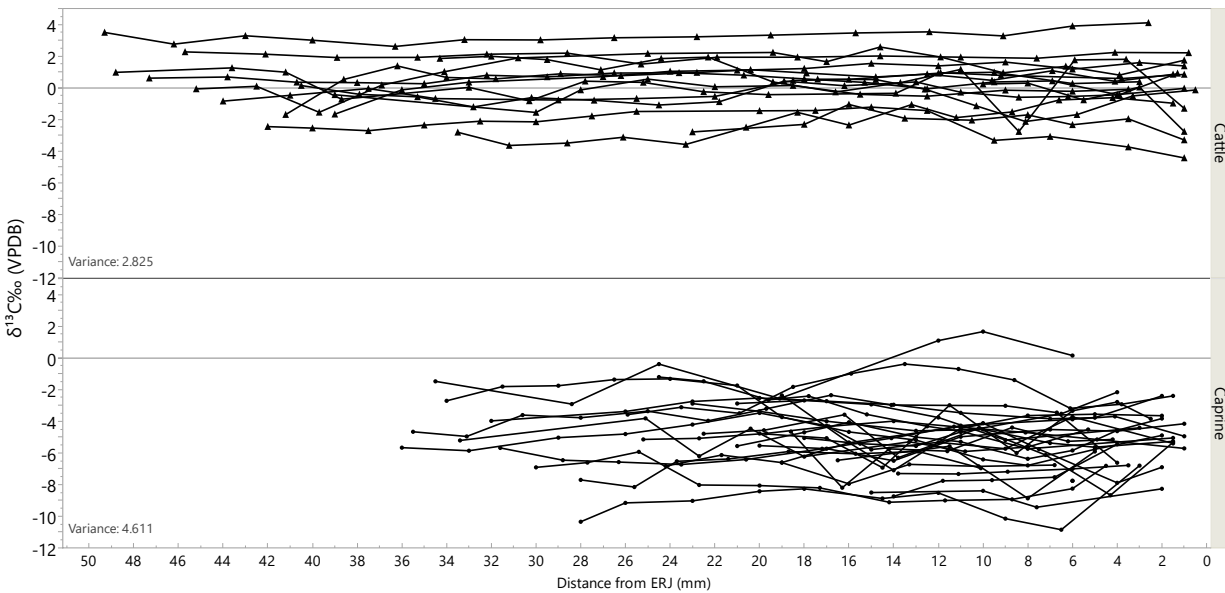


Figure 6.2. Plot of all sampled cattle (top) and caprine (bottom) molar $\delta^{13}\text{C}$ values showing variance in diet over time

The consistency of C_4 dietary inputs over time seen in cattle suggests that the herders took measures, either through mobility or planning, to ensure that cattle had access to preferential fodder despite natural seasonal fluctuations in plant C_3/C_4 plant cover.

A higher variance (2σ) value for the caprine category is not altogether unexpected due to this group including both browsing and grazing species - as discussed (above), however this does not necessarily preclude gross observations at potential differential herding strategies. Problems with $\delta^{18}\text{O}$ amplitude values in comparing domesticated grazers such as sheep and cattle are faced due to differences in physiology and behaviour. The difference in period of tooth mineralisation between the two species is a further factor obfuscating comparisons between values derived from the two species (Balasse et al., 2013).

Table 6.2 Mean values of the ranges of variation in the serial tooth $\delta^{13}\text{C}$ values for grouped cattle and caprines from each site.

SITE	Cattle $\delta^{13}\text{C}$ range	Caprine $\delta^{13}\text{C}$ range
MUT	6.22	8.22
MNR 78	2.54	4.14
MNR 74	4.72	9.52
MNR 04	3.29	4.72
KON	6.87	9.61
MEAN	4.72	7.24

Overall lower mean ranges of variation in the serial tooth isotope ratios (Table 6.2) among cattle may suggest that individuals maintained a more consistent diet over the period of tooth mineralisation (Reid et al., 2019: 8) when compared to caprines. This is taken to be tentative evidence of a dual system of livestock management employed among a common Middle Iron Age agropastoralist society that sought to balance the daily dietary requirements of the communities while maintaining their economic and political status.

The prioritisation of effort and resources expended on maintaining high-value cattle herds as suggested by the data presented here suggests that agropastoralists in the Mapungubwe hinterland were not confined to herding strategies that focused solely on subsistence. Ensuring that cattle as a store of wealth were maintained through social and political networks allowed communities to better leverage the landscape and compound their wealth, while caprine herds could ostensibly fulfil the meat contribution to human diet.

6.2 Conclusion

Subsistence economies are derived from the appropriate selection of seasonal and landscape tools and resources available to a society. Some instances may necessitate a group mooring near a fixed resource such as arable land while some may require a more mobile mechanism as is practised among pastoralists. Complexity in the relationships between people is born when attempts are made to coordinate these different modes of subsistence under a socio-economic system of shared cultural identity. While it is reasonable to assume that a group practicing an agropastoral subsistence economy would utilise their mobility and knowledge of rhythmic shifts in the landscape to secure the best possible area for food production, it is also reasonable to assume that these societies have ambition beyond securing their dietary needs.

The rise of social complexity in southern Africa is underscored by a steady increase in networks of commodity exchange between both domestic and international trade centres. The culmination of an elite class-based society at Mapungubwe Hill demonstrates that with the growth in complexity came a new suite of symbols with which status could be signalled. That the

civilisation which grew out of the Leopard's Kopje ceramic tradition was of the first to seek increasing control of an entire landscape — as opposed to groups seeking only discrete resource exploitation — speaks to a deepening sense of agency realised by actors within the Mapungubwe civilisation.

In order to secure a steady stream of goods and people flowing along the various networks, instances may arise where people are compelled to inhabit areas that are marginal to food production in order to exploit discrete economic resources. Pastoralism affords this kind of resilience to subsistence economy that allows marginal environment occupation. It has been argued that in the Shashe-Limpopo Basin the shift to geographically expanded agropastoral management system arose contemporaneous to the relocation of primary settlement from K2 to Mapungubwe. This is seen as a response to the increased demand for agricultural land required to support the growing population in the Shashe-Limpopo Confluence Area (Smith, 2005: 16). The maintenance of livestock herds, especially cattle, outside the Shashe-Limpopo Confluence Area may also have presented organs of a central political authority seeking to expand influence over the landscape opportunities to mobilise their reach while maintaining the sustainability of the livestock wealth which enables such agency.

The tentative findings of this research suggest that care was taken by the herding societies to ensure that cattle had nutritionally secure diets year-round. Whether this was through transhumant management of herds or the stockpiling of dry season fodder – or a combination of both – remains beyond the purview of this project. However, new textures to the understanding of the Middle Iron Age are presented by probing the stable isotope data presented here through the lens of what is known archaeologically about hinterland societies.

Livestock were not a homogenous component of the subsistence economy of Middle Iron Age societies as indicated by the suggestion of a dual pastoral management system between cattle and caprine herds. Further evaluation and contextualisation of the archaeological contexts of the people behind the animals (Antonites, 2012), and the networks of communities (Antonites & Ashley, 2016) that they formed may help to further elucidate the social dynamics behind such a system. Further, the data presented in this research support the notion that transhumant pastoral practices formed a part of hinterland complexity, and indeed, the Greater Mapungubwe Landscape as a whole.

References

- Antonites, A. 2012. Political and Economic Interactions in the Hinterland of the Mapungubwe Polity, C. AD 1200-1300, South Africa. Yale University. Available: <https://books.google.co.za/books?id=s8-onQEACAAJ>.
- Antonites, A. 2014. Glass beads from Mutamba: patterns of consumption in thirteenth-century southern Africa. *Azania: Archaeological Research in Africa*. 49(3):411–428. DOI: 10.1080/0067270X.2014.959316.
- Antonites, A. 2019a. Mapungubwe’s hinterland: excavations, ceramics and other material culture from Mutamba in the Soutpansberg. *SOUTHERN AFRICAN HUMANITIES*.
- Antonites, A. 2019b. Fiber Spinning During the Mapungubwe Period of Southern Africa: Regional Specialism in the Hinterland. *African Archaeological Review*. 36(1):105–117. DOI: 10.1007/s10437-018-09323-9.
- Antonites, A.R. 2018. A revised chronology for the Zhizo and Leokwe horizons at Schroda. *SOUTHERN AFRICAN HUMANITIES*. 25.
- Antonites, A. & Ashley, C.Z. 2016. The mobilities turn and archaeology: new perspectives on socio-political complexity in thirteenth-century northern South Africa. *Azania: Archaeological Research in Africa*. 51(4):469–488. DOI: 10.1080/0067270X.2016.1249586.
- Antonites, A.R., Uys, S. & Antonites, A. 2016. Faunal remains from MNR 74, a Mapungubwe period settlement in the Limpopo Valley. 6:13.
- Badenhorst, S. 2009. The Central Cattle Pattern During The Iron Age Of Southern Africa: A Critique Of Its Spatial Features. *The South African Archaeological Bulletin*. 64(190):148–155.
- Badenhorst, S. 2015. Intensive hunting during the Iron Age of Southern Africa. *Environmental Archaeology*. 20(1):41–51. DOI: 10.1179/1749631414Y.0000000039.
- Balasse, M. & Ambrose, S.H. 2005. Distinguishing Sheep and Goats Using Dental Morphology and Stable Carbon Isotopes in C4 Grassland Environments. *Journal of Archaeological Science*. 32(5):691–702. DOI: 10.1016/j.jas.2004.11.013.
- Balasse, M., Ambrose, S.H., Smith, A.B. & Price, T.D. 2002. The Seasonal Mobility Model for Prehistoric Herders in the South-western Cape of South Africa Assessed by Isotopic Analysis of Sheep Tooth Enamel. *Journal of Archaeological Science*. 29(9):917–932. DOI: 10.1006/jasc.2001.0787.
- Balasse, M., Smith, A.B., Ambrose, S.H. & Leigh, S.R. 2003. Determining Sheep Birth Seasonality by Analysis of Tooth Enamel Oxygen Isotope Ratios: The Late Stone Age Site of Kasteelberg (South Africa). *Journal of Archaeological Science*. 30(2):205–215. DOI: 10.1006/jasc.2002.0833.

- Balasse, M., Boury, L., Ughetto-Monfrin, J. & Tresset, A. 2012. Stable isotope insights ($\delta^{18}\text{O}$, $\delta^{13}\text{C}$) into cattle and sheep husbandry at Bercy (Paris, France, 4th millennium BC): birth seasonality and winter leaf foddering. *Environmental Archaeology*. 17(1):29–44. DOI: 10.1179/1461410312Z.00000000003.
- Balasse, M., Bălăşescu, A., Janzen, A., Ughetto-Monfrin, J., Mirea, P. & Andreescu, R. 2013. Early herding at Magara-Boldul lui Moş Ivănuş (early sixth millennium BC, Romania): environments and seasonality from stable isotope analysis. *European Journal of Archaeology*. 16(2):221–246. DOI: 10.1179/1461957112Y.00000000028.
- Balasse, M., Bălăşescu, A., Tornero, C., Fremondeau, D., Hovsepyan, R., Gillis, R. & Popovici, D. 2017. Investigating the scale of herding in Chalcolithic pastoral communities settled along the Danube River in the 5th millennium BC: A case study at Borduşani-Popină and Hârşova-tell (Romania). *Quaternary International*. 436:29–40. DOI: 10.1016/j.quaint.2015.07.030.
- Blaise, E. & Balasse, M. 2011. Seasonality and season of birth of modern and late Neolithic sheep from south-eastern France using tooth enamel $\delta^{18}\text{O}$ analysis. *Journal of Archaeological Science*. 38(11):3085–3093. DOI: 10.1016/j.jas.2011.07.007.
- Calabrese, J.A. 2000. Metals, Ideology and Power: The Manufacture and Control of Materialised Ideology in the Area of the Limpopo-Shashe Confluence, c.AD 900 to 1300. *Goodwin Series*. 8:100. DOI: 10.2307/3858051.
- Calabrese, J.A. 2001. Interregional Interaction in Southern Africa: Zhizo and Leopard's Kopje Relations in Northern South Africa, Southwestern Zimbabwe, and Eastern Botswana, AD 1000 to 1200. *African Archaeological Review*. 28.
- Calabrese, J.A. 2005. Ethnicity, Class, and Polity: The Emergence of Social and Political Complexity in the Shashi-Limpopo Valley of Southern Africa, AD 900-1300. PhD Thesis. University of the Witwatersrand.
- Cerling, T.E. & Harris, J.M. 1999. Carbon isotope fractionation between diet and bioapatite in ungulate mammals and implications for ecological and paleoecological studies. *Oecologia*. 120(3):347–363. DOI: 10.1007/s004420050868.
- Cerling, T.E., Harris, J.M. & Passey, B.H. 2003. Diets Of East African Bovidae Based on Stable Isotope Analysis. *Journal of Mammalogy*. 84(2):456–470. DOI: 10.1644/1545-1542(2003)084<0456:DOEABB>2.0.CO;2.
- Chirikure, S., Manyanga, M., Pollard, A.M., Bandama, F., Mahachi, G. & Pikirayi, I. 2014. Zimbabwe Culture before Mapungubwe: New Evidence from Mapela Hill, South-Western Zimbabwe. *PLoS ONE*. 9(10):e111224. DOI: 10.1371/journal.pone.0111224.
- Coertze, R.D. 1986. Livestock In the social and cultural life of African communities.

- Copeland, S.R., Sponheimer, M., Spinage, C.A., Lee-Thorp, J.A., Codron, D. & Reed, K.E. 2009. Stable isotope evidence for impala *Aepyceros melampus* diets at Akagera National Park, Rwanda. *African Journal of Ecology*. 47(4):490–501. DOI: 10.1111/j.1365-2028.2008.00969.x.
- Coplen, T.B. 2011. Guidelines and recommended terms for expression of stable-isotope-ratio and gas-ratio measurement results. *Rapid Communications in Mass Spectrometry*. 25(17):2538–2560. DOI: 10.1002/rcm.5129.
- Coutu, A.N., Whitelaw, G., le Roux, P. & Sealy, J. 2016. Earliest Evidence for the Ivory Trade in Southern Africa: Isotopic and ZooMS Analysis of Seventh–Tenth Century ad Ivory from KwaZulu-Natal. *African Archaeological Review*. 33(4):411–435. DOI: 10.1007/s10437-016-9232-0.
- De Winter, N.J., Snoeck, C. & Claeys, P. 2016. Seasonal Cyclicity in Trace Elements and Stable Isotopes of Modern Horse Enamel. *PLOS ONE*. 11(11):e0166678. DOI: 10.1371/journal.pone.0166678.
- Denbow, J. 1999. Material culture and the dialectics of identity in the Kalahari: AD 700–1700. In *Beyond Chiefdoms*. 1st ed. S.K. McIntosh, Ed. Cambridge University Press. 110–123. DOI: 10.1017/CBO9780511558238.010.
- Denbow, J., Smith, J., Ndobochani, N.M., Atwood, K. & Miller, D. 2008. Archaeological excavations at Bosutswe, Botswana: cultural chronology, paleo-ecology and economy. *Journal of Archaeological Science*. 22.
- Dombrosky, J. 2020. A ~1000-year ¹³C Suess correction model for the study of past ecosystems. *The Holocene*. 30(3):474–478. DOI: 10.1177/0959683619887416.
- Du Piesanie, J. 2009. Understanding the socio-political status of Leokwe society during the Middle Iron Age in the Shashe-Limpopo Basin through a landscape approach. Thesis. Available: <http://wiredspace.wits.ac.za/handle/10539/6967> [2020, June 07].
- Ekblom, A., Gillson, L. & Notelid, M. 2011. A historical ecology of the Limpopo and Kruger National Parks and lower Limpopo Valley. *Journal of Archaeology and Ancient history*. 1(1):1–29.
- Ellis, R.P., Vogel, J.C. & Fuls, A. 1980. Photosynthetic pathways and the geographical distribution of grasses in South West Africa/Namibia. *South African Journal of Science*. 76(7):307–314. DOI: 10.10520/AJA00382353_10244.
- Evers, T.M. 1983. “Oori” or “Moloko”: the origins of the Sotho-Tswana on the evidence of the Iron Age of the Transvaal: reply to R.J. Mason. *South African Journal of Science*. 79:261–264.
- Fricke, H.C. & O’Neil, J.R. 1996. Inter-and intra-tooth variation in the oxygen isotope composition of mammalian tooth enamel phosphate: implications for palaeoclimatological and palaeobiological research. *Palaeogeography, Palaeoclimatology, Palaeoecology*. 126(1–2):91–99.

- Fricke, H.C., Clyde, W.C. & O'Neil, J.R. 1998. Intra-tooth variations in $\delta^{18}\text{O}$ (PO_4) of mammalian tooth enamel as a record of seasonal variations in continental climate variables. 12.
- Gerling, C., Doppler, T., Heyd, V., Knipper, C., Kuhn, T., Lehmann, M.F., Pike, A.W.G. & Schibler, J. 2017. High-resolution isotopic evidence of specialised cattle herding in the European Neolithic. *PLOS ONE*. 12(7):e0180164. DOI: 10.1371/journal.pone.0180164.
- Gillis, R.E., Bulatović, J., Penezić, K., Spasić, M., Tasić, N.N. & Makarewicz, C.A. 2021. Of herds and societies—Seasonal aspects of Vinča culture herding and land use practices revealed using sequential stable isotope analysis of animal teeth. *PLOS ONE*. 16(10):e0258230. DOI: 10.1371/journal.pone.0258230.
- Granovetter, M. 1983. The Strength of Weak Ties: A Network Theory Revisited. *Sociological Theory*. 1:201. DOI: 10.2307/202051.
- Hall, M. 1986. The Role of Cattle in Southern African Agropastoral Societies: More than Bones Alone Can Tell. *Goodwin Series*. 5:83. DOI: 10.2307/3858150.
- Hall, M. 1987. Archaeology and Modes of Production in Pre-Colonial Southern Africa. *Journal of Southern African Studies*. 14(1):1–17.
- Hare, V. & Sealy, J. 2013. Middle Pleistocene dynamics of southern Africa's winter rainfall zone from $\delta^{13}\text{C}$ and $\delta^{18}\text{O}$ values of Hoedjiespunt faunal enamel. *Palaeogeography, Palaeoclimatology, Palaeoecology*. 374:72–80. DOI: 10.1016/j.palaeo.2013.01.006.
- Hogg, A.G., Heaton, T.J., Hua, Q., Palmer, J.G., Turney, C.S., Southon, J., Bayliss, A., Blackwell, P.G., et al. 2020. SHCal20 Southern Hemisphere Calibration, 0–55,000 Years cal BP. *Radiocarbon*. 62(4):759–778. DOI: 10.1017/RDC.2020.59.
- House, M. 2021. Straight from the cow's mouth: investigating procurement and management strategies in cattle supplied to Great Zimbabwe using a multi-isotopic approach: University of Cape Town, 2020 (<https://open.uct.ac.za/handle/11427/32684>). Available: <https://www.tandfonline.com/doi/full/10.1080/0067270X.2021.1891727> [2021, June 22].
- House, M., Sealy, J., Chirikure, S. & Le Roux, P. 2021. Investigating Cattle Procurement at Great Zimbabwe Using $^{87}\text{Sr}/^{86}\text{Sr}$. *Journal of African Archaeology*. 19(2):146–158. DOI: 10.1163/21915784-20210008.
- Huffman, T.N. 1982. Archaeology and Ethnohistory of the African Iron Age. *Annual Review of Anthropology*. 11(1):133–150. DOI: 10.1146/annurev.an.11.100182.001025.
- Huffman, T.N. 1996. Archaeological evidence for climatic change during the last 2000 years in southern Africa. *Quaternary International*. 33:55–60. DOI: 10.1016/1040-6182(95)00095-X.
- Huffman, T.N. 2000. Mapungubwe and the Origins of the Zimbabwe Culture. *Goodwin Series*. 8:14. DOI: 10.2307/3858043.

- Huffman, T.N. 2001. The Central Cattle Pattern and interpreting the past. *Southern African Humanities*. 13:18.
- Huffman, T.N. 2007. *Handbook to the Iron Age: the archaeology of pre-colonial farming societies in Southern Africa*. Scottsville, South Africa: University of KwaZulu-Natal Press.
- Huffman, T.N. 2008. Climate change during the Iron Age in the Shashe-Limpopo Basin, southern Africa. *Journal of Archaeological Science*. 35(7):2032–2047. DOI: 10.1016/j.jas.2008.01.005.
- Huffman, T.N. & Hanisch, E.O.M. 1987. Settlement hierarchies in the Northern Transvaal: Zimbabwe ruins and Venda history. *African Studies*. 46(1):79–116. DOI: 10.1080/00020188708707665.
- Huffman, T.N. & Woodborne, S. 2016. Archaeology, baobabs and drought: Cultural proxies and environmental data from the Mapungubwe landscape, southern Africa. *The Holocene*. 26(3):464–470. DOI: 10.1177/0959683615609753.
- Janzen, A. 2015. Mobility and Herd Management Strategies of Early Pastoralists in South-Central Kenya, 3000-1200 BP. UC Santa Cruz. Available: <https://escholarship.org/uc/item/87x9p4hq#author> [2019, November 05].
- Janzen, A., Balasse, M. & Ambrose, S.H. 2020. Early pastoral mobility and seasonality in Kenya assessed through stable isotope analysis. *Journal of Archaeological Science*. 117:105099. DOI: <https://doi.org/10.1016/j.jas.2020.105099>.
- Jeanjean, M., Haruda, A., Salvagno, L., Schafberg, R., Valenzuela-Lamas, S., Nieto-Espinet, A., Forest, V., Blaise, E., et al. 2022. Sorting the flock: Quantitative identification of sheep and goat from isolated third lower molars and mandibles through geometric morphometrics. *Journal of Archaeological Science*. 141:105580. DOI: 10.1016/j.jas.2022.105580.
- Kintigh, K.W. & Ingram, S.E. 2018. Was the drought really responsible? Assessing statistical relationships between climate extremes and cultural transitions. *Journal of Archaeological Science*. 89:25–31. DOI: 10.1016/j.jas.2017.09.006.
- Kuper, A. 1982. *Wives for cattle: bridewealth and marriage in Southern Africa*. (International library of anthropology). London ; Boston: Routledge & Kegan Paul.
- Lee-Thorp, J. 2002. Two decades of progress towards understanding fossilization processes and isotopic signals in calcified tissue minerals. *Archaeometry*. 44(3):435–446. DOI: 10.1111/1475-4754.t01-1-00076.
- Lee-Thorp, J. & Van der Merwe, N.J. 1987. Carbon isotope analysis of fossil bone apatite. *South African Journal of Science*. 83(11):712–715.

- Lee-Thorp, J., Manning, L. & Sponheimer, M. 1997. Exploring problems and opportunities offered by down-scaling sample sizes for carbon isotope analyses of fossils. *Bull Soc Geol France*. 168.
- Lee-Thorp, J.A., Holmgren, K., Lauritzen, S.-E., Linge, H., Moberg, A., Partridge, T.C., Stevenson, C. & Tyson, P.D. 2001. Rapid climate shifts in the southern African interior throughout the Mid to Late Holocene. *Geophysical Research Letters*. 28(23):4507–4510. DOI: <https://doi.org/10.1029/2000GL012728>.
- Lippert, B.L. 2020. An Investigation of the Material Culture from Five Middle Iron Age Sites in the Limpopo Valley. Unpublished MA thesis. University of Pretoria.
- Loftus, E., Roberts, P. & Lee-Thorp, J.A. 2016. An Isotopic Generation: Four Decades of Stable Isotope Analysis in African Archaeology. *Azania: Archaeological Research in Africa*. 51(1):88–114. DOI: 10.1080/0067270X.2016.1150083.
- Loubser, J.H.N. 1989. Archaeology and Early Venda History. *Goodwin Series*. 6:54. DOI: 10.2307/3858132.
- Loubser, J.H.N. 1991. The ethnoarchaeology of Venda-speakers in southern Africa. *Navorsinge van die Nasionale Museum : Researches of the National Museum*. 7(7):146–464. DOI: 10.10520/AJA00679208_2838.
- Luyt, J. & Sealy, J. 2018. Inter-tooth comparison of $\delta^{13}\text{C}$ and $\delta^{18}\text{O}$ in ungulate tooth enamel from south-western Africa. *Quaternary International*. 495:144–152. DOI: 10.1016/j.quaint.2018.02.009.
- Luyt, J., Hare, V.J. & Sealy, J. 2019. The relationship of ungulate $\delta^{13}\text{C}$ and environment in the temperate biome of southern Africa, and its palaeoclimatic application. *Palaeogeography, Palaeoclimatology, Palaeoecology*. 514:282–291. DOI: 10.1016/j.palaeo.2018.10.016.
- Makarewicz, C.A. 2014. Winter pasturing practices and variable fodder provisioning detected in nitrogen ($\delta^{15}\text{N}$) and carbon ($\delta^{13}\text{C}$) isotopes in sheep dentinal collagen. *Journal of Archaeological Science*. 9.
- Makarewicz, C.A. 2017a. Stable isotopes in pastoralist archaeology as indicators of diet, mobility, and animal husbandry practices. In *Isotopic investigations of pastoralism in prehistory*. Routledge. 141–158.
- Makarewicz, C.A. 2017b. Sequential $\delta^{13}\text{C}$ and $\delta^{18}\text{O}$ analyses of early Holocene bovid tooth enamel: Resolving vertical transhumance in Neolithic domesticated sheep and goats. *Palaeogeography, Palaeoclimatology, Palaeoecology*. 485:16–29. DOI: 10.1016/j.palaeo.2017.01.028.
- Makarewicz, C.A. & Pederzani, S. 2017. Oxygen ($\delta^{18}\text{O}$) and carbon ($\delta^{13}\text{C}$) isotopic distinction in sequentially sampled tooth enamel of co-localized wild and domesticated caprines:

- Complications to establishing seasonality and mobility in herbivores. *Palaeogeography, Palaeoclimatology, Palaeoecology*. 485:1–15. DOI: 10.1016/j.palaeo.2017.01.010.
- Meyer, A. 2000. K2 and Mapungubwe. *Goodwin Series*. 8:4. DOI: 10.2307/3858042.
- Middleton, G.D. 2012. Nothing Lasts Forever: Environmental Discourses on the Collapse of Past Societies. *Journal of Archaeological Research*. 20(3):257–307. DOI: 10.1007/s10814-011-9054-1.
- Moffett, A.J. & Chirikure, S. 2016. Exotica in Context: Reconfiguring Prestige, Power and Wealth in the Southern African Iron Age. *Journal of World Prehistory*. 29(4):337–382. DOI: 10.1007/s10963-016-9099-7.
- Mucina, L., Rutherford, M.C., Powrie, L.W., van Niekerk, A. & van der Merwe, J.H. Eds. 2014. *Vegetation field atlas of continental South Africa, Lesotho and Swaziland*. (Strelitzia no. 33). Pretoria: SANBI.
- Mucina, L. & Rutherford, M.C. Eds. 2006. *The vegetation of South Africa, Lesotho and Swaziland*. (Strelitzia no. 19). Pretoria: South African National Biodiversity Institute.
- O’Leary, M.H. 1981. Carbon isotope fractionation in plants. *Phytochemistry*. 20(4):553–567.
- Pauketat, T. 2001. Practice and history in archaeology: An emerging paradigm. *Anthropological Theory*. 1(1):73–98. DOI: 10.1177/14634990122228638.
- Pederzani, S. & Britton, K. 2019. Oxygen isotopes in bioarchaeology: Principles and applications, challenges and opportunities. *Earth-Science Reviews*. 188:77–107. DOI: 10.1016/j.earscirev.2018.11.005.
- Pilaar Birch, S.E., Scheu, A., Buckley, M. & Çakırlar, C. 2019. Combined osteomorphological, isotopic, aDNA, and ZooMS analyses of sheep and goat remains from Neolithic Ulucak, Turkey. *Archaeological and Anthropological Sciences*. 11(5):1669–1681. DOI: 10.1007/s12520-018-0624-8.
- Plug, I. 2000. Overview of Iron Age Fauna from the Limpopo Valley. *Goodwin Series*. 8:117. DOI: 10.2307/3858053.
- Prinsloo, H.P. & Coetzee, F.P. 2001. Stayt: A 13th century Iron Age site, Soutpansberg District, Northern Province, South Africa. *South African Journal of Ethnology*. 24(3):81.
- Redman, C.L. 2005. Resilience Theory in Archaeology. *American Anthropologist*. 107(1):70–77. DOI: 10.1525/aa.2005.107.1.070.
- Reid, R.E.B., Jones, M., Brandt, S., Bunn, H. & Marshall, F. 2019. Oxygen isotope analyses of ungulate tooth enamel confirm low seasonality of rainfall contributed to the African Humid Period in Somalia. *Palaeogeography, Palaeoclimatology, Palaeoecology*. 534:109272. DOI: 10.1016/j.palaeo.2019.109272.

- van Rooyen, N. 2002. *The Vegetation Types and Veld Condition of Maremani*. Ekotrust CC.
- Rozanski, K., Araguás-Araguás, L. & Gonfiantini, R. 2013. Isotopic Patterns in Modern Global Precipitation. In *Geophysical Monograph Series*. P.K. Swart, K.C. Lohmann, J. Mckenzie, & S. Savin, Eds. Washington, D. C.: American Geophysical Union. 1–36. DOI: 10.1029/GM078p0001.
- Salzman, P.C. 2004. *Pastoralists: Equality, Hierarchy, And The State*. New York: Routledge. DOI: 10.4324/9780429498459.
- Sealy, J.C., Merwe, N.J. van der, Hobson, K.A., Horton, D.R., Lewis, R.B., Parkington, J., Robertshaw, P. & Schwarcz, H.P. 1986. Isotope Assessment and the Seasonal-Mobility Hypothesis in the Southwestern Cape of South Africa [and Comments and Replies]. *Current Anthropology*. 27(2):135–150.
- Sharp, Z. 2017. *Principles of Stable Isotope Geochemistry, 2nd Edition*. 2nd ed. University of New Mexico. Available: https://digitalrepository.unm.edu/unm_oer/1/ [2023, June 07].
- Sinclair, P., Ekblom, A. & Wood, M. 2012. Trade and society on the south-east African coast in the later first millennium AD: the case of Chibuene. *Antiquity*. 86(333):723–737.
- Smith, J.M. 2005. Climate Change and Agropastoral Sustainability in the Shashe/Limpopo River Basin from Ad 900. Thesis. Available: <http://wiredspace.wits.ac.za/handle/10539/1494> [2019, November 05].
- Smith, J., Lee-Thorp, J. & Hall, S. 2007. Climate Change and Agropastoralist Settlement in the Shashe-Limpopo River Basin, Southern Africa: AD 880 to 1700. *The South African Archaeological Bulletin*. 62(186):115–125. DOI: 10.2307/20474967.
- Smith, J., Lee-Thorp, J., Prevec, S., Hall, S. & Späth, A. 2010. Pre-Colonial Herding Strategies in the Shashe-Limpopo Basin, Southern Africa, Based on Strontium Isotope Analysis of Domestic Fauna. *Journal of African Archaeology*. 8(1):83–98. DOI: 10.3213/1612-1651-10154.
- Sponheimer, M. & Lee-Thorp, J.A. 1999. Oxygen Isotopes in Enamel Carbonate and their Ecological Significance. *Journal of Archaeological Science*. 26(6):723–728. DOI: 10.1006/jasc.1998.0388.
- Spyrou, A., Roberts, P., Bleasdale, M., Lucas, M., Crewe, L., Simmons, A. & Webb, J. 2023. DOI: 10.21203/rs.3.rs-2506620/v1.
- Stayt, H.A. 1931. *The Bavenda*. London: Oxford University Press.
- Summers, R. 1950. Iron age cultures in southern Rhodesia. *South African Journal of Science*. 47(4):95. DOI: 10.10520/AJA00382353_2822.

- Tornero, C., Balasse, M., Molist, M. & Saña, M. 2016. Seasonal reproductive patterns of early domestic sheep at Tell Halula (PPNB, Middle Euphrates Valley): Evidence from sequential oxygen isotope analyses of tooth enamel. *Journal of Archaeological Science*.
- Towers, J., Gledhill, A., Bond, J. & Montgomery, J. 2014. An Investigation of Cattle Birth Seasonality using $\delta^{13}\text{C}$ and $\delta^{18}\text{O}$ Profiles within First Molar Enamel. *Archaeometry*. 56(S1):208–236. DOI: 10.1111/arc.12055.
- Traylor, R.B. & Kohn, M.J. 2017. Tooth enamel maturation reequilibrates oxygen isotope compositions and supports simple sampling methods. *Geochimica et Cosmochimica Acta*. 198:32–47. DOI: 10.1016/j.gca.2016.10.023.
- Tyson, P.D., Lee-Thorp, J., Holmgren, K. & Thackeray, J.F. 2002. Changing gradients of climate change in southern Africa during the past millennium: implications for population movements. *Climatic Change*. 52(1–2):129–135.
- Van der Merwe, N.J. 1982. Carbon isotopes, photosynthesis, and archaeology: Different pathways of photosynthesis cause characteristic changes in carbon isotope ratios that make possible the study of prehistoric human diets. *American scientist*. 70(6):596–606.
- Ventresca Miller, A.R. & Makarewicz, C.A. Eds. 2017. *Isotopic Investigations of Pastoralism in Prehistory*. 1st ed. Routledge. DOI: 10.4324/9781315143026.
- Vogel, J.C. 1978. Isotopic assessment of the dietary habits of Ungulates. *South African Journal of Science*,. 74(8):298.
- Voigt, E.A. 1980. Reconstructing Iron Age Economies of the Northern Transvaal: A Preliminary Report. *The South African Archaeological Bulletin*. 35(131):39. DOI: 10.2307/3888724.
- Voigt, E.A. 1983. *Mapungubwe: An Archaeozoological Interpretation of an Iron Age Community*. V. 1. Available: https://journals.co.za/doi/abs/10.10520/AJA090799001_126.
- Voigt, E.A. 1986. Iron Age Herding: Archaeological and Ethnoarchaeological Approaches to Pastoral Problems. *Goodwin Series*. 5:13. DOI: 10.2307/3858141.
- Voigt, E.A. & Plug, I. 1984. Happy rest: the earliest Iron Age fauna from the Soutpansberg. *South African Journal of Science*. 80(5):221. DOI: 10.10520/AJA00382353_6717.
- Wiedemann, F.B., Bocherens, H., Mariotti, A., Driesch, A. von den & Grupe, G. 1999. Methodological and Archaeological Implications of Intra-tooth Isotopic Variations ($\delta^{13}\text{C}$, $\delta^{18}\text{O}$) in Herbivores from Ain Ghazal (Jordan, Neolithic). *Journal of Archaeological Science*. 26(6):697–704. DOI: 10.1006/jasc.1998.0392.
- Wood, M. 2000. Making Connections: Relationships between International Trade and Glass Beads from the Shashe-Limpopo Area. *Goodwin Series*. 8:78. DOI: 10.2307/3858049.

Woodborne, S., Hall, G., Robertson, I., Patrut, A., Rouault, M., Loader, N.J. & Hofmeyr, M. 2015. A 1000-year carbon isotope rainfall proxy record from South African baobab trees (*Adansonia digitata* L.). *PLoS One*. 10(5).

Woodborne, S., Gandiwa, P., Hall, G., Patrut, A. & Finch, J. 2016. A Regional Stable Carbon Isotope Dendro-Climatology from the South African Summer Rainfall Area. *PLOS ONE*. 11(7):e0159361. DOI: 10.1371/journal.pone.0159361.

Wright, L.E. 2017. Oxygen Isotopes. In *Encyclopedia of Geoarchaeology*. Springer Netherlands : Dordrecht. 567–574. DOI: 10.1007/978-1-4020-4409-0_22.

Appendix A - Sampled animal profiles by site

Individual No.	Accession number	Tooth (Side)	Species
Mutamba			
Bos taurus			
1	MUT/2012/F08	M3(L)	Bos taurus
	MUT/2012/F09	M2(L)	Bos taurus
	MUT/2012/F10	M1(L)	Bos taurus
2	MUT/1031/F07	M $\bar{1}$ (L)	Bos taurus
3	MUT/2099/F09	M $\bar{3}$ (R)	Bos taurus
4	MUT/2167/F01	M $\bar{3}$ (L)	Bos taurus
Capra Hircus			
1	MUT/2003/F04	M $\bar{3}$ (L)	Capra Hircus
Ovis aries			
1	MUT/1011/F13/01	M1(L)	Ovis aries
	MUT/1011/F13/02	M2(L)	Ovis aries
	MUT/2019/F20/03	M $\bar{1}$ (R)	Ovis aries
2	MUT/2019/F20/04	M $\bar{2}$ (R)	Ovis aries
	MUT/2019/F20/05	M $\bar{3}$ (R)	Ovis aries
Ovis/Capra			
1	MUT/1170/F05/01	M1(L)	Ovis/capra
	MUT/1170/F05/02	M2(L)	Ovis/capra
	MUT/1170/F05/03	M3(L)	Ovis/capra
2	MUT/2177/F02	M1(R)	Ovis/capra
	MUT/2177/F03	M2(R)	Ovis/capra
Wild Grazer			
1	MUT/1037/F07	M $\bar{2}$ (R)	Alcelaphus buselaphus (Hartebeest)
2	MUT/1159/F04	M $\bar{2}$ (R)	Alcelaphus Buselaphus (Grazer)
3			
Wild Browser			
1	MUT/2003/F05/05	M $\bar{1}$ (L)	Pelea capreolus (Common rhebok)
Wild Mixed Feeder			
1	MUT/1051/F09/01	M2(L)	Aepyceros melampus
	MUT/1051/F09/02	M1(L)	(Impala)
MNR78			

Bos taurus			
1	MNR78/231/05	M $\bar{3}$ (R)	Bos taurus
	MNR78/231/06	M $\bar{2}$ (R)	Bos taurus
Ovis/Capra			
1	MNR78/123/03	M $\bar{2}$ (R)	Ovis/capra

MNR74			
Bos taurus			
1	MNR74/B063/01 MNR74/B063/02	M $\bar{3}$ (R) M $\bar{2}$ (R)	Bos taurus
2	MNR/B024	M $\bar{2}$ (L)	Bos taurus
Ovis/Capra			
1	MNR74/B065/01	M1(L)	Ovis/capra
	MNR74/B065/02	M2(L)	Ovis/capra
2	MNR74/B255/02 MNR74/B255/03	M $\bar{2}$ (R) M $\bar{3}$ (R)	Ovis/capra
3	MNR74/B068	M1(L)	Ovis/capra
Wild Grazer			
1	MNR74/B011	M1(R)	Equid (c.f. Zebra)

MNR 04

Bos taurus

1 MNR04/341/08 M1̄ Bos taurus

Ovis/Capra

1 MNR04/289/10 M2(R)
MNR04/289/09 M3(R) Ovis/Capra

2 MNR04/2021/11/02 M2(L)
MNR04/2021/11/01 M3(R) Ovis/Capra

Ovis aries

1 MNR04/205/10 M1̄ (L) Ovis aries

2 MNR04/239/09 M3̄(L) Ovis aries

KON

Individual No. Accession number Tooth (Side)

Bos taurus

1 KON/100 M1(U)
KON/114 M2(U) Bos taurus

2 KON/295 M2(U) Bos taurus

3 KON/T4 M2(U) Bos taurus

Ovis/Capra

1	KON/106/01 KON/106/02 KON/106/03	M1 (R) M2 (R) M3 (R)	Ovis/Capra
2	KON/192	M2(L)	Ovis/Capra
3	KON/161	M3(U)	Ovis/Capra
4	KON/40	M3(L)	Ovis/Capra
Wild			
1	KON/156	M1(U)	Aepyceros melampus Impala Mixed feeder

Appendix B – Stable Isotope Results

Lower case letter indicates sample position on tooth. a = enamel root junction (ERJ)

ID	13C	13Cerr	18O	18Oerr
MUT/2177/F03/j	-1.21	0.13	-0.99	0.12
MUT/2177/F03/i	-1.48	0.04	0.11	0.17
MUT/2177/F03/h	-2.65	0.14	0.10	0.24
MUT/2177/F03/g	-2.42	0.05	0.36	0.04
MUT/2177/F03/f	-3.57	0.11	0.84	0.16
MUT/2177/F03/e	-4.32	0.09	-1.03	0.12
MUT/2177/F03/d	-4.64	0.05	0.52	0.10
MUT/2177/F03/c	-5.74	0.06	-0.10	0.08
MUT/2177/F03/b				
MUT/2177/F03/a	-5.06	0.14	-2.36	0.19
MUT/2177/F02/f	-6.47	0.17	-2.41	0.19
MUT/2177/F02/e				
MUT/2177/F02/d	-5.58	0.19	-1.20	0.23
MUT/2177/F02/c				
MUT/2177/F02/b	-5.91	0.16	-2.16	0.12
MUT/2167/F01/h	0.54	0.06	-0.88	0.13
MUT/2167/F01/g	0.51	0.10	-0.89	0.20
MUT/2167/F01/f	-0.09	0.10	-1.68	0.20
MUT/2167/F01/e	-1.15	0.08	-4.07	0.20
MUT/2167/F01/d	-2.13	0.09	-3.27	0.18
MUT/2167/F01/c	-1.70	0.04106093	-2.20	0.10
MUT/2167/F01/b	-0.52	0.09	-3.42	0.16
MUT/2167/F01/a	-0.14	0.020549	-2.12	0.11
MUT/2099/F09/q	0.6046853	0.05	-2.05	0.14
MUT/2099/F09/p	0.68	0.08	-1.75	0.13
MUT/2099/F09/o	0.35	0.05	-2.89	0.11
MUT/2099/F09/n	0.32	0.07	-1.53	0.14
MUT/2099/F09/m	0.25	0.05	-2.38	0.18
MUT/2099/F09/l	0.79	0.05	-2.61	0.14
MUT/2099/F09/k	0.68	0.06	-2.62	0.15
MUT/2099/F09/j	0.93	0.04	-1.71	0.10
MUT/2099/F09/i	0.94	0.06	-2.68	0.10

ID	13C	13Cerr	18O	18Oerr
MUT/2099/F09/h	0.79	0.03	-1.40	0.11
MUT/2099/F09/g	0.56	0.03	-2.03	0.10
MUT/2099/F09/f	0.34	0.08	-0.08	0.23
MUT/2099/F09/e	-0.07	0.09	-1.08	0.17
MUT/2099/F09/d	0.36	0.11	-2.06	0.21
MUT/2099/F09/c	0.43	0.008583	-2.80	0.11
MUT/2099/F09/b	-0.44	0.05	-1.07	0.11
MUT/2099/F09/a	-0.04	0.05	-0.66	0.14
MUT/2019/F20/05/m	-5.22	0.04	-5.59	0.10
MUT/2019/F20/05/j	-3.82	0.08	-3.10	0.17
MUT/2019/F20/05/i	-6.21	0.09	-4.98	0.13
MUT/2019/F20/05/h	-4.47	0.02	-4.29	0.04
MUT/2019/F20/05/g	-6.24	0.08	-4.96	0.10
MUT/2019/F20/05/f				
MUT/2019/F20/05/e	-5.30	0.07	-4.84	0.13
MUT/2019/F20/05/d	-5.91	0.02	-5.06	0.25
MUT/2019/F20/05/c	-5.63	0.02	-5.23	0.06
MUT/2019/F20/05/b	-4.53	0.04	-4.84	0.11
MUT/2019/F20/04/n	-4.67	0.07	-2.22	0.18
MUT/2019/F20/04/m	-4.96	0.07	-3.28	0.12
MUT/2019/F20/04/l	-3.61	0.07	-3.66	0.12
MUT/2019/F20/04/k	-3.78	0.05	-3.64	0.07
MUT/2019/F20/04/j	-3.37	0.06	-3.25	0.22
MUT/2019/F20/04/i	-3.98	0.15	-2.78	0.06
MUT/2019/F20/04/h	-3.22	0.09	-2.19	0.06
MUT/2019/F20/04/g	-2.36	0.09	-2.04	0.12
MUT/2019/F20/04/f	-2.98	0.14	-3.05	0.15
MUT/2019/F20/04/d	-3.03	0.05	-4.08	0.15
MUT/2019/F20/04/c	-3.46	0.11	-3.74	0.17
MUT/2019/F20/04/b	-6.62	0.13	-3.92	0.26
MUT/2019/F20/03/h	-4.66	0.07	-1.06	0.13
MUT/2019/F20/03/g	-8.20	0.04	-3.27	0.16
MUT/2019/F20/03/f	-5.75	0.05	-2.01	0.20
MUT/2019/F20/03/e	-5.89	0.04	-2.71	0.18
MUT/2019/F20/03/d	-4.40	0.09	-2.48	0.06
MUT/2019/F20/03/c	-5.27	0.03	-1.67	0.13
MUT/2019/F20/03/b	-5.15	0.06	-3.20	0.11

ID	13C	13Cerr	18O	18Oerr
MUT/2012/F10/n	-2.81	0.13	-0.18	0.21
MUT/2012/F10/m	-3.65	0.19	-2.17	0.25
MUT/2012/F10/l	-3.50	0.21	-2.15	0.18
MUT/2012/F10/k	-3.13	0.16	-1.77	0.21
MUT/2012/F10/j	-3.58	0.13	-3.10	0.15
MUT/2012/F10/i	-2.50	0.11	-2.64	0.13
MUT/2012/F10/h	-1.56	0.21	-2.56	0.15
MUT/2012/F10/g	-2.36	0.17	-2.87	0.20
MUT/2012/F10/f	-1.07	0.25	-1.81	0.20
MUT/2012/F10/e	-1.89	0.05	-3.05	0.21
MUT/2012/F10/d	-1.53	0.14	-2.73	0.13
MUT/2012/F10/c	-0.78	0.03	-1.95	0.19
MUT/2012/F10/b	-0.63	0.26	-1.33	0.21
MUT/2012/F10/a	-0.98	0.07	-0.24	0.13
MUT/2012/F09/q				
MUT/2012/F09/p	-1.70	0.10	-0.63	0.19
MUT/2012/F09/o	0.52	0.05	0.43	0.27
MUT/2012/F09/n	1.37	0.21	-0.47	0.29
MUT/2012/F09/m	0.65	0.17	-1.77	0.20
MUT/2012/F09/l	0.56	0.15	-2.34	0.22
MUT/2012/F09/k	0.88	0.10	-2.05	0.22
MUT/2012/F09/j	0.76	0.13	-2.86	0.11
MUT/2012/F09/i	0.96	0.17	-3.02	0.13
MUT/2012/F09/h	1.14	0.18	-2.96	0.28
MUT/2012/F09/g	0.93	0.12	-3.74	0.19
MUT/2012/F09/f	0.68	0.13	-4.21	0.06
MUT/2012/F09/e	0.86	0.26	-3.95	0.13
MUT/2012/F09/d	0.47	0.08	-4.04	0.21
MUT/2012/F09/c	1.07	0.19	-3.34	0.23
MUT/2012/F09/b	0.40	0.21	-3.61	0.13
MUT/2012/F09/a	0.84	0.14	-2.53	0.17
MUT/2012/F08/s	0.97	0.25	-2.95	0.14
MUT/2012/F08/r				
MUT/2012/F08/q	1.25	0.16	-2.34	0.17
MUT/2012/F08/p	0.98	0.19	-2.91	0.19
MUT/2012/F08/o	-0.72	0.12	-1.72	0.22
MUT/2012/F08/m	0.02	0.11	-3.17	0.10
MUT/2012/F08/l	-0.83	0.11	-3.88	0.16
MUT/2012/F08/k	0.41	0.06	-4.06	0.13

ID	13C	13Cerr	18O	18Oerr
MUT/2012/F08/j	0.34	0.09	-3.84	0.14
MUT/2012/F08/i	-0.26	0.05	-3.84	0.08
MUT/2012/F08/h	-0.44	0.10	-3.49	0.18
MUT/2012/F08/g	-3.17	0.12	-3.72	0.13
MUT/2012/F08/f	-0.35	0.18	-3.23	0.07
MUT/2012/F08/e	0.95	0.11	-3.65	0.25
MUT/2012/F08/d	0.78	0.15	-3.26	0.17
MUT/2012/F08/c				
MUT/2012/F08/b	0.58	0.17	-1.01	0.09
MUT/2012/F08/a	0.84	0.11	-2.94	0.19
MUT/2003/F05/05/g	-7.99	0.12	-2.62	0.17
MUT/2003/F05/05/f				
MUT/2003/F05/05/e	-7.14	0.09	-1.18	0.08
MUT/2003/F05/05/d	-7.91	0.06	-0.18	0.13
MUT/2003/F05/05/c	-8.23	0.10	-0.32	0.20
MUT/2003/F05/05/b	-7.41	0.11	-2.76	0.08
MUT/2003/F05/05/a	-7.57	0.09	-2.11	0.21
MUT/2003/F04/h	-4.79	0.06	-4.42	0.18
MUT/2003/F04/g	-4.57	0.12	-4.17	0.17
MUT/2003/F04/f	-3.59	0.10	-4.19	0.20
MUT/2003/F04/e	-6.31	0.16	-7.21	0.14
MUT/2003/F04/d	-4.46	0.04	-5.20	0.16
MUT/2003/F04/c	-6.13	0.04	-7.21	0.26
MUT/2003/F04/b	-8.67	0.15	-7.72	0.14
MUT/2003/F04/a	-5.34	0.10	-5.20	0.17
MUT/1170/F05/03/i	-7.71	0.15	-5.49	0.24
MUT/1170/F05/03/h	-8.16	0.08	-6.14	0.14
MUT/1170/F05/03/g	-6.53	0.11	-4.24	0.21
MUT/1170/F05/03/f	-6.39	0.09	-3.60	0.04
MUT/1170/F05/03/e	-5.92	0.18	-3.93	0.12
MUT/1170/F05/03/d	-6.06	0.06	-2.55	0.06
MUT/1170/F05/03/c	-5.91	0.07	-2.77	0.12
MUT/1170/F05/03/b	-6.97	0.07	-1.50	0.19
MUT/1170/F05/03/a				
MUT/1170/F05/02/l	-6.92	0.20	-0.13	0.15
MUT/1170/F05/02/k	-6.61	0.16	0.50	0.27

ID	13C	13Cerr	18O	18Oerr
MUT/1170/F05/02/j	-5.94	0.09	-0.63	0.06
MUT/1170/F05/02/i	-8.03	0.17	-0.11	0.28
MUT/1170/F05/02/h	-8.06	0.14	-3.11	0.07
MUT/1170/F05/02/g	-8.21	0.09	-2.56	0.20
MUT/1170/F05/02/f	-9.12	0.14	-3.00	0.14
MUT/1170/F05/02/e	-9.00	0.11	-4.18	0.19
MUT/1170/F05/02/d	-8.94	0.05	-4.62	0.13
MUT/1170/F05/02/c	-8.26	0.16	-5.77	0.08
MUT/1170/F05/02/b	-6.82	0.14	-3.09	0.16
MUT/1170/F05/01/g				
MUT/1170/F05/01/f	-8.50	0.17	-0.79	
MUT/1170/F05/01/e				
MUT/1170/F05/01/d	-8.40	0.17	-0.25	0.17
MUT/1170/F05/01/c	-9.43	0.13	-0.82	0.12
MUT/1170/F05/01/a	-8.27	0.18	-1.56	0.23
MUT/1159/F04/g	-3.50	0.19	-3.87	0.23
MUT/1159/F04/f	-1.92	0.05	-1.60	0.17
MUT/1159/F04/e	-3.37	0.08	-2.37	0.18
MUT/1159/F04/d	-4.77	0.14	-4.18	0.16
MUT/1159/F04/c	-2.15	0.08	-2.18	0.15
MUT/1159/F04/b	-2.41	0.04	-0.78	0.19
MUT/1159/F04/a	-3.53	0.08	-3.04	0.18
MUT/1051/F09/02/d	-7.37	0.09	1.32	0.21
MUT/1051/F09/02/c	-7.35	0.06	-0.38	0.19
MUT/1051/F09/02/b	-8.49	0.03	0.12	0.11
MUT/1051/F09/01/f	-7.51	0.16	-2.44	0.15
MUT/1051/F09/01/e	-7.14	0.13	-1.55	0.17
MUT/1051/F09/01/d	-8.30	0.06	0.62	0.09
MUT/1051/F09/01/c	-8.77	0.13	-0.56	0.15
MUT/1051/F09/01/b	-9.05	0.18	-0.28	0.18
MUT/1037/F07/o	1.00	0.03	-3.23	0.09
MUT/1037/F07/n	1.00	0.05	-3.11	0.17
MUT/1037/F07/m	-0.77	0.02	-2.81	0.07
MUT/1037/F07/l	0.00	0.10	-2.95	0.07
MUT/1037/F07/k	0.25	0.08	-3.15	0.22
MUT/1037/F07/j	0.34	0.05	-3.42	0.15
MUT/1037/F07/i	-0.40	0.07	-2.74	0.13

ID	13C	13Cerr	18O	18Oerr
MUT/1037/F07/h	0.25	0.09	-3.87	0.16
MUT/1037/F07/f	-1.51	0.05	-2.49	0.07
MUT/1037/F07/e	0.45	0.08	-4.02	0.22
MUT/1037/F07/d	0.38	0.17	-3.29	0.13
MUT/1037/F07/c	0.68	0.08	-3.93	0.20
MUT/1037/F07/b	-0.53	0.08	-2.78	0.17
MUT/1037/F07/a				
MUT/1031/F07/q	-0.08	0.07	-0.15	0.07
MUT/1031/F07/p	0.09	0.05	0.03	0.18
MUT/1031/F07/o	-1.55	0.14	-0.13	0.11
MUT/1031/F07/n	0.16	0.12	0.23	0.22
MUT/1031/F07/m	1.01	0.04	-0.31	0.07
MUT/1031/F07/l	1.88	0.03	-0.25	0.23
MUT/1031/F07/k				
MUT/1031/F07/j	2.16	0.04	-0.51	0.08
MUT/1031/F07/i	0.87	0.05	-1.18	0.11
MUT/1031/F07/h	2.23	0.11	-1.94	0.20
MUT/1031/F07/g	1.64	0.14	-1.90	0.19
MUT/1031/F07/f	2.57	0.10	-2.28	0.12
MUT/1031/F07/e	1.94	0.05	-1.94	0.21
MUT/1031/F07/d	0.94	0.08	-2.34	0.18
MUT/1031/F07/c	1.35	0.04	-3.07	0.11
MUT/1031/F07/b	0.80	0.10	-1.75	0.18
MUT/1031/F07/a	1.73	0.08	-0.71	0.09
MUT/1011/F13/02/f	-8.75	0.09	-4.75	0.18
MUT/1011/F13/02/e	-7.77	0.08	-3.78	0.13
MUT/1011/F13/02/d	-7.72	0.06	-3.25	0.15
MUT/1011/F13/02/c	-7.54	0.16	-2.41	0.18
MUT/1011/F13/02/b	-5.46	0.11	-2.52	0.11
MUT/1011/F13/02/a				
MUT/1011/F13/01/c	-7.76	0.15	-0.80	0.09
MUT/1011/F13/01/a				
MNR78/231/06/m	-0.44	0.06	-1.95	0.09
MNR78/231/06/k	-0.44	0.05	-0.27	0.09
MNR78/231/06/j	-1.56	0.06	-3.18	0.12
MNR78/231/06/i	-0.14	0.16	-3.00	0.12
MNR78/231/06/h	0.54	0.11	-1.70	0.09
MNR78/231/06/g	0.06	0.10	-1.93	0.13

ID	13C	13Cerr	18O	18Oerr
MNR78/231/06/f	0.14	0.07	-1.70	0.14
MNR78/231/06/e	-0.42	0.16	-2.15	0.11
MNR78/231/06/d	-0.54	0.13	-2.77	0.10
MNR78/231/06/c	-0.16	0.10	-3.18	0.13
MNR78/231/06/b	-0.23	0.07	-3.04	0.10
MNR78/231/06/a	-0.10	0.04	-3.20	0.05
MNR78/231/05/n	-0.85	0.06	-3.90	0.06
MNR78/231/05/m	-0.48	0.09	-2.37	0.15
MNR78/231/05/l	-0.05	0.05	-2.67	0.07
MNR78/231/05/k	-0.69	0.06	-3.88	0.13
MNR78/231/05/j				
MNR78/231/05/i	-0.78	0.07	-2.12	0.14
MNR78/231/05/h	-0.69	0.04	-2.30	0.15
MNR78/231/05/g	-0.55	0.09	-2.13	0.06
MNR78/231/05/f	0.46	0.04	-1.61	0.20
MNR78/231/05/e	0.53	0.09	-2.64	0.07
MNR78/231/05/d	0.92	0.06	-3.54	0.14
MNR78/231/05/c	0.98	0.10	-3.64	0.11
MNR78/231/05/b	0.26	0.12	-3.58	0.16
MNR78/231/05/a	0.38	0.09	-3.03	0.13
MNR78/123/03/h	-4.78	0.04	-2.36	0.07
MNR78/123/03/g	-5.07	0.12	-2.84	0.12
MNR78/123/03/f	-6.93	0.07	-4.74	0.10
MNR78/123/03/e	-2.99	0.02	-1.72	0.10
MNR78/123/03/d	-6.01	0.11	-3.16	0.16
MNR78/123/03/c	-3.35	0.06	-2.44	0.08
MNR78/123/03/b	-2.79	0.06	-3.95	0.13
MNR78/123/03/a	-3.85	0.08	-2.22	0.10
MNR74/B255/03/j	-10.35	0.12	-1.78	0.16
MNR74/B255/03/i	-9.16	0.06	-1.57	0.10
MNR74/B255/03/h	-9.03	0.13	-1.38	0.14
MNR74/B255/03/g	-8.43	0.06	-0.98	0.15
MNR74/B255/03/f	-8.27	0.06	-1.80	0.14
MNR74/B255/03/e	-8.88	0.14	-1.11	0.24
MNR74/B255/03/d	-8.53	0.10	-3.23	0.09
MNR74/B255/03/c	-10.15	0.08	-4.62	0.16
MNR74/B255/03/b	-10.85	0.07	-1.78	0.18
MNR74/B255/03/a	-6.81	0.04	-2.87	0.16

ID	13C	13Cerr	18O	18Oerr
MNR74/B255/02/g	-6.61	0.02	-2.51	0.17
MNR74/B255/02/f	-5.37	0.04	-3.85	0.12
MNR74/B255/02/d	-4.12	0.17	-1.48	0.03
MNR74/B255/02/c	-5.77	0.10	-4.25	0.08
MNR74/B255/02/b	-7.89	0.05	-3.93	0.13
MNR74/B255/02/a	-6.91	0.11	-3.49	0.10
MNR74/B068/i	-5.57	0.08	-4.50	0.16
MNR74/B068/h	-4.70	0.12	-4.84	0.04
MNR74/B068/g	-4.07	0.14	-4.32	0.16
MNR74/B068/f	-5.01	0.09	-3.21	0.10
MNR74/B068/e	-5.30	0.11	-4.42	0.15
MNR74/B068/d	-6.38	0.10	-5.88	0.17
MNR74/B068/c	-5.85	0.11	-3.64	0.12
MNR74/B068/b	-4.58	0.06	-4.36	0.19
MNR74/B068/a	-3.83	0.12	-5.81	0.13
MNR74/B065/02/m	-2.71	0.03	-3.34	0.07
MNR74/B065/02/l	-1.82	0.06	-3.43	0.10
MNR74/B065/02/k	-1.76	0.07	-2.73	0.10
MNR74/B065/02/j	-1.37	0.13	-1.57	0.15
MNR74/B065/02/i	-1.33	0.04	-1.40	0.08
MNR74/B065/02/h	-1.75	0.07	-1.34	0.08
MNR74/B065/02/g	-3.74	0.11	-2.07	0.14
MNR74/B065/02/f	-4.68	0.06	-0.52	0.12
MNR74/B065/02/e	-5.19	0.10	-2.12	0.16
MNR74/B065/02/d	-6.41	0.09	-1.79	0.14
MNR74/B065/02/c	-6.79	0.10	-3.66	0.19
MNR74/B065/02/b	-5.77	0.16	-4.01	0.06
MNR74/B065/02/a	-4.90	0.05	-2.27	0.11
MNR74/B065/01/h	-5.06	0.05	-0.84	0.09
MNR74/B065/01/g	-5.42	0.08	-1.88	0.09
MNR74/B065/01/f	-5.57	0.10	-1.49	0.21
MNR74/B065/01/e	-4.68	0.11	-2.48	0.11
MNR74/B065/01/c	-3.53	0.07	-1.38	0.14
MNR74/B065/01/b	-2.17	0.06	-2.20	0.13
MNR74/B065/01/a				
MNR74/B063/02/k				

ID	13C	13Cerr	18O	18Oerr
MNR74/B063/02/j	-2.79	0.06	-4.14	0.09
MNR74/B063/02/i	-2.79	0.17	-0.22	0.14
MNR74/B063/02/h	-2.32	0.12	-6.50	0.10
MNR74/B063/02/g	-1.06	0.10	-5.62	0.15
MNR74/B063/02/f	-1.93	0.09	-5.20	0.16
MNR74/B063/02/e	-2.05	0.15	-6.16	0.10
MNR74/B063/02/d	-1.71	0.03	-4.94	0.07
MNR74/B063/02/c	-2.34	0.06	-3.55	0.11
MNR74/B063/02/b	-1.97	0.08	-4.34	0.06
MNR74/B063/02/a	-3.30	0.06	-2.87	0.11
MNR74/B063/01/e	0.23	0.07	-4.86	0.22
MNR74/B063/01/d	0.29	0.03	-4.92	0.18
MNR74/B063/01/c	-0.77	0.09	-4.95	0.20
MNR74/B063/01/b	0.04	0.04	-4.25	0.14
MNR74/B063/01/a	-2.76	0.05	-5.36	0.10
MNR74/B024/q	-2.46	0.08	0.01	0.12
MNR74/B024/p	-2.55	0.06	0.32	0.18
MNR74/B024/o	-2.72	0.13	-1.13	0.15
MNR74/B024/n	-2.36	0.10	-1.02	0.12
MNR74/B024/m	-2.12	0.09	-1.94	0.10
MNR74/B024/l	-2.15	0.14	-2.86	0.21
MNR74/B024/k	-1.79	0.12	-1.79	0.18
MNR74/B024/j	-1.50	0.06	-2.63	0.16
MNR74/B024/i				
MNR74/B024/h	-1.46	0.07	-2.35	0.04
MNR74/B024/g	-1.44	0.06	-2.43	0.14
MNR74/B024/f	-1.22	0.04	-2.44	0.18
MNR74/B024/e	-1.44	0.12	-2.98	0.12
MNR74/B024/d	-3.32	0.04	-5.20	0.17
MNR74/B024/c	-3.08	0.09	-4.89	0.13
MNR74/B024/b	-3.74	0.10	-5.09	0.24
MNR74/B024/a	-4.43	0.06	-5.87	0.14
MNR74/B011/o	-6.16	0.03	-3.69	0.09
MNR74/B011/n	-2.25	0.08	-1.81	0.18
MNR74/B011/m	-0.97	0.07	-1.35	0.10
MNR74/B011/l	-1.21	0.07	-1.80	0.09
MNR74/B011/k	-0.93	0.07	-1.55	0.12
MNR74/B011/j	-0.76	0.07	-1.97	0.12

ID	13C	13Cerr	18O	18Oerr
MNR74/B011/i	-3.00	0.10	-3.79	0.15
MNR74/B011/h				
MNR74/B011/g	0.13	0.05	-5.41	0.05
MNR74/B011/f	0.22	0.08	-5.09	0.09
MNR74/B011/e	0.13	0.05	-3.62	0.20
MNR74/B011/d	0.26	0.09	-4.85	0.09
MNR74/B011/c	-0.45	0.08	-4.83	0.05
MNR74/B011/b	0.31	0.08	-3.49	0.13
MNR74/B011/a	0.02	0.03	-3.92	0.20
MNR04/341/08/o	-3.35	0.10	-3.57	0.19
MNR04/341/08/n	-1.67	0.02	-3.64	0.12
MNR04/341/08/m	-0.14	0.02	-3.57	0.21
MNR04/341/08/l	0.35	0.10	-3.15	0.17
MNR04/341/08/k	-5.36	0.04	-5.70	0.16
MNR04/341/08/j	0.70	0.05	-4.12	0.13
MNR04/341/08/i	1.03	0.08	-4.22	0.14
MNR04/341/08/h	1.10	0.13	-4.20	0.12
MNR04/341/08/g	1.21	0.06	-3.47	0.11
MNR04/341/08/f	1.53	0.08	-2.96	0.16
MNR04/341/08/e	1.38	0.05	-3.62	0.17
MNR04/341/08/d	1.62	0.04	-2.54	0.14
MNR04/341/08/c	1.17	0.04	-2.49	0.11
MNR04/341/08/b	1.58	0.06	-1.78	0.11
MNR04/341/08/a	1.38	0.10	-2.04	0.10
MNR04/289/10/g	-2.37	0.06	-1.83	0.10
MNR04/289/10/f	-5.35	0.05	-3.03	0.18
MNR04/289/10/e	-7.10	0.04	-4.44	0.08
MNR04/289/10/d	-4.45	0.12	-3.64	0.10
MNR04/289/10/c	-3.65	0.08	-3.25	0.18
MNR04/289/10/b	-3.56	0.07	-4.25	0.07
MNR04/289/10/a	-3.65	0.04	-3.63	0.08
MNR04/289/09/k	-3.98	0.08	-4.28	0.12
MNR04/289/09/j				
MNR04/289/09/i	-3.39	0.07	-4.96	0.09
MNR04/289/09/h	-2.76	0.07	-4.90	0.14
MNR04/289/09/g	-2.54	0.14	-5.87	0.10
MNR04/289/09/f	-2.74	0.04	-5.29	0.14
MNR04/289/09/e	-2.96	0.03	-4.16	0.06

ID	13C	13Cerr	18O	18Oerr
MNR04/289/09/d	-3.47	0.07	-3.71	0.17
MNR04/289/09/c	-3.85	0.06	-4.57	0.14
MNR04/289/09/b	-3.78	0.13	-5.25	0.21
MNR04/289/09/a	-2.40	0.05	-6.24	0.14
MNR04/239/09/g	-2.88	0.08	-3.00	0.14
MNR04/239/09/f	-2.69	0.07	-1.74	0.14
MNR04/239/09/e	-2.94	0.08	-3.74	0.12
MNR04/239/09/d	-3.77	0.06	-3.04	0.22
MNR04/239/09/c	-5.19	0.09	-2.84	0.08
MNR04/239/09/a	-4.42	0.06	-4.04	0.14
MNR04/205/10/h	-2.89	0.05	-5.88	0.08
MNR04/205/10/g	-3.38	0.09	-5.42	0.13
MNR04/205/10/f	-4.00	0.04	-5.10	0.15
MNR04/205/10/e	-4.61	0.13	-5.07	0.10
MNR04/205/10/d	-4.52	0.06	-3.79	0.12
MNR04/205/10/c	-5.38	0.05	-4.51	0.14
MNR04/205/10/b	-5.64	0.08	-5.13	0.15
MNR04/205/10/a	-5.27	0.10	-6.11	0.15
MNR04/2021/11/02/g	-4.16	0.09	-3.69	0.04
MNR04/2021/11/02/f	-4.63	0.08	-4.18	0.09
MNR04/2021/11/02/e	-4.53	0.08	-4.06	0.12
MNR04/2021/11/02/d	-4.98	0.06	-4.90	0.10
MNR04/2021/11/02/c	-6.50	0.05	-5.43	0.13
MNR04/2021/11/02/b	-5.73	0.06	-4.65	0.10
MNR04/2021/11/02/a	-5.54	0.09	-5.45	0.09
MNR04/2021/11/01/l	-5.67	0.05	-4.80	0.10
MNR04/2021/11/01/k	-5.87	0.06	-4.72	0.07
MNR04/2021/11/01/j	-5.04	0.04	-5.39	0.09
MNR04/2021/11/01/i	-4.81	0.12	-5.04	0.12
MNR04/2021/11/01/h	-4.21	0.05	-4.04	0.02
MNR04/2021/11/01/g	-3.48	0.07	-3.57	0.11
MNR04/2021/11/01/f	-4.29	0.10	-3.43	0.18
MNR04/2021/11/01/e	-5.79	0.14	-3.71	0.19
MNR04/2021/11/01/d	-5.33	0.07	-3.57	0.19
MNR04/2021/11/01/c	-5.74	0.12	-3.50	0.11
MNR04/2021/11/01/b	-3.73	0.05	-5.12	0.19
MNR04/2021/11/01/a	-5.40	0.09	-4.41	0.04

ID	13C	13Cerr	18O	18Oerr
KON/40/k	-3.58	0.05	-6.48	0.16
KON/40/j	-3.12	0.04	-5.41	0.20
KON/40/i	-3.50	0.14	-8.78	0.22
KON/40/h	-1.83	0.15	-6.71	0.17
KON/40/g	-1.00	0.02	-4.91	0.20
KON/40/f	-0.39	0.05	-4.96	0.14
KON/40/e	-0.70	0.18	-3.91	0.18
KON/40/d	-1.40	0.15	-4.49	0.16
KON/40/c	-3.19	0.06	-3.58	0.09
KON/40/b	-2.93	0.10	-6.08	0.19
KON/40/a	-2.40	0.10	-4.74	0.20
KON/295/o	3.49	0.08	-3.74	0.18
KON/295/n	2.75	0.05	-4.40	0.13
KON/295/m	3.28	0.13	-2.78	0.12
KON/295/l	3.00	0.05	-3.73	0.12
KON/295/k	2.60	0.09	-3.44	0.09
KON/295/j	3.03	0.09	-3.31	0.19
KON/295/i	3.02	0.04	-3.53	0.11
KON/295/h	3.15	0.07	-3.80	0.17
KON/295/g	3.21	0.04	-4.75	0.07
KON/295/f	3.32	0.04	-5.59	0.12
KON/295/e	3.46	0.15	-5.91	0.13
KON/295/d	3.53	0.07	-5.65	0.07
KON/295/c	3.27	0.08	-6.47	0.12
KON/295/b	3.89	0.10	-5.74	0.16
KON/295/a	4.10	0.11	-5.47	0.17
KON/192/i	-1.48	0.07	-4.88	0.18
KON/192/h	-2.57	0.16	-3.49	0.22
KON/192/g	-2.92	0.10	-4.71	0.19
KON/192/f	-0.39	0.11	-2.98	0.11
KON/192/c	1.09	0.05	-3.51	0.13
KON/192/b	1.66	0.07	-1.63	0.13
KON/192/a	0.14	0.15	-1.55	0.09
KON/161/l	-5.69	0.13	-0.97	0.13
KON/161/k	-6.46	0.08	-0.92	0.20
KON/161/j	-6.58	0.07	-1.49	0.12
KON/161/i	-6.74	0.07	-2.75	0.18

ID	13C	13Cerr	18O	18Oerr
KON/161/h	-6.42	0.13	-2.95	0.14
KON/161/g	-5.74	0.11	-2.50	0.17
KON/161/f	-5.07	0.03	-2.43	0.20
KON/161/e	-4.28	0.04	0.36	0.09
KON/161/c	-3.88	0.06	-1.37	0.12
KON/161/b	-3.70	0.03	-2.09	0.12
KON/161/a	-4.95	0.11	-1.66	0.28
KON/106/03/i	-5.15	0.10	1.11	0.09
KON/106/03/h	-5.08	0.05	0.64	0.18
KON/106/03/g	-4.77	0.06	-0.62	0.15
KON/106/03/f	-4.33	0.06	-1.03	0.13
KON/106/03/e	-4.00	0.06	-2.37	0.18
KON/106/03/d	-4.35	0.04	-1.47	0.17
KON/106/03/c	-4.71	0.09	0.33	0.12
KON/106/03/b	-5.15	0.10	1.62	0.16
KON/106/03/a	-5.72	0.02	1.21	0.16
KON/T4/n	2.26	0.05	-5.91	0.16
KON/T4/m	2.12	0.06	-5.46	0.20
KON/T4/l	1.90	0.06	-5.25	0.19
KON/T4/k	1.91	0.10	-5.08	0.17
KON/T4/j	2.11	0.10	-4.14	0.18
KON/T4/i	2.18	0.07	-3.67	0.19
KON/T4/h	1.49	0.16	-3.32	0.03
KON/T4/g	1.92	0.03	-3.09	0.13
KON/T4/f	1.93	0.10	-1.50	0.15
KON/T4/e	2.00	0.06	-1.86	0.17
KON/T4/d	1.93	0.07	-2.83	0.20
KON/T4/c	1.86	0.06	-3.09	0.19
KON/T4/b	2.23	0.04	-3.05	0.18
KON/T4/a	2.20	0.02	-3.14	0.19
KON/156/a	-7.90	0.06	-3.23	0.15
KON/156/b	-7.62	0.07	-3.80	0.07
KON/156/c	-7.30	0.10	0.01	0.05
KON/114/p	0.14	0.06	-5.15	0.06
KON/114/o	-0.42	0.14	-5.97	0.18
KON/114/n	-0.58	0.08	-5.43	0.16
KON/114/m	-1.21	0.06	-5.98	0.07

ID	13C	13Cerr	18O	18Oerr
KON/114/l	-0.63	0.05	-3.69	0.09
KON/114/k	-0.79	0.12	-4.79	0.18
KON/114/j	-1.09	0.05	-4.83	0.17
KON/114/i	-0.89	0.06	-4.69	0.12
KON/114/h	0.42	0.05	-3.46	0.15
KON/114/g	0.13	0.03	-5.02	0.07
KON/114/f	0.36	0.11	-4.82	0.13
KON/114/e	-0.29	0.06	-4.53	0.13
KON/114/d	-0.60	0.10	-5.00	0.11
KON/114/c	-0.56	0.09	-4.64	0.09
KON/114/b	-0.45	0.04	-4.67	0.17
KON/114/a	0.91	0.07	-5.10	0.12
KON/106/02/i	-6.83	0.12	-2.26	0.09
KON/106/02/h	-6.14	0.07	-4.11	0.16
KON/106/02/g	-6.62	0.07	-1.84	0.17
KON/106/02/f	-7.96	0.15	-2.45	0.10
KON/106/02/e	-6.73	0.05	-0.61	0.15
KON/106/02/d	-6.85	0.06	-0.69	0.07
KON/106/02/c	-6.77	0.06	-1.55	0.04
KON/106/02/b				
KON/106/02/a				
KON/106/01/f	-7.30	0.07	-1.75	0.11
KON/106/01/e	-7.33	0.05	-1.27	0.14
KON/106/01/d	-7.19	0.04	-2.90	0.12
KON/106/01/c	-7.01	0.16	-2.28	0.15
KON/106/01/b	-6.79	0.07	-3.70	0.18
KON/100/n	1.85	0.05	-2.81	0.12
KON/100/m	1.98	0.05	-2.59	0.09
KON/100/l	1.77	0.08	-3.01	0.16
KON/100/k	1.13	0.06	-3.95	0.15
KON/100/j	1.84	0.04	-4.20	0.14
KON/100/i	1.93	0.03	-3.41	0.15
KON/100/h	0.36	0.08	-4.72	0.15
KON/100/g	-0.27	0.09	-5.36	0.13
KON/100/f	0.32	0.04	-4.72	0.16
KON/100/e	1.16	0.06	-5.19	0.16
KON/100/d	-2.77	0.08	-6.52	0.08

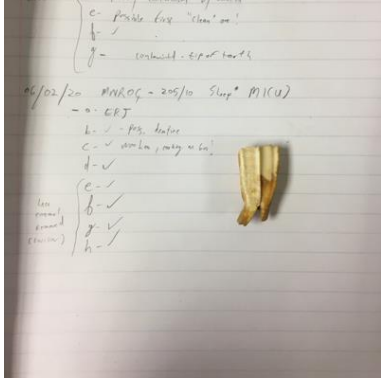
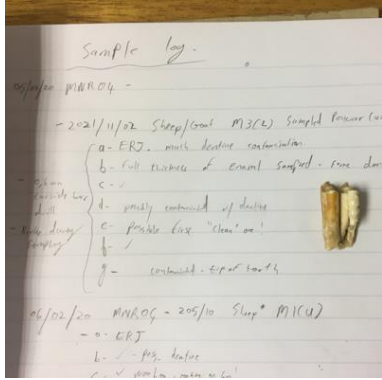
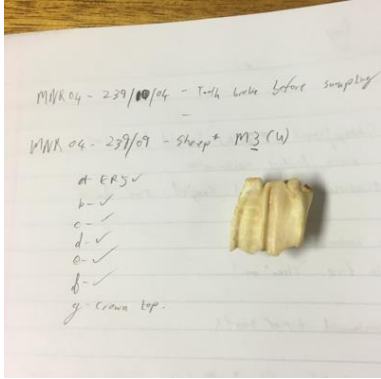
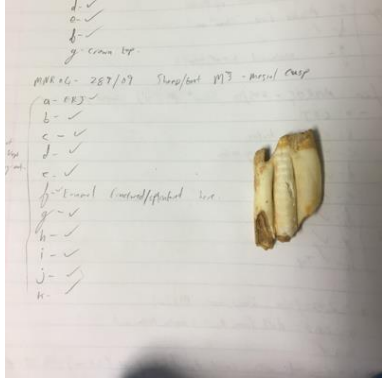
ID	13C	13Cerr	18O	18Oerr
KON/100/c	1.75	0.09	-3.75	0.16
KON/100/b	1.79	0.07	-4.00	0.19
KON/100/a	-1.31	0.08	-5.43	0.10

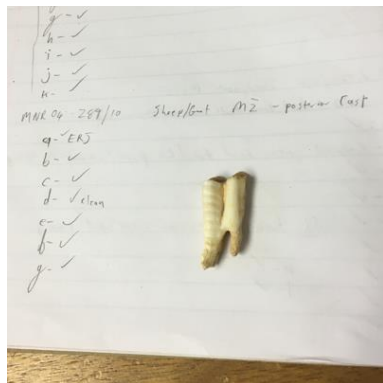
Reference Standards Results

Date	Sample ID	$\delta^{13}\text{C}$	$\delta^{18}\text{O}$
28_07_2021	GS35/87	1.05	-2.57
	GS35/88	0.86	-3.07
	GS35/89	1.67	-3.09
	GS35/90	1.42	-3.20
	GS35/91	1.03	-3.20
	GS35/92	1.09	-2.93
	GS35/93	1.28	-2.77
	GS35/75	-7.57	-1.16
	21_07_2021	GS35/77	1.12
GS35/76		1.25	-3.08
GS35/78		1.16	-3.15
GS35/79		1.11	-2.92
GS35/82		1.27	-2.86
GS35/84		1.28	-2.55
GS35/81		1.14	-2.80
GS35/83		1.11	-2.89
GS35/85		1.15	-2.98
GS35/50		1.12	-2.94
15-07-2021	GS35/58	1.33	-3.00
	GS35/69	1.06	-3.05
	GS35/68	1.18	-2.90
	GS35/71	1.38	-2.89
	GS35/59	0.99	-2.85
	GS35/73	1.03	-2.96
	GS35/55	0.99	-2.86
	GS35/62	1.35	-2.83
12-07-2021	GS35/54	1.44	-2.89
	GS35/63	1.02	-2.85
	GS35/53	1.14	-3.23
	GS35/64	1.22	-3.42
	GS35/60	0.99	-3.02
	GS35/38	1.19	-2.91

Date	Sample ID	$\delta^{13}\text{C}$	$\delta^{18}\text{O}$
	GS35/40	1.05	-2.96
8-07-2021	GS35/43	1.30	-2.85
	GS35/42	1.38	-2.87
	GS35/46	1.16	-3.12
	GS35/45	0.79	-3.33
	GS35/44	1.39	-2.85
	GS35/49	1.13	-2.91
	GS35/28	1.17	-2.60
	GS35/17	1.20	-3.36
6-07-2021	GS35/30	0.96	-2.98
	GS35/31	1.21	-3.16
	GS35/35	1.40	-2.98
	GS35/27	1.16	-2.67
	GS35/32	1.35	-2.91
	GS35/33	1.36	-2.58
	GS35/29	0.73	-3.40
	GS35/11	1.01	-2.78
	GS35/18	1.31	-2.54
5-07-2021	GS35/19	1.37	-3.31
	GS35/20	1.08	-3.78
	GS35/22	1.14	-2.54
	GS35/23	1.22	-2.75
	GS35/3	1.07	-2.88
	GS35/2	1.08	-2.74
2021/06/25	GS35/1	1.14	-2.75
	GS35/10	1.21	-3.24
	GS35/8	1.66	-3.39
	GS35/4	1.20	-3.13
	GS35/14	1.28	-2.94
	GS35/12	0.83	-2.85
	GS35/7	1.08	-2.74

Appendix C – Sample Images

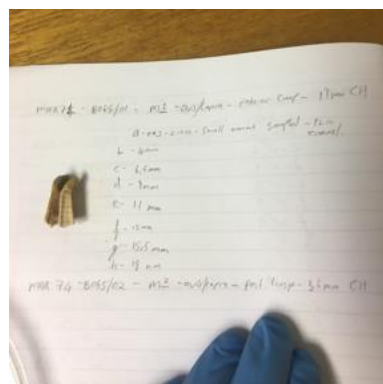
	
<p style="text-align: center;">MNR04/205/10. M₁. <i>O. aries</i></p>	<p style="text-align: center;">MNR04 / 2021/11/02.M₃. <i>O. aries</i> / <i>C. hircus</i></p>
	
<p style="text-align: center;">MNR04/239/09. M₃. <i>O. aries</i></p>	<p style="text-align: center;">MNR04/289/09. M₃. <i>O. aries</i> / <i>C. hircus</i></p>



MNR04/289/10. M $\bar{2}$. *O. aries/C. hircus*



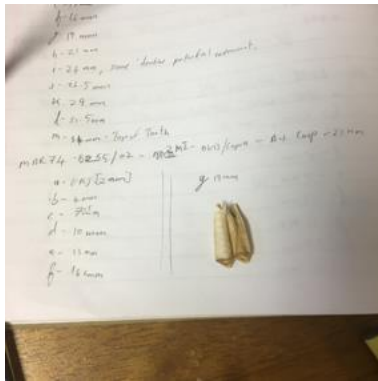
MNR04/341/08. M $\bar{2}$. *B. taurus*



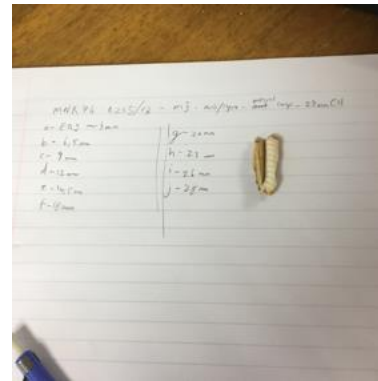
MNR74/B065/01. M $\bar{1}$. *O. aries/C. hircus*



MNR74/B065/02. M $\bar{2}$. *O. aries/C. hircus*



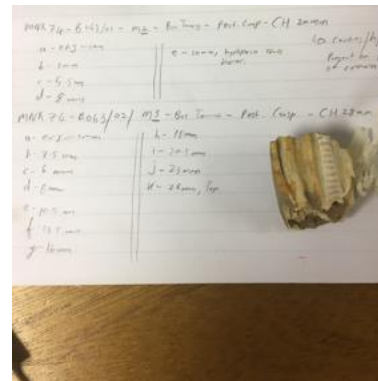
MNR74/B255/02. M $\bar{2}$. *O. aries*/C. hircus



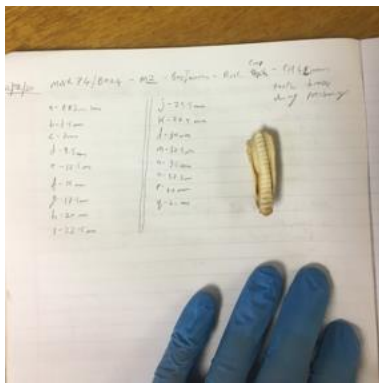
MNR74/B255/03. M $\bar{3}$. *O. aries*/C. hircus



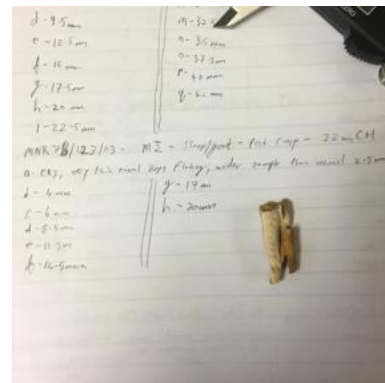
MNR74/B063/01. M $\bar{2}$. *B. taurus*



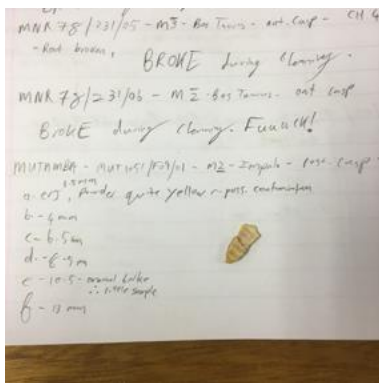
MNR74/B063/02. M $\bar{3}$. *B. taurus*



MNR74/B024. M₂. *B. taurus*



MNR78/123/03. M₂. *O. aries/C. hircus*



MUT1051/F09/01. M₂. *A. melampus*



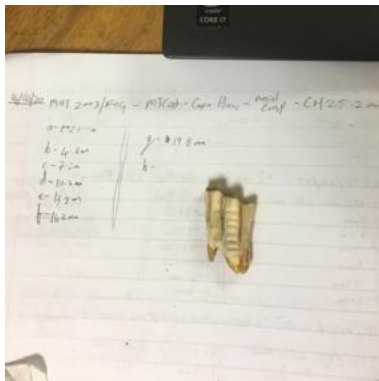
MUT1051/F09/02. M₁. *A. melampus*



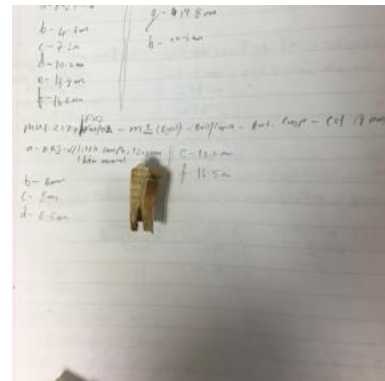
MNR78/231/05. M $\bar{3}$. *B. taurus*



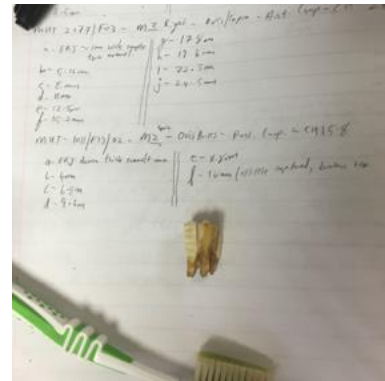
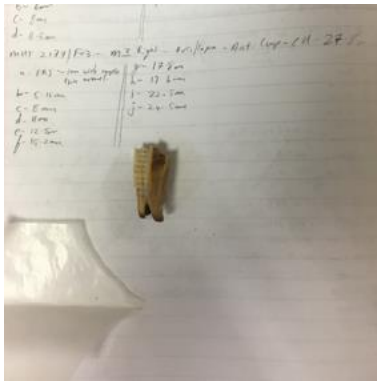
MNR78/231/06. M $\bar{2}$. *B. taurus*



MUT2003/F04. M $\bar{3}$. *C. hircus*

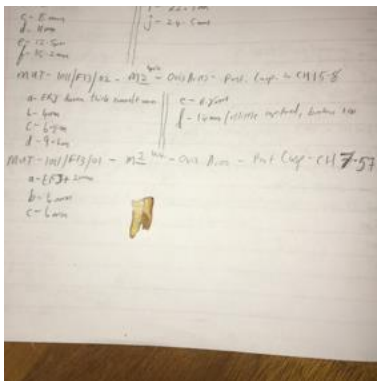


MUT2177/F02. M $\bar{1}$. *O. aries/C. hircus*



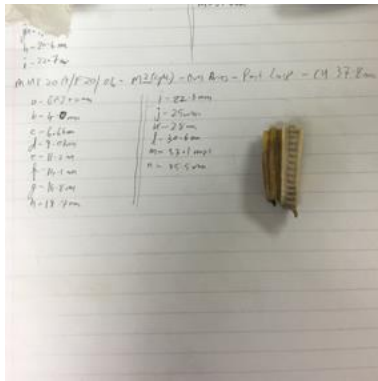
MUT2177/F03. M2. *O. aries*/*C. hircus*

MUT1011/F13/02. M2. *O. aries*

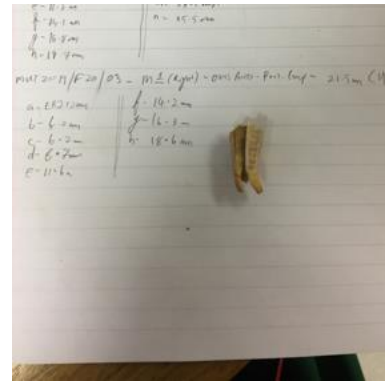


MUT1011/F13/01. M1. *O. aries*

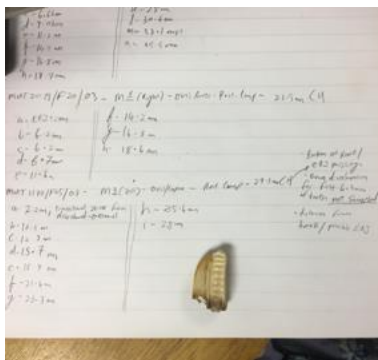
MUT2018/F20/05. M3. *O. aries*



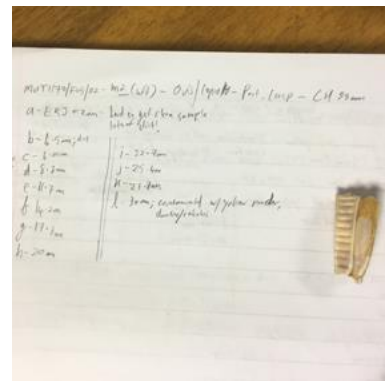
MUT2018/F20/04. M₂. *O. aries*



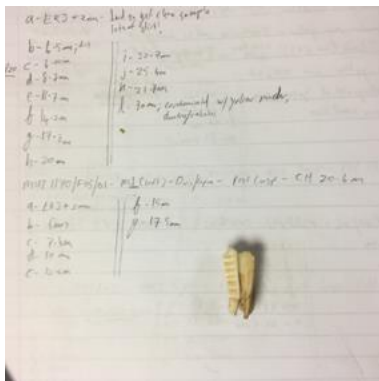
MUT2018/F20/03. M₁. *O. aries*



MUT1170/F05/03. M₁. *O. aries*

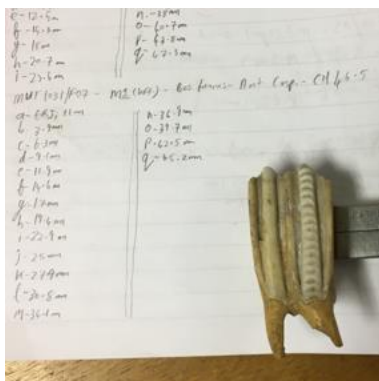


MUT1170/F05/02. M₂. *O. aries*/*C. hircus*



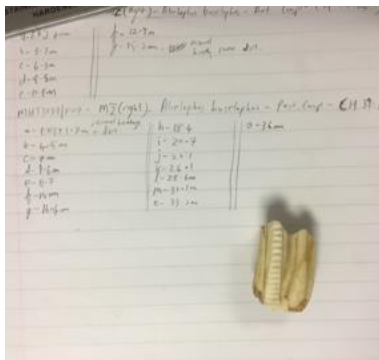
MUT1170/F05/01. M1. *O. aries*/*C. hircus*

MUT2099/F09. M3. *B. taurus*

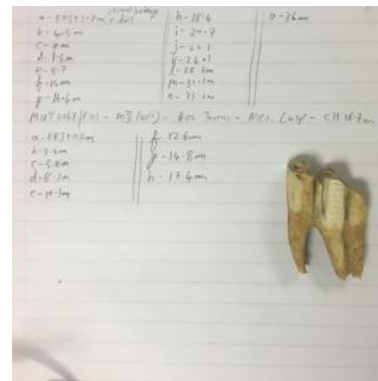


MUT1031/F07. M1. *B. taurus*

MUT1159/F04. M2. *A. buselaphus*



MUT1037/F07. M2. *A. buselaphus*



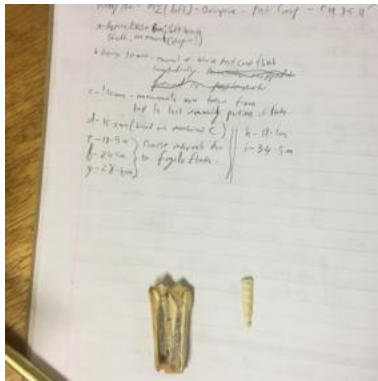
MUT2167/F01. M3. *B. taurus*



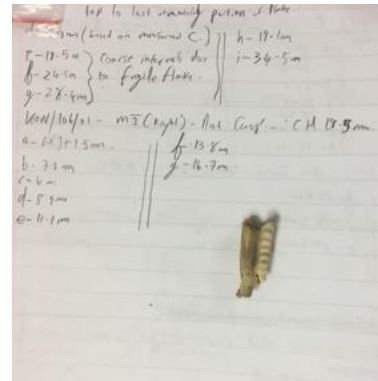
KON/40. M3. *O. aries/C. hircus*



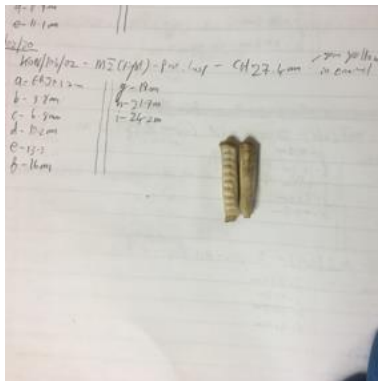
KON/161. M3. *O. aries/C. hircus*



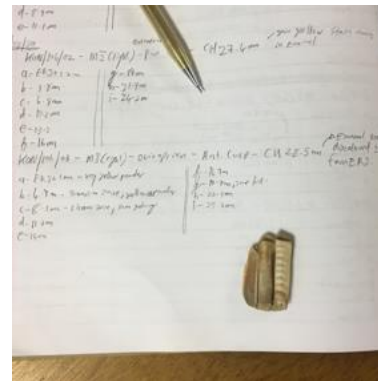
KON/192. M $\bar{2}$. *O. aries* / *C. hircus*



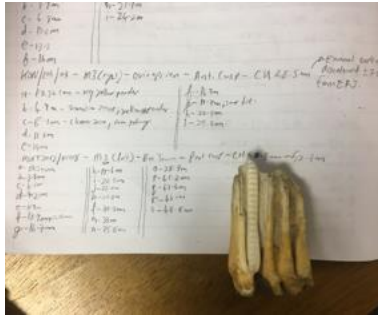
KON/1106/01. M $\bar{1}$. *O. aries* / *C. hircus*



KON/106/02. M $\bar{2}$. *O. aries* / *C. hircus*



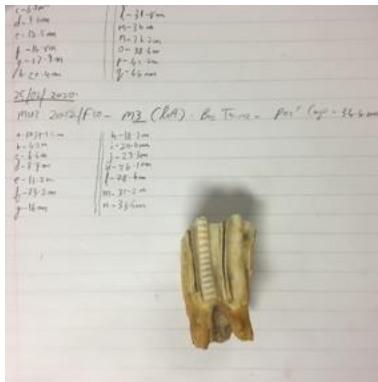
KON/106/03. M $\bar{3}$. *O. aries* / *C. hircus*



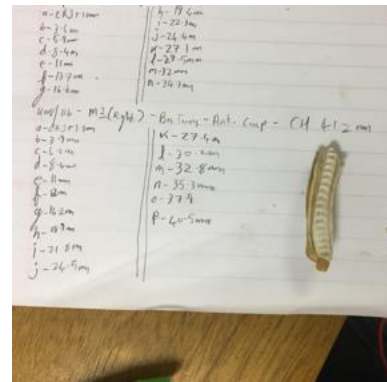
MUT2012/F08. M3. *B. taurus*



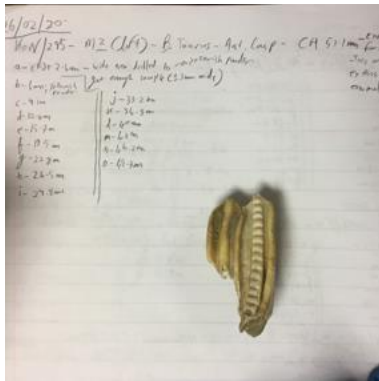
MUT2012/F09. M2. *B. taurus*



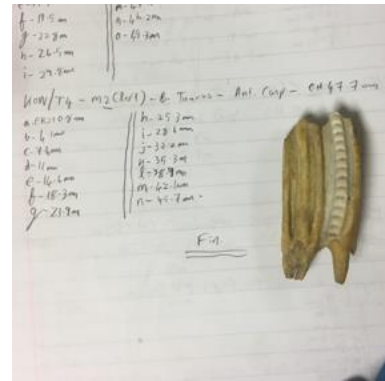
MUT2012/F10. M3. *B. taurus*



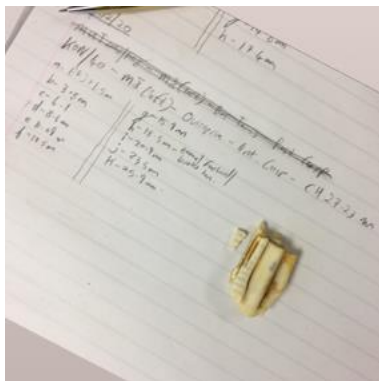
KON/114. M2. *B. taurus*



KON/295. M₂. *B. taurus*



KON/T4. M₂. *B. taurus*



KON/40. M₃. *O. aries/C. hircus*